

Universität für Bodenkultur Wien
University of Natural Resources and Life Sciences Vienna

Department for Water, Atmosphere and Environment
Institute for Hydrology and Water Management (HyWa)



Water temperature estimation by analysing runoff components

Master thesis

in fulfilment of the requirements for the degree of Diplom-Ingenieur

submitted by

Christoph Kugler

Supervisor: Hubert Holzmann, Ao.Univ.Prof. Dipl.-Ing. Dr.nat.techn.

Vienna, April 2019

Declaration of academic honesty

I hereby declare that I am the sole author of this work. No assistance other than that which is permitted has been used. Ideas and quotes taken directly or indirectly from other sources are identified as such. This written work has not yet been submitted in any part.

Eidesstattliche Erklärung

Ich erkläre eidesstattlich, dass ich die Arbeit selbständig angefertigt habe. Es wurden keine anderen als die angegebenen Hilfsmittel benutzt. Die aus fremden Quellen direkt oder indirekt übernommenen Formulierungen und Gedanken sind als solche kenntlich gemacht. Diese schriftliche Arbeit wurde noch an keiner Stelle vorgelegt.

Christoph Kugler, April 2019

Acknowledgements

First of all I want to thank Professor Holzmann for having a sympathetic ear for all my small and big questions and for the many meetings where we could discuss them in person.

Jakob spent many weekends with me at the library, I want to thank him for the company and the conversations over coffee and tea.

When things got too stressful Oskar helped me to appreciate the really important things in life like jumping in puddles and smelling flowers and taking naps.

I want to thank Petra, Andi, Resi, Johannes, Judith, my parents, my parents-in-law, Conny and Stefan for taking over my part in the puddle-jumping business when I had university stuff to do.

Most of all I want to thank Katrin, for listening to my enthusiasm and my rants, for supporting me all these years through my studies, for uplifting my spirits when I was down and for carrying much of the load, so that I could finish this thesis. I could not have done it without you!

Finally I want to thank my dog Zora for forcing me out into nature every day regardless of snow, wind, sun or rain, probably for the better.

Abstract

Water temperature is vastly important for aquatic environments, it influences these ecosystems in a variety of ways as it affects biological as well as chemical processes. Water temperature has also huge (socio-)economic implications because of its impact on drinking water production, thermoelectric power production and fishing.

The aim of this thesis is to investigate if knowledge about the size of contributing runoff components and their respective temperature distributions improves the estimation of stream temperature. To achieve this a discharge-weighted stream temperature model is compared with several other temperature models.

The discharge of a river can come from several sources, e.g. groundwater, melting water, surface flow or subsurface flow. These runoff components have different volumes and different temperature distributions. This thesis uses a simplified concept by assuming that the runoff of a river can roughly be divided into two components, a slow component and a fast component.

A simplified conceptual water balance model is used to estimate these two components, by modelling dominant hydrological processes for the upper catchment area of the river Pielach at gauge Hofstetten.

The fast component is influenced by the air temperature which has been obtained from several gauges in or near the catchment area. The associated temperature of the slow component has been obtained from a groundwater temperature gauge near the catchment area. It has a lower frequency and a smaller amplitude than the air temperature.

To estimate the stream temperature, the fast and slow component (expressed as percentages of the total discharge) are used as weights for their associated temperature distributions.

The results show that the discharge-weighted temperature model overestimates the temperature at the beginning and the end of a given year, presumably because the groundwater temperature is overemphasized.

Kurzfassung

Die Wassertemperatur ist für Gewässer von großer Bedeutung. Sie übt großen Einfluss auf diese Ökosysteme in vielfältiger Weise aus, da sie sowohl biologische als auch chemische Prozesse beeinflusst. Außerdem hat sie enorme sozioökonomische Auswirkungen, da sie die Trinkwassergewinnung, die thermoelektrische Stromerzeugung und die Fischerei beeinträchtigen kann.

Ziel dieser Arbeit ist es herauszufinden, ob die Kenntnis über Größe und Temperaturverläufe von Abflussbestandteilen die Abschätzung der Flusstemperatur verbessert. Um dies zu erreichen, wird ein abflussgewichtetes Temperaturmodell mit mehreren anderen Temperaturmodellen verglichen.

Der Abfluss eines Flusses setzt sich aus mehreren Quellen zusammen, z.B. Grundwasser, Schmelzwasser, Oberflächenabfluss oder Zwischenabfluss. Diese Abflussbestandteile haben unterschiedliche Volumina und Temperaturverteilungen. Vereinfachend wird angenommen dass der Abfluss eines Flusses grob in zwei Bestandteile unterteilt werden kann, einem langsamen und einem schnellen Bestandteil.

Zur Abschätzung der beiden Bestandteile wird ein vereinfachtes konzeptionelles Wasserhaushaltsmodell verwendet, das dominante hydrologische Prozesse für das obere Einzugsgebiet der Pielach an der Messstelle Hofstetten modelliert.

Der schnelle Bestandteil wird durch die Lufttemperatur beeinflusst, welche von mehreren Messstellen im oder nahe dem Einzugsgebiet ermittelt wurde. Die dem langsamen Bestandteil zugehörige Grundwassertemperatur wurde von einer Messstelle in der Nähe des Einzugsgebietes ermittelt. Die Grundwassertemperatur hat eine niedrigere Frequenz und eine kleinere Amplitude als die Lufttemperatur.

Um die Flusstemperatur abzuschätzen, werden die schnellen und langsamem Bestandteile als Gewichtungsfaktoren für die jeweiligen Temperaturverläufe verwendet.

Die Ergebnisse zeigen, dass das abflussgewichtete Temperaturmodell die Temperatur zu Beginn und am Ende eines Jahres überschätzt, da die Grundwassertemperatur hier überrepräsentiert ist.

Table of Contents

1	INTRODUCTION AND LITERATURE REVIEW.....	1
1.1	IMPORTANCE OF WATER TEMPERATURE.....	1
1.1.1	<i>Environmental relevance.....</i>	<i>1</i>
1.1.2	<i>Economic relevance.....</i>	<i>3</i>
1.2	INFLUENCING FACTORS ON STREAM TEMPERATURE.....	6
1.2.1	<i>External temperature drivers.....</i>	<i>6</i>
1.2.2	<i>Internal structure of the stream.....</i>	<i>6</i>
1.2.3	<i>Human influence on stream structures.....</i>	<i>8</i>
1.3	OVERVIEW OF STREAM TEMPERATURE MODELS.....	10
1.3.1	<i>Ca. 1900 to the 1970s – (Smith, 1972).....</i>	<i>11</i>
1.3.2	<i>1970s to mid-1980s – (Ward, 1985).....</i>	<i>13</i>
1.3.3	<i>Mid-1980s to mid-2000s – (Caissie, 2006).....</i>	<i>16</i>
1.3.4	<i>Interlude – (Webb et al., 2008).....</i>	<i>19</i>
1.3.5	<i>Mid-2000s to mid-2010s – (Hannah & Garner, 2015).....</i>	<i>20</i>
1.4	AIM OF THIS THESIS.....	20
2	METHODOLOGY.....	22
2.1	INTRODUCTORY REMARKS.....	22
2.2	STUDY AREA AND DATA.....	22
2.2.1	<i>Gauge Loich.....</i>	<i>22</i>
2.2.2	<i>Gauge Hofstetten.....</i>	<i>24</i>
2.2.3	<i>Discharge and stream temperature.....</i>	<i>26</i>
2.2.4	<i>Precipitation.....</i>	<i>27</i>
2.2.5	<i>Air temperature.....</i>	<i>29</i>
2.2.6	<i>Groundwater temperature.....</i>	<i>31</i>
2.2.7	<i>Altitude distribution.....</i>	<i>32</i>
2.3	HYDROLOGICAL MODEL.....	34
2.3.1	<i>Introduction to MODMOD.....</i>	<i>34</i>
2.3.2	<i>Preparation of input data.....</i>	<i>36</i>
2.3.3	<i>Used Modules of MODMOD.....</i>	<i>36</i>
2.3.4	<i>Execution of the hydrological model.....</i>	<i>39</i>
2.3.5	<i>Preparation of the output data.....</i>	<i>40</i>
2.3.6	<i>Goodness of fit and parameter adaption.....</i>	<i>40</i>
2.4	STATISTICAL MODEL.....	46
2.4.1	<i>Discharge-weighted hydrology-based model.....</i>	<i>46</i>
2.4.2	<i>Linear regression model.....</i>	<i>46</i>
2.4.3	<i>Non-linear regression model.....</i>	<i>46</i>
3	RESULTS AND DISCUSSION.....	48
3.1	HYDROLOGICAL MODEL.....	48
3.1.1	<i>Comparing modelled discharge values with observed values (calibration period)</i>	<i>48</i>
3.1.2	<i>Comparing fast and slow runoff (validation period).....</i>	<i>48</i>
3.2	STATISTICAL MODEL.....	50
3.2.1	<i>Preparations.....</i>	<i>50</i>
3.2.2	<i>Model results.....</i>	<i>54</i>
3.2.3	<i>Comparison to the linear regression model.....</i>	<i>56</i>
3.2.4	<i>Comparison to the non-linear regression model.....</i>	<i>57</i>
3.2.5	<i>Comparison to the unweighted model.....</i>	<i>58</i>

4	CONCLUSION.....	64
5	APPENDICES.....	I
6	BIBLIOGRAPHY.....	IX

List of Figures

Figure 1: Diurnal cycle of air[L] and water[W] temperature at the mouth of Rasen at 9.8.1953 [Tagesgang der Luft- und Wassertemperatur an der Rasenmündung (9.8.1953)], from Schmitz (1954).....	11
Figure 2: Diurnal cycle of the water temperature of the creek Rase on 1.9.1953 at a clear summer day at various distances from the source. [Tagesgang der Wassertemperatur des Rase-Baches an einem heiteren Sommertag (1.9.1953) in verschiedener Entfernung der Quelle] from Schmitz (1954).....	12
Figure 3: Dependency of stream temperature on the distance to the source. Month August, observations in the morning. The dashed curves connect gauges of same sea level.[Abhängigkeit der Flußtemperatur von der Ursprungsentfernung. Monat August, Morgenbeobachtungen. Die strichlierten Kurven verbinden Meßstellen gleicher Meereshöhe.] from Steinhauser et al. (1960).....	13
Figure 4: Relationships between sine curve amplitude, annual mean temperature and site altitude, from Johnson (1971).....	14
Figure 5: Relationship of discharge and maximum daily river temperature, from Hockey, Owens & Tapper (1982).....	16
Figure 6: Simple regression model and logistic regression model, from Caissie (2006).....	17
Figure 7: Gauge Loich daily runoff.....	19
Figure 8: Loich basin with characteristic values.....	23
Figure 9: Daily air temperature (black) from station Frankenfels and water temperature (red) from gauge Loich.....	23
Figure 10: Basin Hofstetten.....	25
Figure 11: Gauge Hofstetten, daily mean discharge values from 1991 to 2015; dotted red line: long-term daily mean for this period (6.28 m ³ /s), blue line daily long-term daily mean from 1957 to 2015 (6.47m ³ /s).....	26
Figure 12: Gauge Hofstetten, daily mean water temperature values from 1991 to 2015.....	27
Figure 13: Area of influence of the eight precipitation stations, the scale shows the sum of the precipitation over the whole period in mm.....	28
Figure 14: Daily areal precipitation of the basin of gauge Hofstetten in mm.....	29
Figure 15: Areas of influence of air temperature stations, the scale shows the mean temperature in °C for the whole period.....	30
Figure 16: Weighted daily mean air temperature of basin Hofstetten, 1991-2015.....	30
Figure 17: Daily air temperature (black) from station St. Pölten (Autobahnmeisterei) and water temperature (red) from gauge Hofstetten.....	31
Figure 18: Monthly values of groundwater temperature at station Ochsenburg, Br 253.....	32
Figure 19: Drainage area of gauge Hofstetten categorized into eleven elevation bands.....	33
Figure 20: Model structure, modified from Holzmann et al. (2014a).....	35
Figure 21: Module 1 (Holzmann et al., 2014a).....	37
Figure 22: Module 3 (Holzmann et al., 2014a).....	37
Figure 23: Module 4 (Holzmann et al., 2014a).....	38
Figure 24: Module 5 (Holzmann et al., 2014a).....	38
Figure 25: Module 6 (Holzmann et al., 2014a).....	39
Figure 26: Module 9 (Holzmann et al., 2014a).....	39
Figure 27: Daily values of observed and modelled discharge using the starting parameter set.....	43

Figure 28: Daily values of observed and modelled discharge after 20 iterations of parameter optimization.....	43
Figure 29: Daily values of observed and modelled discharge, final parameter set....	43
Figure 30: Starting parameter set - sample year 1997.....	44
Figure 31: After 20 iterations - sample year 1997.....	44
Figure 32: Final parameter set after 51 iterations - sample year 1997.....	44
Figure 33: Monthly comparison of observed and simulated runoff values (calibration period).....	45
Figure 34: Monthly comparison of observed and simulated discharge values (validation period).....	45
Figure 35: Schematic representation of the logistic function parameters(O. Mohseni et al., 1998).....	47
Figure 36: Fast (red) and slow (blue) runoff components of the validation period (of the hydrological model).....	49
Figure 37: Fast (red) and slow (blue) runoff components of the year 2005.....	49
Figure 38: Time series of observed water temperature (gap divides calibration and validation period).....	51
Figure 39: Cross-correlation of groundwater temperature and stream temperature, highest value at lag 4 with 0.86.....	52
Figure 40: Comparison of air (AT) and groundwater (GWT) temperature.....	53
Figure 41: Cross-correlation of air and stream temperature, highest value at lag 0 with 0.98.....	54
Figure 42: Discharge-weighted model without lagged groundwater temperature (blue line: model, black dots: observed values), for the validation period.....	55
Figure 43: Discharge-weighted model with lagged groundwater temperature (blue line: model, black dots: observed values), for the validation period.....	56
Figure 44: Linear regression model (blue line: model, black dots: observed values), for the validation period.....	57
Figure 45: Non-linear regression model (blue line: model, black dots: observed values), for the validation period.....	58
Figure 46: Unweighted-discharge model without lagged groundwater temperature (blue line: model, black dots: observed values), for the validation period.....	59
Figure 47: Unweighted-discharge model with lagged groundwater temperature (blue line: model, black dots: observed values), for the validation period.....	60
Figure 48: Observed discharge (blue) and simulated discharge (red) which is split up into the fast (grey) and slow (green) component.....	61
Figure 49: Temperature distributions of air (red), groundwater (green) and stream (blue) temperature.....	62
Figure 50: Observed temperature (blue), discharge-weighted model output (red), unweighted model output (green) for the year 2010.....	63

List of Tables

Table 1: Stream structures that influence insulating and buffering characteristics, Poole and Berman (2001).....	7
Table 2: List of used stations, in bold are the cut-off points (beginning respectively ending) which limit the used period.....	26
Table 3: Precipitation stations.....	28
Table 4: Air temperature stations.....	29
Table 5: Area per elevation band.....	34

Table 6: Modules of ModMod (in bold: used for the model for this thesis).....	35
Table 7: Change of parameters due to parameter optimization.....	42
Table 8: Intercept and coefficients of the multiple linear regression model.....	56
Table 9: Parameters of the non-linear regression model.....	57
Table 10: Comparison of stream temperatures, observed values, linear regression model, discharge-weighted and unweighted model with lagged groundwater temperature (all values in °C) with closest values in bold.....	60
Table 11: Discharge components, temperature components and model results for January 2010.....	62

Appendices

Appendix I: inputmodna.txt (Gauge Hofstetten, for the validation period).....	I
Appendix II: alt_hofstn.txt.....	III
Appendix III: ALL_DATA.txt.....	III

List of Abbreviations and Symbols

GPP	Gross primary production
ER	Ecosystem respiration
CO ₂	Carbon dioxide
et al.	and others
e.g.	for example (lat. <i>exempli gratia</i>)
°C	degree Celsius
USD	United States dollar
ha	Hectare (10000m ²)
yr	Year
c.f.	compare (lat. <i>confer</i>)
USA	United States of America
UK	United Kingdom
a.s.l.	Above sea level
m	Meter
s	Second
kg	Kilogram
J	Joule
W	Watt
ANN	Artificial Neural Networks
k-NN	k-Nearest Neighbours
km	Kilometers
BMLFUW	Bundesministerium für Land- und Forstwirtschaft, Umwelt und Wasserwirtschaft (Federal Ministry of Agriculture, Forestry, Environment and Water Management) [now: BMNT]
BMNT	Bundesministerium für Nachhaltigkeit und Tourismus (Federal Ministry of Sustainability and Tourism)
mm	Milimeters
Lat	Latitude
Lon	Longitude
d	Day
HZB	Hydrographisches Zentralbüro (Hydrographical Central Office)
HZB no.	Number of gauge (assigned by the HZB)
DEM	Digital elevation model
SRTM	Shuttle Radar Topography Mission
GIS	Geographic Information System
GRASS	Geographic Resources Analysis Support System
GDAL	Geospatial Data Abstraction Library
IDE	Integrated development environment
K	Kelvin
API	Antecedent Precipitation Index
ψ	Runoff coefficient
NSE	Nash-Sutcliffe Efficiency
KGE	Kling-Gupta Efficiency
ED	Euclidian distance
n.b.	note well (lat. <i>nota bene</i>)

1 Introduction and literature review

This thesis consists of four parts. At first, the importance of water temperature as an environmental and economic factor will be considered, the factors which influence stream temperature will be described and an overview of stream temperature models will be given. The second part focusses on the methodology and is titled accordingly. In the third part, “Results and Discussion”, the results of the model and a comparison to other models are presented. In the fourth part “Conclusion”, these findings are put into a wider context.

1.1 Importance of water temperature

1.1.1 Environmental relevance

Water temperature is vastly important for aquatic environments¹. Water temperature influences these ecosystems in a variety of ways, it affects biological processes e.g. organism growth rate, organism metabolism or organism behaviour (Lillehammer, Brittain, Saltveit, & Nielsen, 1989), (Kingsolver, 2009), (Poertner & Peck, 2011). Rising water temperatures accelerate chemical processes (European Environment Agency, European Commission, & World Health Organization, 2008), (Schulte, 2011), the Arrhenius equation states that for an increase of 10 °C the rate of chemical reactions is doubled (Delpla, Jung, Baures, Clement, & Thomas, 2009). Higher water temperatures lead to higher gross primary production (GPP)² of rivers but also to higher ecosystem respiration (ER)³, where GPP is increasing faster with rising temperature than ER. This means that habitats downstream get lower nutrition, potentially avoiding eutrophic conditions, at the cost of emitting more CO₂ to the atmosphere (Demars et al., 2011). Rising groundwater temperatures could lead to more salinity as there is more evaporation and more intensive water-rock interaction also described by the Arrhenius equation (European Environment Agency et al., 2008).

¹ As this thesis is concerned with the modelling of stream temperature, only fresh water in lotic systems and groundwater will be explicitly considered.

² The GPP represents the total biomass generated by primary producers

³ The ER represents the sum of respiration of all living organisms of a particular ecosystem

1.1.1.1 Fish

The next few paragraphs will deal with the impact of temperature on fish. The literature on how water temperature impacts fish is more abundant than for other species.

For fish, there are several thermal limits of growth. The temperature range for short term survival is much wider than the temperature range where somatic growth is possible and the range for reproductive development is even narrower (Jobling, 1997). Most fish are poikilothermic⁴ ectotherms⁵ which means that their body temperature fluctuates with the external temperature of their environment (Schulte, 2011).

Rising temperatures may result in the loss of habitat for e.g. bull trout, and even moderate temperature changes may have large negative effects, as medium and large habitat patches are getting lost faster than general habitat area, which means mainly smaller (less valuable) ones remain (E. Rieman et al., 2007).

Rising temperatures and the corresponding thermalscapes⁶ will determine and confine especially the habitat of cold-water-species. Cold water could be used as a climate shield which can attenuate harming effects of rising temperatures by providing so-called climate refugia. To forecast climate refugia one has to overlay biological datasets, temperature maps and habitat occupancy models (Isaak, Young, Nagel, Horan, & Groce, 2015). These potential refugia raise hope, especially when the temperature can be kept stagnating because, as Crozier, Zabel, Hockersmith, & Achord (2010) show, rising temperatures exacerbate the negative effects which high population densities have on growth.

Even as temperature changes can directly influence the growth processes of fish, it should not be considered without taking food availability into account, which is also an important factor in growth (Crozier et al., 2010). Rice, Breck, Bartel, & Kitchell (1983) make the same point, linking growth patterns of thin bass primarily to seasonally variable consumption instead of temperature.

The next section will look at other freshwater organisms which are of course also affected by water temperature (Webb, Hannah, Moore, Brown, & Nobilis, 2008).

⁴ Organisms whose body temperature varies (“poikilos”: Greek for “varied”).

⁵ Organisms whose body temperature is dependent on the temperature of the environment (“ektós”: Greek for “outside”)

⁶ A connected network of streams with sufficient thermal quality where the probability is high that fish populations can be maintained under rising temperatures because of climate change.

1.1.1.2 Other freshwater organisms

Each plant species has its own optimal temperature or optimal temperature range, which differ seasonally and geographically. Growth accelerates when approaching the optimum and often drastically declines when it is exceeded (Carr, Duthie, & Taylor, 1997).

In cold glacial-fed (kryal) streams only some algae and aquatic mosses are present and fauna is also sparse. Even though in such habitats there is a paucity of nutrition and generally rough living conditions, the most important factor for the small number of taxa is probably the temperature. In krenal streams, which are fed by groundwater, the relatively constant thermal (more specifically: physicochemical) conditions may be the reason for the reduced diversity of insects.⁷ The higher variability of physicochemical conditions in rhithral (snowmelt-fed) streams allows for more diversity of fauna and flora. If the conditions are too extreme though, this changes and krenal streams may be more species-rich (Ward, 1994).

In low mountainous small streams mean temperatures are highly correlated with insect composition (for medium-sized streams the correlation is much smaller), while maximum temperatures are connected to species growth. Temperature is apparently at least partly responsible for quantitative differences in small and medium streams (Haidekker & Hering, 2008).

Ward and Stanford (1982) found that many aquatic insects are able to grow at or just above 0 °C (which suggests that their ancestral populations originated in cold headwater habitats.)

What has to be kept in mind though, is that Hawkins, Hogue, Decker, & Feminella (1997) showed that assemblage structure of common insect taxa is more influenced by sampling date than by stream temperature.

1.1.2 Economic relevance

As seen above (section 1.1.1) water temperature influences the rate of chemical reactions and consequently the gross primary production and ecosystem respiration which obviously has economic impacts. (Costanza et al. (1997) estimate an average global value of lakes and rivers of 41 USD ha⁻¹ yr⁻¹ for food production alone.) More specifically, water temperature influences the quality of drinking water – rising water temper-

⁷ Probably because to initiate life cycle events most insects need external trigger events.

ature leads to a higher risk of waterborne disease which indirectly has high economic costs (McMichael, Woodruff, & Hales, 2006), (Hunter, 2003).

Some other (socio-)economic areas which are directly or indirectly affected by water temperature are recreation, tourism, thermoelectric power production, drinking water production and fishing (Hannah & Garner, 2015). The next subsections will look at the last three points, as there is indeed an abundant literature about climate change and tourism and recreation(c.f. Haas et al. (2018), Pröbstl et al. (2008) or Hamilton, Madison, & Tol (2005), to name a few), but there is not much literature with a specific regard to water temperature and tourism.

1.1.2.1 Thermoelectric power production

Climate change induced discharge reduction will lead to struggles for water distribution between different sectors, also affecting the thermoelectric power sector where water is used to cool the plants. The cooling water is not consumed but discharged back into the river, albeit with a higher temperature (Foerster & Lilliestam, 2010). In countries where thermoelectric power plants are obliged to comply with water quality regulations (concerning water temperature) water use could be severely restricted as water temperatures are continuing to rise (European Environment Agency, 2008). Electricity prices are projected to rise for most European countries as electricity production gets more expensive because of the need of adapting power plants to rising water temperatures⁸ (van Vliet, Vögele, & Rübhelke, 2013). The need to adapt power plants show van Vliet et al. (2011) as a projected rise of 4 °C in air temperature and a reduction of discharge of 40 % led to 104 days per year where power plants would have to be shut down because the legally permissive maximum temperature for cooling would be exceeded.

1.1.2.2 Quality of drinking water

Again it has to be pointed out that water temperature controls the rate of chemical reactions and is thereby a crucial factor for the quality of drinking water, particularly important are the accelerated growth rates of microorganisms (World Health Organization, 2017) and the temperature induced reduction of the concentration of dissolved gases, like oxygen (Delpla et al., 2009).

⁸ Hydro-power plants also play a role here as they are affected by decreasing discharge.

In areas where rivers or river-fed groundwater are the main sources of drinking water, high water temperature can lead to worse bank filtration because of higher algae growth, leading to problems with water quality. In hot summers, Dutch drinking water companies are struggling with keeping the water temperatures below 25°C to secure biologically safe water production (Ramaker, Meuleman, Bernhardt, & Cirkel, 2005)

1.1.2.3 Fishing

As showed above in section 1.1.1.1, fish are severely affected by changes in water temperatures. Because fish are easily harvested or produced, they are vital in developing countries where they are used as protein supplier for billions of people. In industrialized countries fish is not as elemental for nutrition but the disappearance of recreational fisheries e.g. because of a climate change induced alteration of the fish assemblage (Pletterbauer, Melcher, Ferreira, & Schmutz, 2015) may result in high economic costs (Ficke, Myrick, & Hansen, 2007).

After looking at the relevance of water temperature, the next section covers the factors which are influencing water temperature.

1.2 Influencing factors on stream temperature

Stream temperature is influenced by the amount of energy delivered to the stream and the internal structure of the stream which determines the distribution of the temperature in-stream.

The major factors for stream temperature can be grouped into external, mostly climatic drivers and internal structure like stream morphology, groundwater and riparian vegetation (Poole & Berman, 2001). There are two subsections for each of the mentioned groups. A third subsection deals with human influences on stream temperature.

1.2.1 External temperature drivers

External drivers control how much energy is delivered to the stream. The most important drivers can be summarised under “climatic drivers” which are described in this subsection, the specific drivers which naturally often influence each other are in bold.

The most important external driver by far for stream temperature is the (short wave) **solar radiation**. It is influenced by **cloud cover** and **solar angle** and can averagely account for 70% of the incoming energy⁹ (Webb et al., 2008). Other major factors are the (net) **long-wave radiation** and **evaporation**, which are both comparable in size but considerably smaller than the short wave radiation (Caissie, 2006). Even smaller in size, but still important, is the **convection**, driven by temperature differences between the water temperature and the **air temperature** and heavily influenced by **wind speed** and **relative humidity** of the air (S. L. Johnson, 2004). Though contributing, **precipitation** is less relevant compared to the factors above (Pletterbauer, Melcher, & Graf, 2018).

1.2.2 Internal structure of the stream

This subsection and the next rely heavily on Poole & Berman (2001). Internal structures like stream morphology, groundwater and riparian vegetation account for the resistance of the stream against heating or cooling, see Table 1.

⁹ Even up to 99% of the incoming energy in Antarctic meltwaters.

Table 1: Stream structures that influence insulating and buffering characteristics, Poole and Berman (2001)

Component and characteristic	Determined by	Ecological influence over
Channel		
Slope	catchment topography	flow rate
Substrate	flow regime, sediment sources, stream power	resistance to groundwater flux; channel roughness and therefore flow rate and thermal stratification
Width	flow regime, sediment sources, stream power, bank stability	surface area for convective heat exchange
Streambed topography	flow regime, sediment sources, stream power, bank stability, large roughness elements (e.g., large woody debris)	gradients that drive hyporheic flux
Pattern	flow regime, sediment sources, stream power, bank stability, large roughness elements, valley shape	gradients that drive hyporheic flux; potential shade from riparian vegetation
Riparian zone		
Vegetation	flow regime, vegetation height, density, growth form, rooting pattern	shade to reduce solar radiation; windspeed, advective heat transfer, conductive heat transfer; bank stability
Width	(same as channel pattern)	potential for hyporheic flux; potential for shade
Alluvial aquifer		
Sediment particle size	(same as channel substrate)	potential for hyporheic flux
Sediment particle sorting	(same as channel substrate)	diversity of subsurface temperature patterns by determining stratigraphy; extent of hyporheic flux
Aquifer depth	(same as channel pattern)	extent of hyporheic flux

1.2.2.1 Stream morphology

Water temperature in the channel is dependent on heat load and discharge, properties of the channel which influence these two have influence on the water temperature. Slope is another factor which influences discharge and the stream pattern, which in turn affects the hyporheic flux on different spatial levels and the impact of the riparian vegetation, see below. Substrate controls the stream temperature by influencing the groundwater flux, see the subsection groundwater. The channel width is important as it controls the influence of the riparian vegetation on the stream, see the subsection riparian vegetation. The greater the width of the channel, the more intense is the heat exchange between stream and atmosphere, allowing the river to absorb more heat. Channels with intricate streambed topography have a higher rate of flows between the channel and the aquifer (hyporheic flows) which may, similarly to “normal” groundwater act as a thermal buffer (Poole & Berman, 2001).

1.2.2.2 Groundwater

Groundwater can be recharged at different times and keep to a certain degree the thermal characteristics of this period. When cool groundwater (recharged in the cooler

periods of a year) feeds into the stream, the heat content is diluted and thus the water temperature decreases. When the groundwater constitutes a substantial volume of the stream it can function as a strong buffer against warming, especially when the cold groundwater influx occurs at a time when the air temperature influenced stream temperatures are highest. Conversely, when the recharging appears in the warmer periods of the year, the temperature can possibly even increase (Poole & Berman, 2001).

1.2.2.3 Riparian vegetation

The riparian vegetation reduces the amount of heat reaching the stream by shadowing it, this effect is stronger at narrower streams than at wide ones. Vegetation also reduces the heat exchange between the stream and the surrounding environment by reducing wind-speed and thus insulating it (Poole & Berman, 2001).

1.2.3 Human influence on stream structures

This subsection also relies heavily on Poole & Bermann (2001) and only looks at the human influence on stream structures, although humans also have some influence on climatic drivers (McMichael et al., 2006).

1.2.3.1 Dams

Dams influence the water temperature directly downstream of the dams. As there is water temperature stratification over the depth of the reservoir, the temperature of the outflow depends on the location of the outlet. Water temperature is also affected by the discharge reduction as the stream loses (part of) its thermal assimilative capacity and the hyporheic flow loses its ability to buffer temperature fluctuations.

1.2.3.2 Water withdrawals

As with dams, water withdrawals lead to reduced discharge with all the consequences mentioned above. If water is returned to the stream it has often a much higher temperature. Soil water which is removed by tile drainage is fed back into the river, but often at higher temperatures, as the pipes of the drainage may be routed above ground. A third case of water withdrawals are wells, which if used excessively can deplete groundwater bodies, lower the groundwater table and thus reduce the ability to buffer water temperature.

1.2.3.3 Channel engineering

Channel engineering which aims to inhibit lateral flow is responsible for a reduced exchange between channel and aquifer and thus reduced buffering capacity.

1.2.3.4 Removal of vegetation

As written above, riparian vegetation is paramount for insulating narrow channels by reducing direct solar radiation and wind speed and by trapping air. Removing it not only removes these insulating features, but can also lead to more soil erosion and an influx of fine sediments which may alter the permeability of the river bed with all its consequences (see above).

1.3 Overview of stream temperature models

The following subsections will summarize the most relevant literature on the history of stream temperature models using the five available review papers which are introduced below as starting points.

Smith (1972) gives an overview of the underlying physical processes and human impacts on thermal pollution and only shortly touches water temperature modelling.

Ward (1985) notes that there is a paucity of data outside the USA, Europe and Japan and that there is only one review paper (the one from Smith, mentioned above) dealing with the thermal conditions of lotic environments. He consequently focusses on the Southern Hemisphere looking at influences on the thermal regime and anthropogenic factors, mentioning water temperature only incidentally. He concludes, based on the scarce data, that “it would appear that *the distinctiveness of Southern Hemisphere lotic ecosystems is one of degree and not of kind.*” (Ward, 1985; emphasis in original). By showing the multitude of factors which influence the thermal regime, Ward (1985) is one of the papers which led to the conclusion that the thermal regime of rivers is too complex to be sorted into neat categories by simple criteria, an assumption which was under scrutiny since the 1970s.

Twenty-one years later, Caissie (2006) looks at the natural processes which affect water temperature and presents several different approaches to water temperature modelling. He gives an overview of how human activities can influence the rivers’ thermal regime.

Webb et al. (2008) review the literature since 1990 focussing on the gained understanding of fundamental controls of water temperature, heterogeneity, human impacts and past and future trends. They merely touch on water temperature modelling, referring to Caissie (2006) for more information.

Hannah and Garner (2015) although focussing on the United Kingdom, look at research worldwide to put the situation in the UK into a global context. They describe the underlying dynamics of water temperature and how water temperature has and probably will change.

The next subsection will deal in more detail with the development of water temperature models, drawing mainly on the aforementioned review papers as a baseline.

1.3.1 Ca. 1900 to the 1970s – (Smith, 1972)

The first studies on water temperature have been concerned with measuring rather than modelling it. Pioneer A. E. Förster (as cited in Smith, 1972) in his dissertation (published 1894) focussed on observing the water temperature in lotic systems in Central Europe. At the beginning of the 20th-century stream temperature research was based in Central and Northern Europe, with later research emerging from the USA and Japan (Smith, 1972). As the factors influencing stream temperature are quite complex (see above), efforts were made to simplify the models. One such attempt is to condense these several factors into just one, namely air temperature and then look at the relationship between it and the water temperature. This approach was used for example in Japan by Miyake and Takeuchi (1951 as cited in Smith, 1972) who used long-term air temperature data. In general researchers in Europa and Japan in this period relied more on analysing long-term data than researchers in the UK and the USA. In Germany Schmitz (1954) also looked at the relation of air and water temperature, see Figure 1 and the change of water temperature when moving further away from the source, see Figure 2.

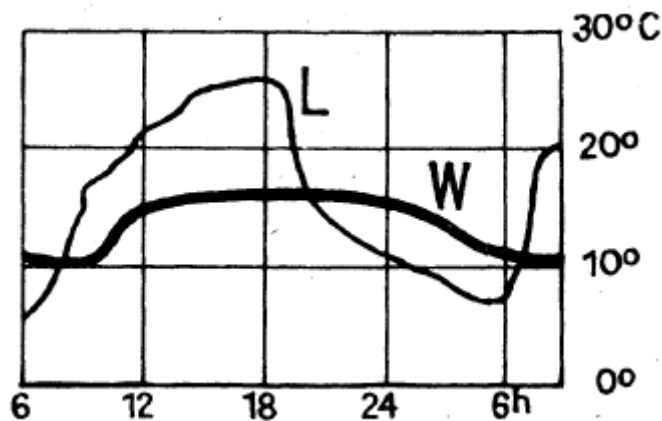


Figure 1: Diurnal cycle of air[L] and water[W] temperature at the mouth of Rasen at 9.8.1953 [Tagesgang der Luft- und Wassertemperatur an der Rasenmündung (9.8.1953)], from Schmitz (1954)

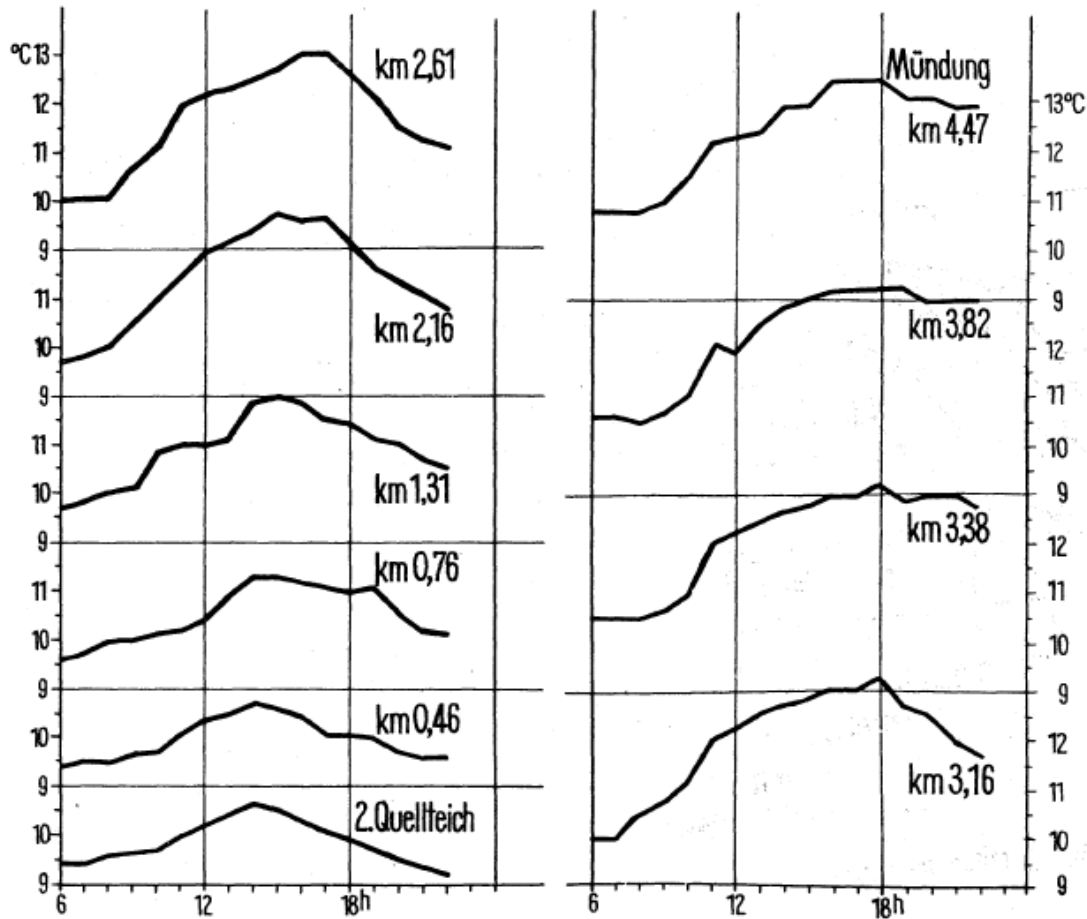


Figure 2: Diurnal cycle of the water temperature of the creek Rase on 1.9.1953 at a clear summer day at various distances from the source. [Tagesgang der Wassertemperatur des Rase-Baches an einem heiteren Sommertag (1.9.1953) in verschiedener Entfernung der Quelle] from Schmitz (1954)

In similar vein some efforts were made to categorize rivers by altitude, in Japan by Kurashige (1934, as cited in Smith, 1972) who included air-water-temperature correlations or in Austria by Steinhauser, Eckel, & Lauscher (1960) who describe a weak relationship between m a.s.l and water temperature for different rivers, see Figure 3.

Starting in the 1940s more complex heat budget approaches were carried out. In Austria Eckel & Reuter (1950) found an iterative graphical solution for a differential equation model with physical input parameters for stream temperature estimation, in Japan Nishizawa (1966 and 1967 as cited in Smith, 1972) modelled heat balance processes.

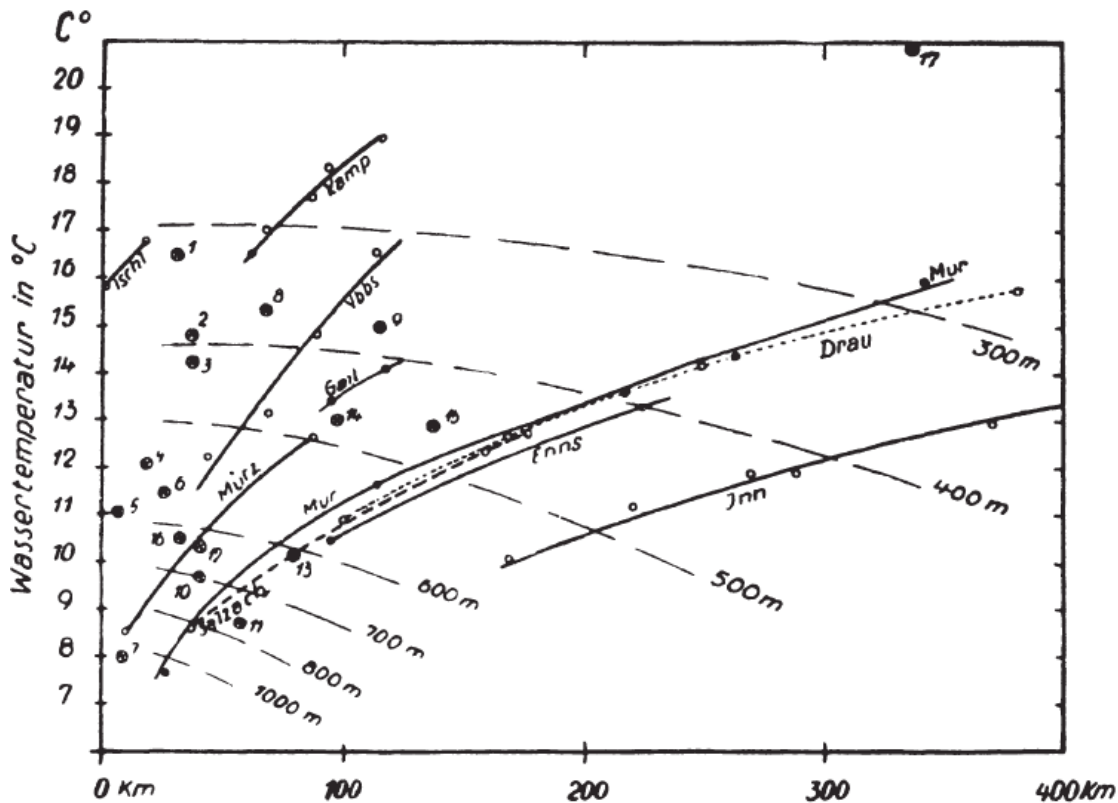


Figure 3: Dependency of stream temperature on the distance to the source. Month August, observations in the morning. The dashed curves connect gauges of same sea level. [Abhängigkeit der Flußtemperatur von der Ursprungsentfernung. Monat August, Morgenbeobachtungen. Die strichlierten Kurven verbinden Meßstellen gleicher Meereshöhe.] from Steinhauser et al. (1960)

In the USA statistical models were designed which use harmonic analysis (Ward, 1963 and Collins, 1969 as cited in Smith, 1972), other models which use the net rate of heat exchange, more specifically the equilibrium temperature and exchange coefficient (Edinger, Duttweiler, & Geyer, 1968), and models which use several (micro)meteorological input parameters. Brown (1969) used e.g. barometric pressure, thermal radiation, wind speed air temperature and humidity, and Morse (1970) additionally used cloud cover. A picture started to emerge, in which stream temperature is of much more complex nature than previously assumed. This led eventually to the discontinuation of attempts to categorize the thermal regime of rivers in the 1980s.

1.3.2 1970s to mid-1980s – (Ward, 1985)

The paper by Ward (1985) sheds some light on the developments concerning mainly the drivers of stream temperature and the human influence on it, since the last review paper 15 years earlier. None-the-less, there are some references to stream temperature modelling. As the next paragraphs focus on the Southern Hemisphere like Ward, there

will be no literature about Europe, Japan and the USA – as a matter of fact, the only studies in this review which deal with water temperature modelling were conducted in Australia and New Zealand. For example Johnson (1971) uses a method proposed by Ward to fit sine curves to monthly water temperature data of six streams, see equation (1).

$$T = a * \sin(bx + c) + \bar{T} \quad (1)$$

With:

- T = stream temperature °C on any given day x
- a = Amplitude of the sine curve °C
- b = 0.987°/day
- x = Number of days since 1st November (Nov. 1st x= 1)
- c = Phase coefficient of the sine curve in degrees
- \bar{T} = Annual mean daily temperature °C

He relates (among other things) altitude to sine curve amplitude and annual mean water temperature, respectively, see Figure 4.

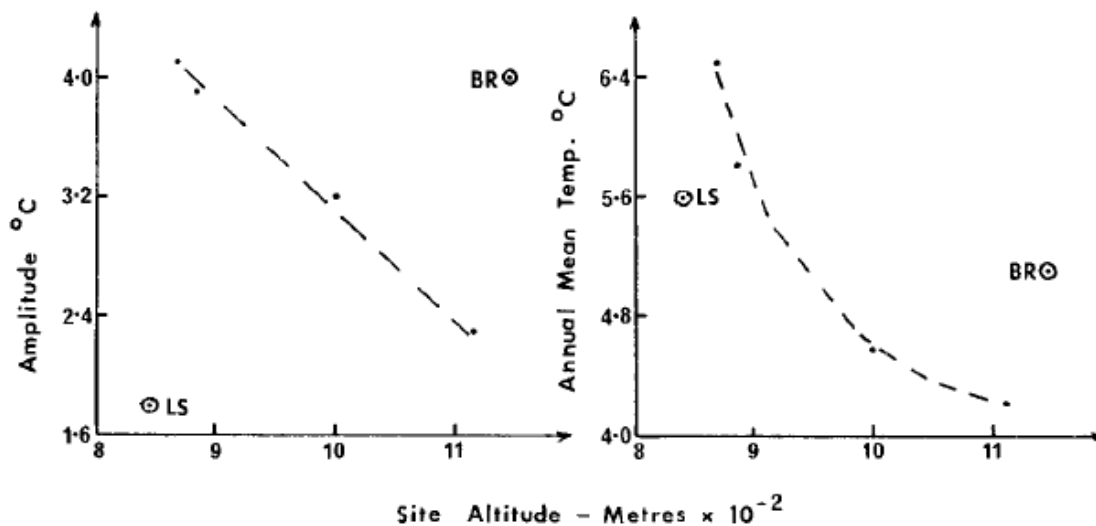


Figure 4: Relationships between sine curve amplitude, annual mean temperature and site altitude, from Johnson (1971)

He also looks at the correlation of air and water temperature and concludes that for water temperature estimation one has also to take topographic characteristics into account.

This is what Walker and Lawson (1977) do, by designing two models which use either both, air temperature and altitude or the water temperature upstream to predict water temperatures in a catchment in Victoria, Australia. The first model is described

by equations (2), (3) and (4), the second model is the same in principle but uses water temperature instead of air temperature.

$$T_w = a_0 + a_1 * T_a \quad (2)$$

$$a_0 = 0.3075 + 0.0122 \Delta a + 0.0001993 \Delta a^2 \quad (3)$$

$$a_1 = 0.8944 - 0.0017 \Delta a + 0.0000124 \Delta a^2 \quad (4)$$

With:

- T_w = water temperatures
- a_0, a_1 = coefficients
- T_a = air temperature
- Δa = difference in elevation (m) between used air temperature station and the water temperature station.

Grant (1977) uses stepwise regression to model the maximum water temperature of a stream in New Zealand using the air temperature of the same day and the day before, see equation (5).

$$Max WT(d) = 0.31 Max AT(d) + 0.55 Max AT(d-1) + 1.2 \quad (5)$$

Hockey, Owens & Tapper (1982) utilize two models, a statistical and a physical model, see equations (6) and (7), respectively.

$$T_w = 12.6 + 0.31 T_a(max) - 1.5 \ln(Q) \quad (6)$$

With:

- T_w = water temperature
- $T_a(max)$ = maximum daily air temperature
- $\ln(Q)$ = natural logarithm of discharge

$$\frac{dT}{dt} = \frac{\phi^*(T)}{\rho c_p h} \quad (7)$$

With:

- T = river temperature ($^{\circ}C$)
- t = time (s)
- ρ = river water density (kg/m^3)
- c_p = specific heat of river water ($J kg^{-1} ^{\circ}C^{-1}$)
- h = mean river depth (m)
- $\phi^*(T)$ = river surface temperature exchange (W/m^2), a function of T

In the statistical model of Hockey et al. discharge and air temperature explain 30% and 50%, respectively, of water temperature variance of a New Zealand stream. Their physical model which used an energy balance equation predicts for lower flows a decrease of maximum water temperature by 0.1°C per $1 \text{ m}^3/\text{s}$ increase of discharge, see Figure 5.

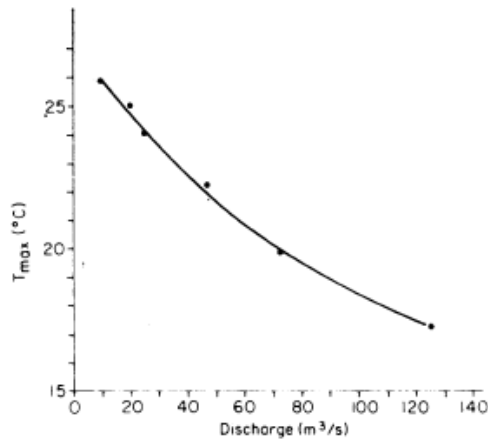


Figure 5: Relationship of discharge and maximum daily river temperature, from Hockey, Owens & Tapper (1982)

The scarcity in predictive modelling of Southern Hemisphere rivers probably lies in their perceived unpredictability as annual stream temperatures of Australian rivers are called unpredictable by nature (when compared to streams of the Northern Hemisphere) by Lake (1982 as cited in Ward, 1985), an assessment which Ward does not share, see his quote above, in section 1.3.

1.3.3 Mid-1980s to mid-2000s – (Caissie, 2006)

Caissie (2006) gives an overview over past discoveries of influences on water temperature, from the equilibrium temperature where the average water temperature equals the average air temperature (Macan, 1958) to altitude and aspect (Hynes 1960, as cited in Caissie, 2006), timber harvesting (Brown and Krygier, 1967 as cited in Caissie, 2006), to peak flow and snowmelt (Smith, 1975).

Caissie categorizes water temperature models into three groups, deterministic, stochastic and regression models. Regression models are further divided into linear, multiple and logistic regression models, with examples given for each subcategory. Linear models use air temperature as the input parameter and are applied widely at timescales where the water temperature is not autocorrelated, which is mostly the case at weekly and monthly timescales. Slope and intercept of the linear regression change

with different timescales. The slope increases with increasing timescale (H. G. Stefan & Preud'homme, 1993, among others) and different stream types, streams which are not dominated by groundwater have steeper slopes than groundwater-dominated streams (Erickson & Stefan, 2000 and Mackey & Berrie, 1991 both as cited in Caissie, 2006), see Figure 6.

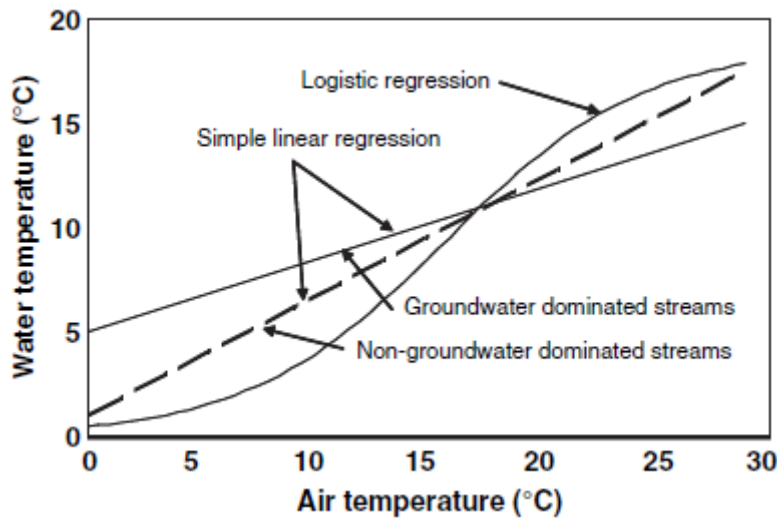


Figure 6: Simple regression model and logistic regression model, from Caissie (2006).

Multiple regression models use more than one parameter for water temperature prediction, for example air temperature and altitude (Walker & Lawson, 1977), see above, or air temperature, solar radiation and depth of water (Jeppesen & Iversen, 1987, as cited in Caissie, 2006).

Mohseni et al. (1998) found that a logistic regression describes the relationship of air and water temperature better at very low and high temperatures where this relationship is not linear because of water freezing at about 0 °C and evaporative cooling at increasing temperatures. See section 2.4.3 for the equation used by Mohseni et al. The logistic regression model is mostly used at a weekly timescale – there were no research found which used monthly time steps¹⁰, probably because the evaporative cooling is averaged out (Caissie, 2006) and logistic regression shows poor performance at daily time steps (Caissie, El-Jabi & Satish, 2001 as cited in Caissie, 2006).

For daily time steps stochastic or deterministic models can be used. Stochastic models are more simple, they just use air temperature as the input parameter and decompose the time series into long-term and short-term components. The long-term component can be described with a sinusoidal or Fourier series and represents the sea-

¹⁰ This thesis applies a logistic regression on a monthly timescale non-the-less, to be able to compare the output to other kinds of models, see section 4.3

sonality of the annual cycle, the short-term component represents the deviations from the seasonality and can be modelled with a Markov process (Caissie, 2006).

Deterministic models need meteorological and hydrological data as input. They mathematically describe the underlying physics of the heat exchange between river and environment. The whole energy flux is described and then water temperature changes are modelled according to energy flux changes (Caissie, 2006). Early deterministic water temperature models focussed solely on the air/water surface to quantify energy fluxes (Marcotte & Duong, 1973 as cited in Caissie, 2006), later models started to also take the river bed into account (Sinokrot & Stefan, 1993), see equation (8).

$$\frac{\partial T}{\partial t} = -U \frac{\partial T}{\partial x} + D_L \frac{\partial^2 T}{\partial x^2} + \frac{S}{\rho c_p d} \quad (8)$$

With:

- T = water temperature
- t = time
- x = streamwise distance
- D_L = dispersion coefficient in the direction of flow (x-direction)
- S = source or sink (includes heat transfers with the surrounding environment)
- U = mean channel velocity
- d = mean channel depth
- ρ = density of water
- c_p = specific heat of water

For daily and hourly data deterministic models are similarly precise as stochastic models, for hourly the river bed becomes more important for getting good results. Deterministic models are more complex but they benefit from the possibility of simulating specific scenarios (Benyahya, Caissie, St-Hilaire, Ouarda, & Bobée, 2007). Deterministic models can be carried out multidimensional in contrast to regression and stochastic models which can only be applied to specific sites (zero-dimensional). The most used deterministic model is the one-dimensional model, where the water temperature is modelled longitudinally (Caissie, 2006).

Benyahya et al. (2007) refine the classification of statistical models, they categorize them in two subclasses, parametric and non-parametric. The parametric models can be further divided into regression models and stochastic models, both have been described above.

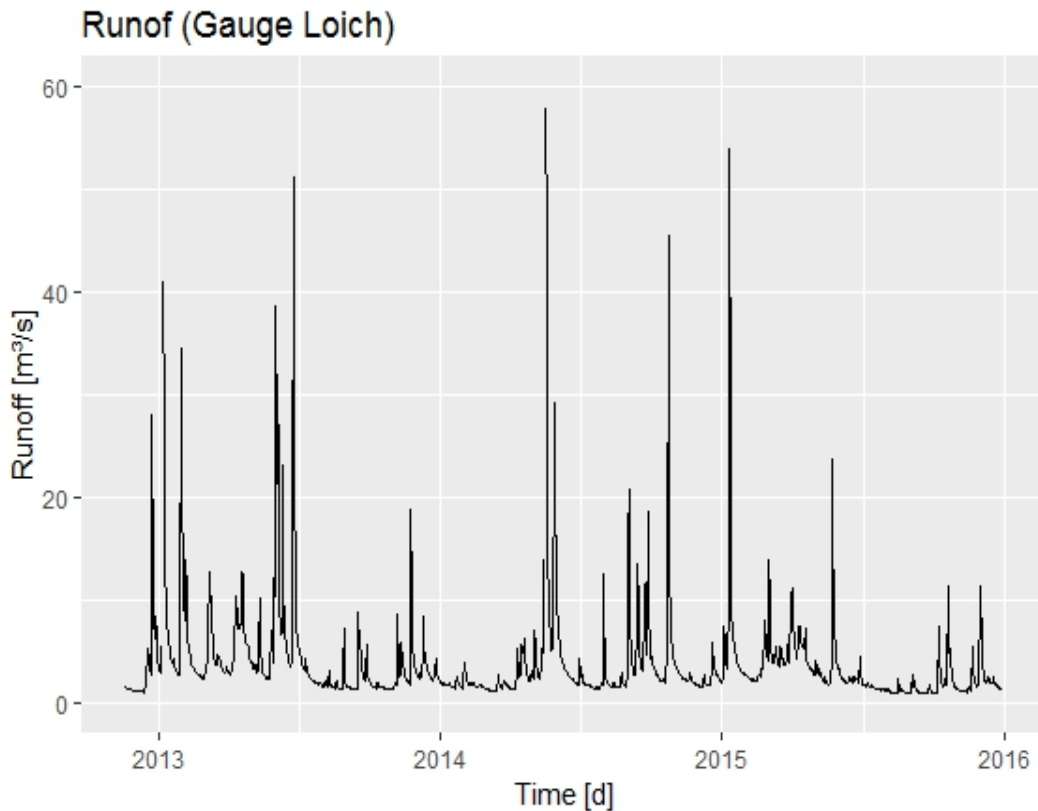


Figure 7: Gauge Loich daily runoff

The non-parametric models differ from parametric models as their model structure is not predefined by the modeller but relies mostly on the data. These models “learn” from past values and cannot be used to predict values outside the range of the pre-existing values. Benyahya et al. (2007) give two examples for non-parametric models, Artificial Neural Networks (ANN) and k-Nearest Neighbours (k-NN). ANN result in similar results as linear regression (Olden and Jackson, 2002 as cited in Benyahya et al., 2007) and k-NN give similar results as a periodic autoregressive model (Benyahya, St-Hilaire, Ouarda, Bobée, & Dumas, 2008).

1.3.4 Interlude – (Webb et al., 2008)

Published shortly after Caissie (2006) Webb et al. (2008) skip treatment of temperature modelling (and also biological processes) and decide to focus on areas not covered by Caissie, namely “to identify current interests, advances in understanding and potentially profitable directions for future studies.” (Webb et al., 2008)

They note that there is currently (2008) more interest in describing past trends than in projecting future trends but also that this may change with increasing concern about how temperature is affected by climate change.

1.3.5 Mid-2000s to mid-2010s – (Hannah & Garner, 2015)

Hanna & Garner (2015) review the literature dealing with future water temperature trends and find that the most extensive studies have been conducted in North America. They describe a study by van Vliet et al. (2011) who adapted the formula from Mohseni et al. (1998), see above, by including a discharge term additional to air temperature which resulted in an improved model for 87% of the stations. Two years later a deterministic model was applied to predict global river water temperatures from 2071-2100 in comparison to 1971-2000 (Van Vliet et al., 2013a as cited in Hannah & Garner, 2015). The period of the 2050s to the 2080s was modelled by using a deterministic model which found that changes in river water temperature were driven mainly by discharge, with winter and early spring temperatures decreasing and summer and late spring water temperatures increasing (MacDonald et al., 2014 as cited in Hannah & Garner, 2015).

1.4 Aim of this thesis

It is assumed that the water temperature of a river is dependent on air temperature and, to a lesser extent, on the composition of discharge.

Air temperature is a proxy for the solar radiation and many studies have shown a close relationship between air and water temperature for longer (weekly or monthly) timescales.

The discharge of a river can come from several sources, e.g. groundwater, melting water, surface flow or subsurface flow (Sun, Chen, Li, & Li, 2016). These runoff components have different volumes and different temperature distributions. This concept will be simplified by assuming that the runoff of a river can roughly be divided into two components, a slow component and a fast component. A simplified conceptual water balance model is used to estimate these two components.

The fast component represents the overland flow and fast subsurface runoff which are influenced by the highly fluctuating air temperature. The air temperature will be obtained from several stations in or near the catchment area. The slow component represents the groundwater flow with an associated temperature which will be obtained

from a groundwater temperature station near the catchment area. It has a lower frequency and a smaller amplitude than the air temperature.

In conclusion, the hypothesis of this thesis is that the knowledge of the size of contributing runoff components and their respective temperature distributions improves the estimation of stream temperature.

2 Methodology

2.1 Introductory remarks

Modelled discharge data and temperature data were combined to estimate stream water temperature of the Pielach river at the gauges Loich and Hofstetten.

Input datasets (Air temperature, water temperature, groundwater temperature, discharge, precipitation) came from the Office of the Provincial Government of Lower Austria, specifically the Department of Hydrology and Geoinformation, from ehyd.gv.at and the “H2O Fachdatenbank”. For modelling the discharge data, the hydrological model BOKU_ModMod (Holzmann, Massmann, & Stangl, 2014b) was used. For pre- and post-processing the data the programming language R was used.

2.2 Study area and data

The study area comprises the catchment area of the upper course of the Pielach river. It is located in the Mostviertel, in the south-western quarter of Lower Austria. For the purposes of the water legisprudence the Pielach is situated in the sub-basin of the Danube between the rivers Enns and March. The Pielach river originates in the “Schwarzenbachgegend” at an elevation of about 950 m a.s.l. (Hemsen, 1967) and runs 69 km where it joins the Danube at 208 m a.s.l. (Mandlbürger, Hauer, Wieser, & Pfeifer, 2015). It reaches stream order 4 according to Strahler (Melcher & Schmutz, 2010). The entire catchment area is 593.1 km² (BMLFUW, 2014).

2.2.1 Gauge Loich

At the river Pielach there are two gauges which record water temperature, the gauge Loich at km 53.60 with a catchment area of 144.5 km² (BMNT, 2018b) and the gauge Hofstetten at km 36.10 whose catchment area is approximately twice as large (BMNT, 2018a). The gauge Loich was established in August 2011, its basin can be seen in Figure 8 and the daily runoff in Figure 7. The relationship between the daily water temperature and the daily air temperature (of the nearby weather station Frankenfels) is made visible in Figure 9. To get accustomed to the hydrological modelling process with ModMod, the gauge Loich was used in a first test run, because of its smaller catchment area and its shorter associated time series. The model structure was defined a priori and under theoretical considerations of the properties of the basin.

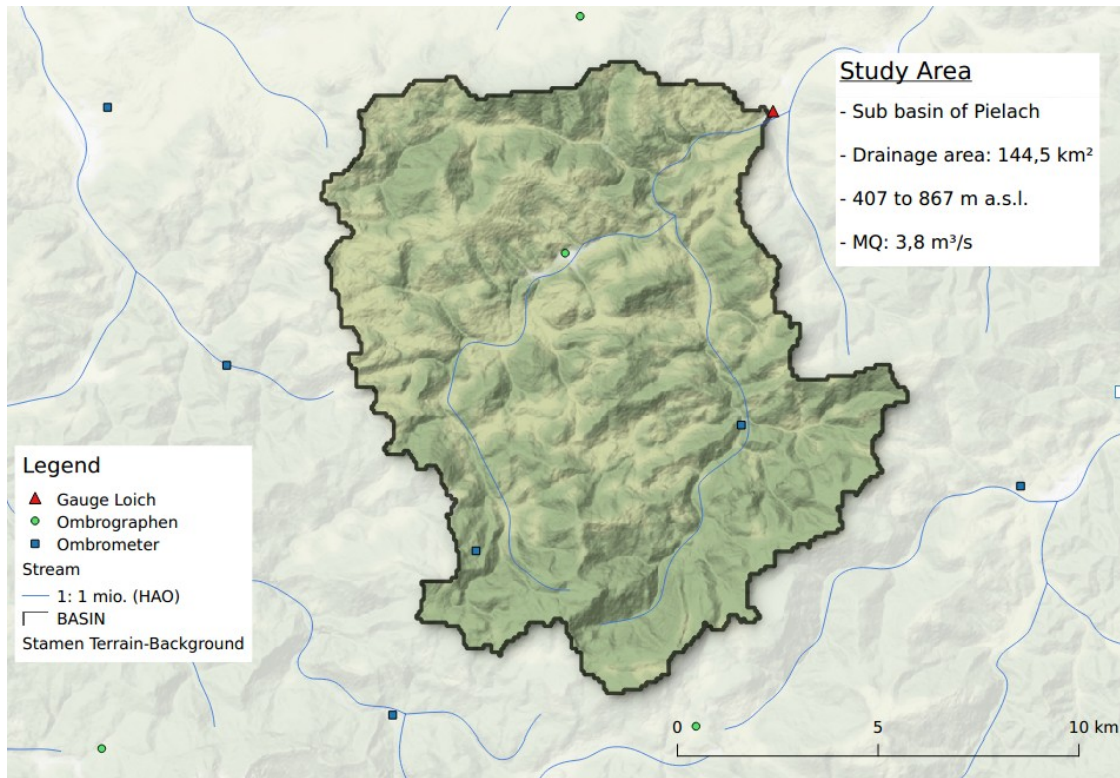


Figure 8: Loich basin with characteristic values

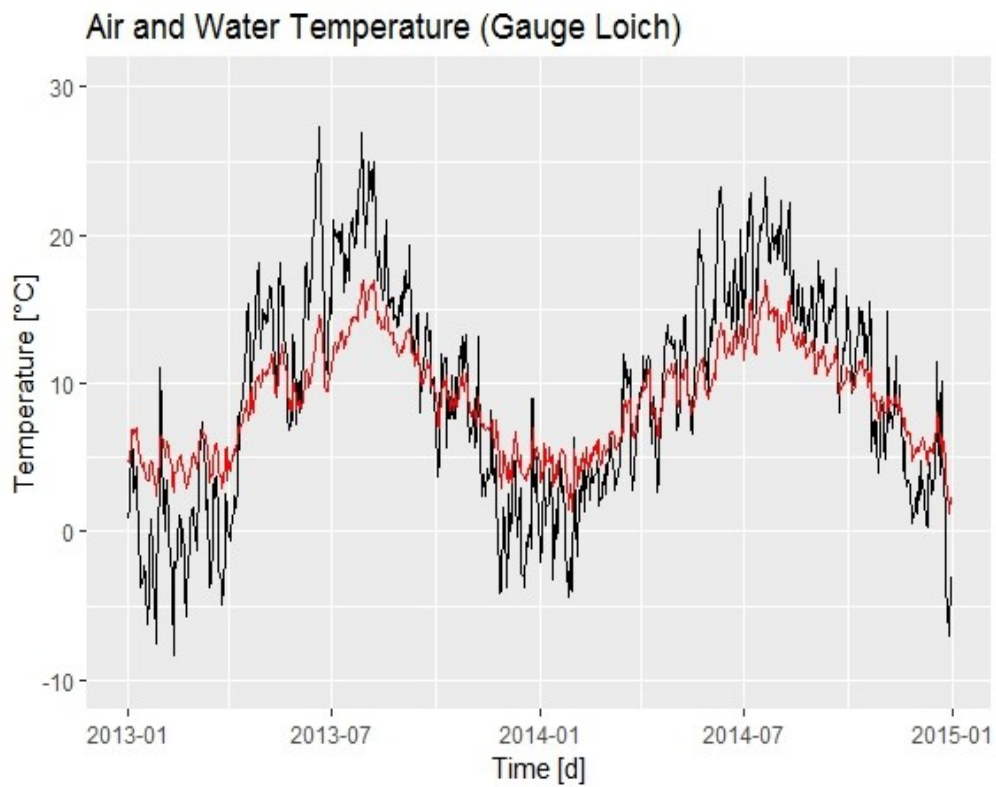


Figure 9: Daily air temperature (black) from station Frankenfels and water temperature (red) from gauge Loich.

The results for gauge Loich showed that the water temperature model was not very accurate but as the modelling period was just one year, the model structure was reused for the bigger catchment Hofstetten, see section 2.3.1 for a graphical representation.

2.2.2 Gauge Hofstetten

Hofstetten proved to be a more suitable gauge with longer data series available, hence the modelling in this thesis is based on this gauge. As stated above, it is situated at river km 36.10 at about 311 m a.s.l. The drainage area (displayed in Figure 10) is 289.5 km² and the daily long-term (1951-2015) mean discharge is 6.47m³/s (BMNT, 2018a). The river is categorized as a riffle-pool type (Mandlbürger et al., 2015) with a mean slope of 1.77%.

For the hydrological model, the longest continuous (no gaps) period of complete years (where all stations had data) was selected. That period consists of the years 1991 to 2015. The effective, processed period is from 1991 to 2014. Table 2 gives an overview of the different kinds of gauges (which are described in more detail below), the source where the data came from and the available period.

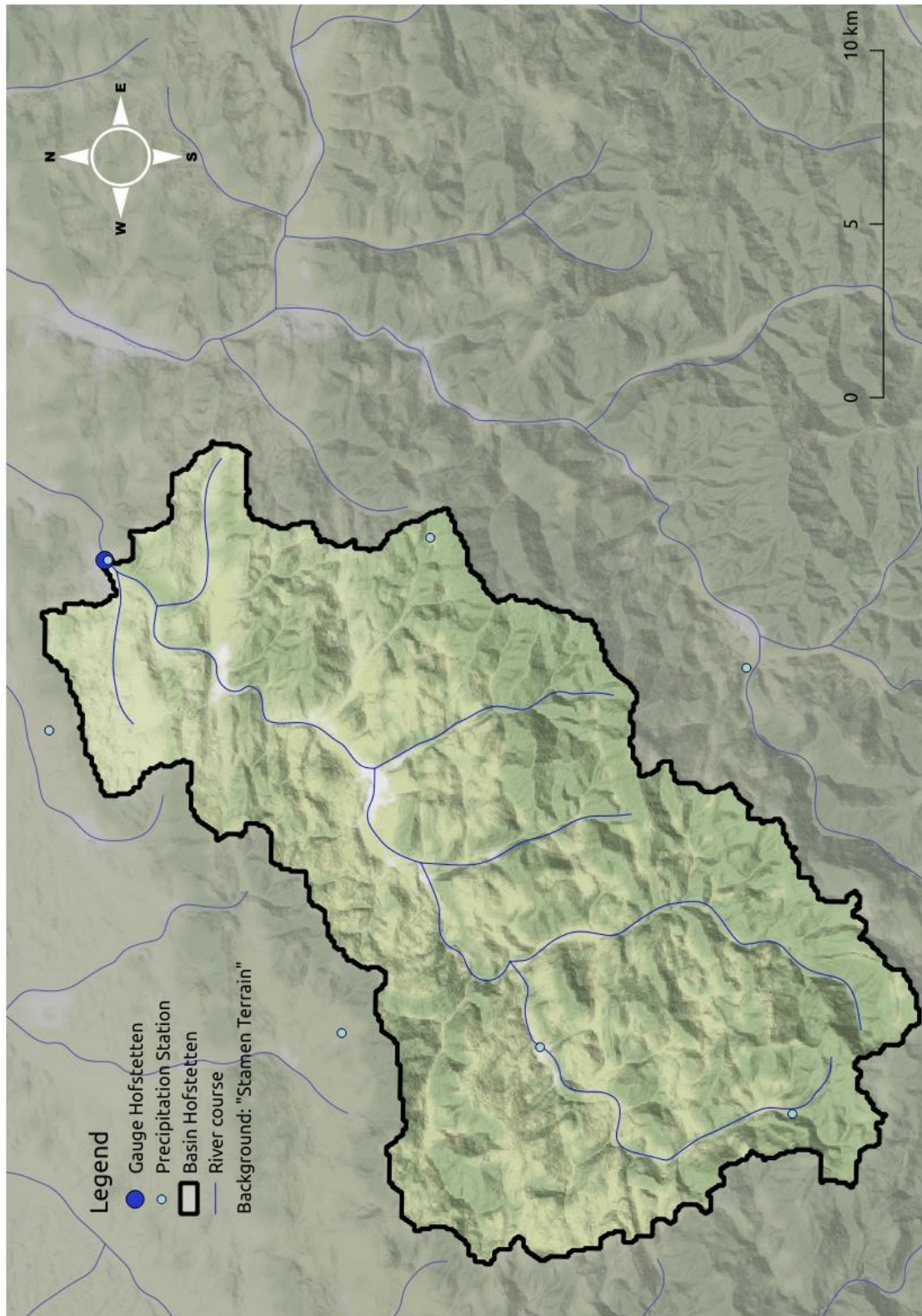


Figure 10: Basin Hofstetten

Table 2: List of used stations, in bold are the cut-off points (beginning respectively ending) which limit the used period.

Kind of station(s)	Source of data	Period
Discharge	Office of Provincial Government of Lower Austria	1981 - 2015
Precipitation	www.ehyd.gv.at	1971 - 2017
Air temperature	www.ehyd.gv.at	1991 - 2016
Stream temperature	Office of Provincial Government of Lower Austria	1976 - 2017
Groundwater temperature	www.ehyd.gv.at	1989 - 2015

2.2.3 Discharge and stream temperature

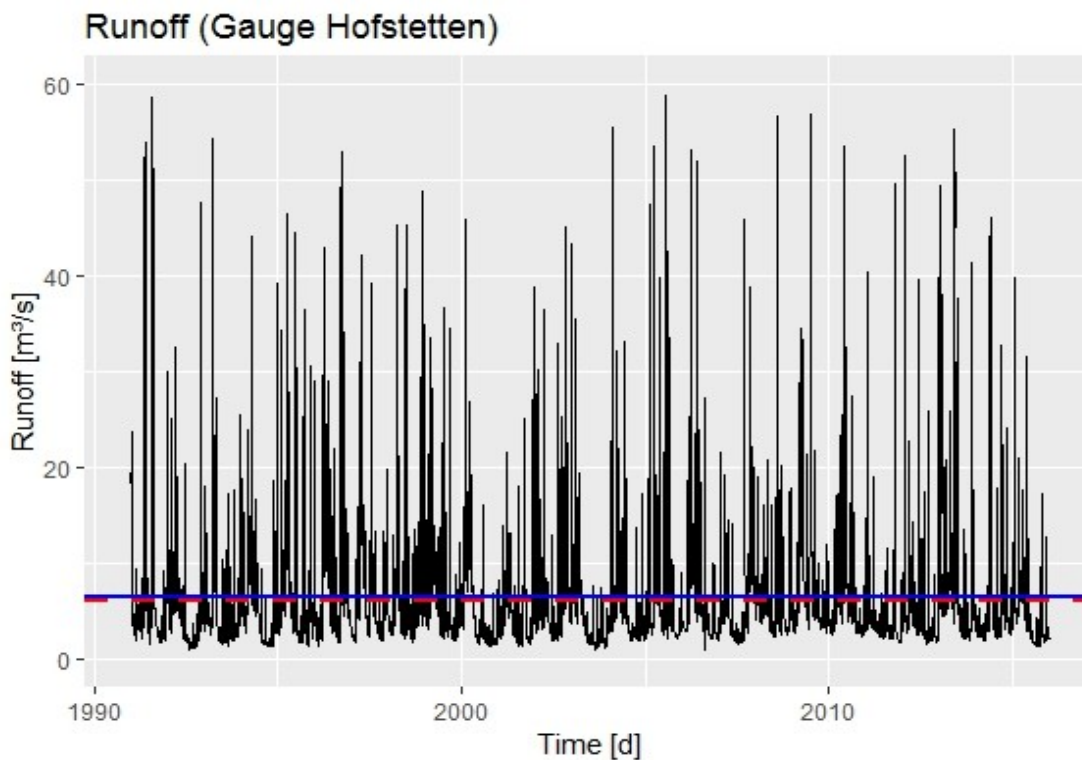


Figure 11: Gauge Hofstetten, daily mean discharge values from 1991 to 2015; dotted red line: long-term daily mean for this period ($6.28 \text{ m}^3/\text{s}$), blue line daily long-term daily mean from 1957 to 2015 ($6.47 \text{ m}^3/\text{s}$)

Discharge data of the gauge Hofstetten was made available by the Department of Hydrology and Geoinformation of the Office of the Provincial Government of Lower Austria as daily mean (in m^3/s) from 01.01.1971 to 31.12.2015 with no missing data points. For the analysis the data beginning at 01.01.1991 was used, see Figure 11. Stream temperature data at this gauge was also made available by the Department of Hydrology and Geoinformation as daily mean (in $^{\circ}\text{C}$) from 02.01.1976 to 28.02.2017 with 863 missing entries; whereby the period from the 23.06.2004 to the 23.10.2006

accounted for the major part, with 853 missing entries. This time series was also subsetted to the period from 01.01.1991 to the 31.12.2015, see Figure 12.

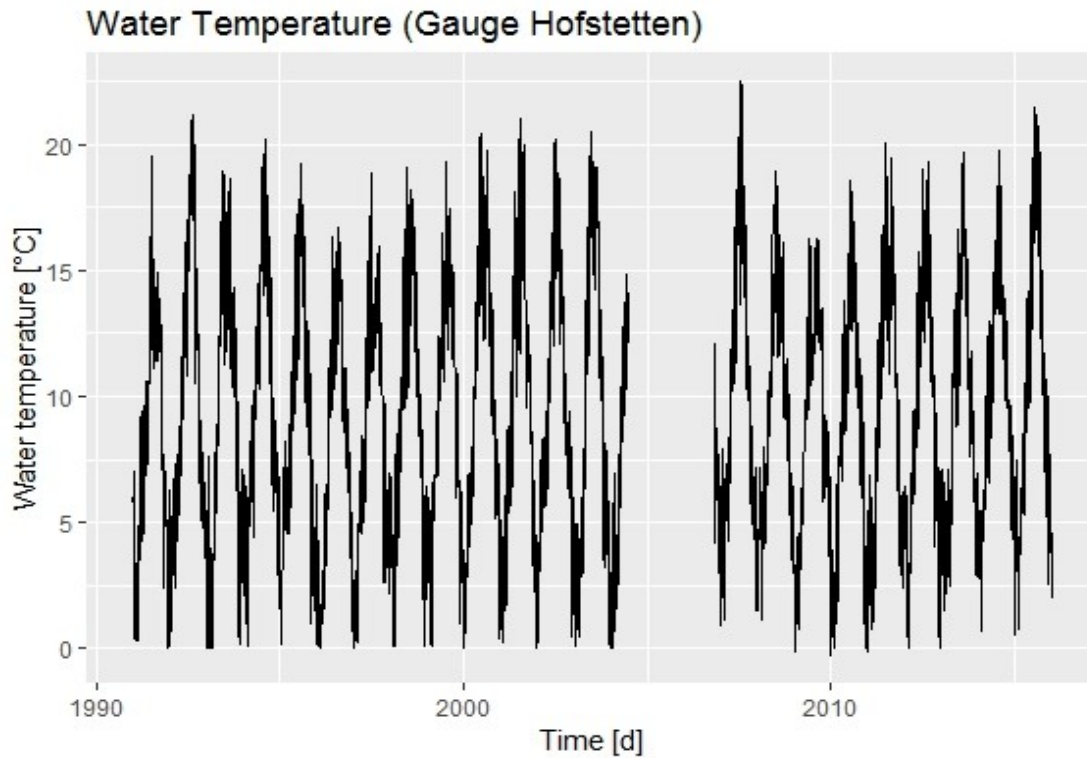


Figure 12: Gauge Hofstetten, daily mean water temperature values from 1991 to 2015

2.2.4 Precipitation

Precipitation data was made available by www.ehyd.gv.at as daily sums in mm. Eight stations were used to interpolate the precipitation data to get the daily areal precipitation. The stations are presented in Table 3. As depicted in Figure 13, Thiessen polygons were used to calculate the area of influence of each station in the basin. For each day, the areal precipitation of each segment was summed up to get the total daily areal precipitation. The resulting time series can be seen in Figure 14.

Table 3: Precipitation stations

Station name	HZB no.	Period	Weight	Alt. (m a.s.l.)	Lat	Lon
Scheibbs	107193	1971-2015	0,01%	440	15 09 51	48 0148
Wastl / Wald	107177	1971-2015	16,4%	1079	15 18 12	47 53 55
Frankenfels	107300	1971-2015	27,5%	468	15 19 40	47 58 57
Hofstetten	107318	1971-2015	8,5%	318	15 30 50	48 05 45
Türnitz	107466	1971-2015	12,5%	480	15 28 30	47 55 49
Kilb	107334	1971-2015	11,7%	295	15 24 52	48 06 38
Texing	109074	1981-2015	9,7%	469	15 19 56	48 02 02
Christenthal	109082	1981-2015	13,7%	650	15 31 26	48 00 45

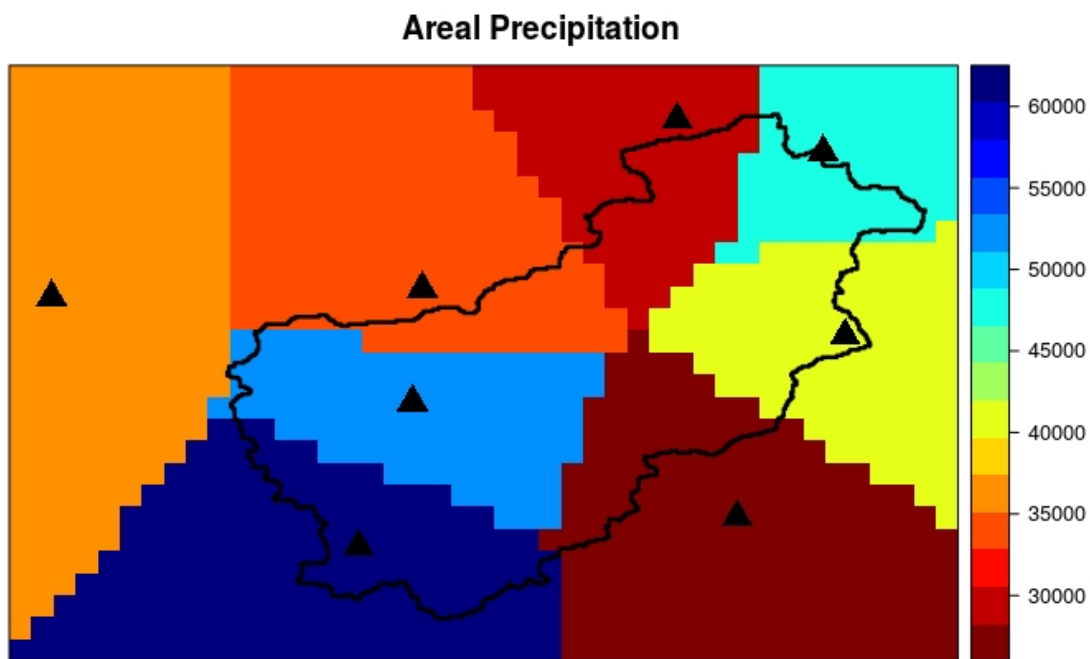


Figure 13: Area of influence of the eight precipitation stations, the scale shows the sum of the precipitation over the whole period in mm.

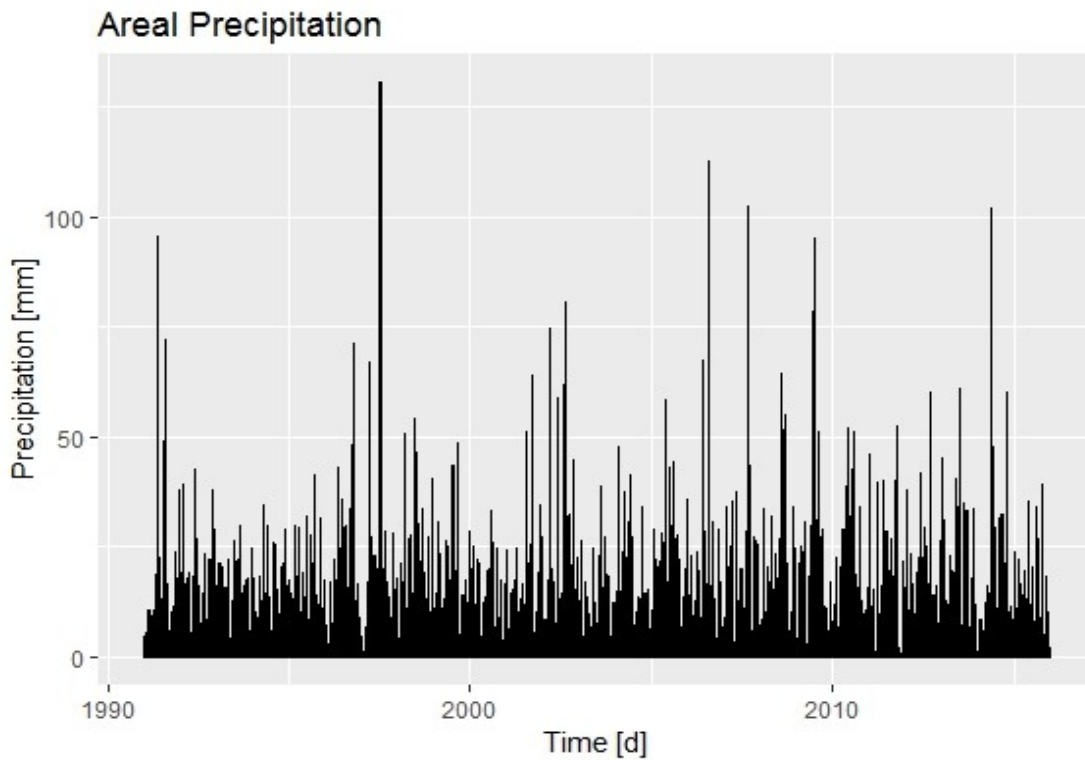


Figure 14: Daily areal precipitation of the basin of gauge Hofstetten in mm

2.2.5 Air temperature

Air temperature data was also made available by the Department of Hydrology and Geoinformation, as daily mean in degree Celsius ($^{\circ}\text{C}$). As seen in Table 4, three air temperature stations were used to get interpolated daily data. Once more, Thiessen polygons were used to get the influence of each station on the catchment area, see Figure 15. The weighted mean temperature was calculated to get a representative daily air temperature of the whole catchment, see Figure 16.

Table 4: Air temperature stations

Station name	HZB no.	Period	Weight	Alt. (m a.s.l.)	Lat	Lon
Frankenfels	107300	1991-2016	58,0%	468	15 19 40	47 58 57
Türnitz	107466	1991-2016	36,6%	480	15 28 30	47 55 49
St.Pölten	115642	1991-2016	5,4%	285	15 36 55	48 10 29

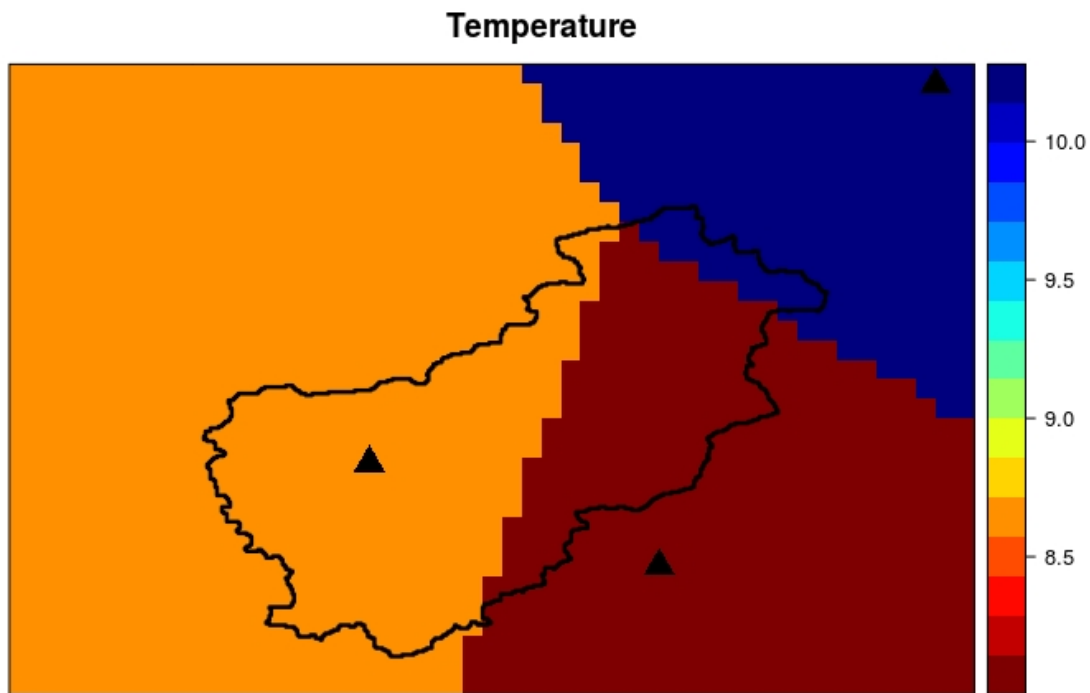


Figure 15: Areas of influence of air temperature stations, the scale shows the mean temperature in °C for the whole period.

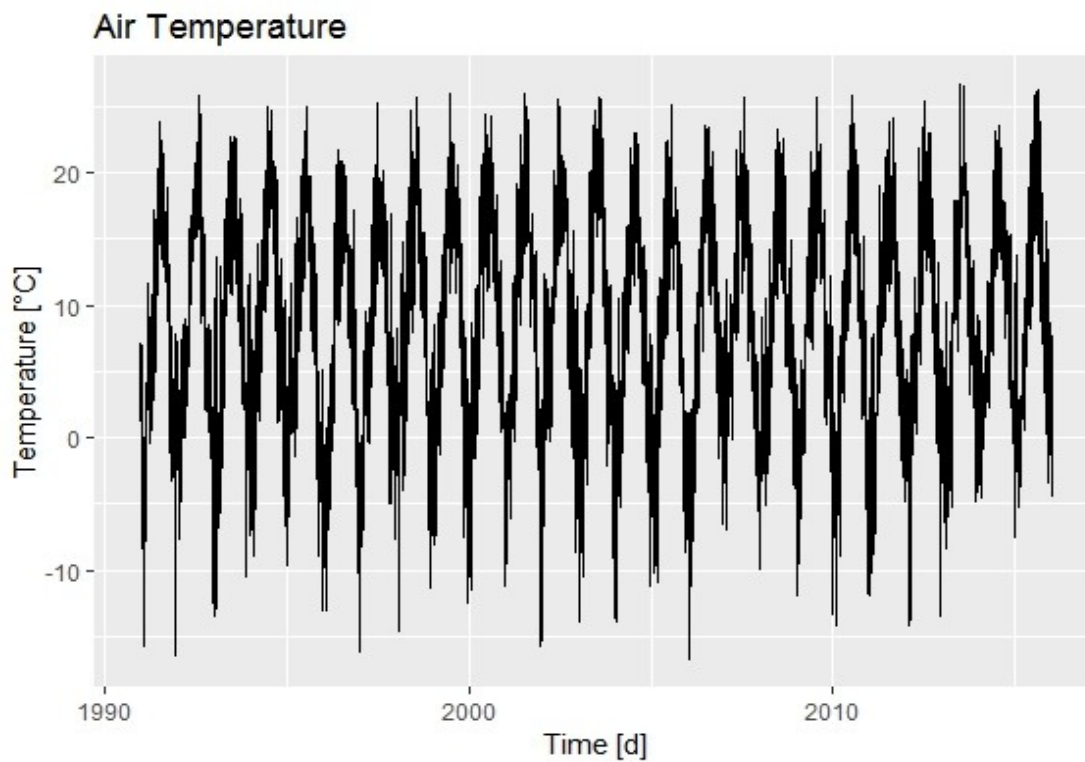


Figure 16: Weighted daily mean air temperature of basin Hofstetten, 1991-2015

To make the relationship between air temperature and water temperature visible, both are presented over a period of two years in Figure 17. The air temperature is taken from gauge St. Pölten (Autobahnmeisterei).

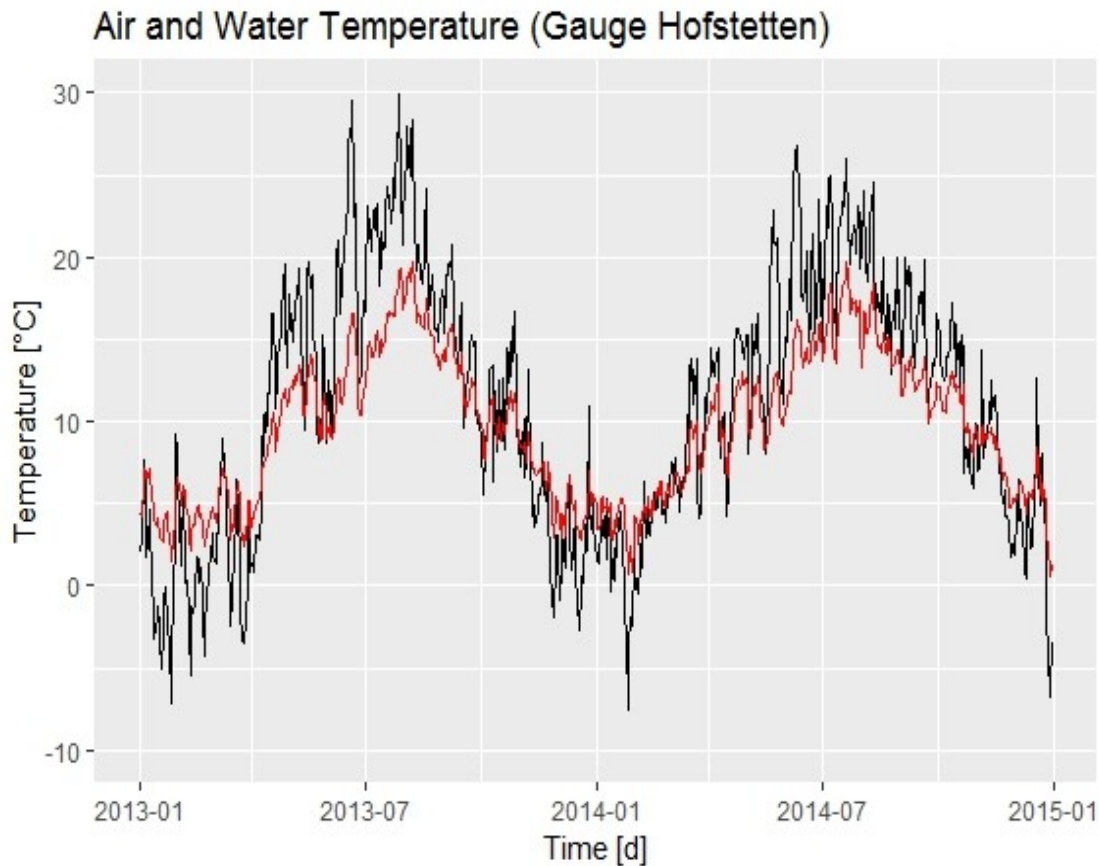


Figure 17: Daily air temperature (black) from station St. Pölten (Autobahnmeisterei) and water temperature (red) from gauge Hofstetten.

2.2.6 Groundwater temperature

Groundwater temperature data was available from the station Ochsenburg as monthly means (in °C) from ehyd.gv.at. The data was available from January 1989 to December 2015 with the following ten missing entries: seven entries from July 1995 to January 1996, and August 1997, December 1998 and January 1999. In Figure 18 the values are plotted, like the other time series, for the time period of 1991 to 2015.

A comparison to air temperature can be seen in Figure 40 in section 3.2.1.2.

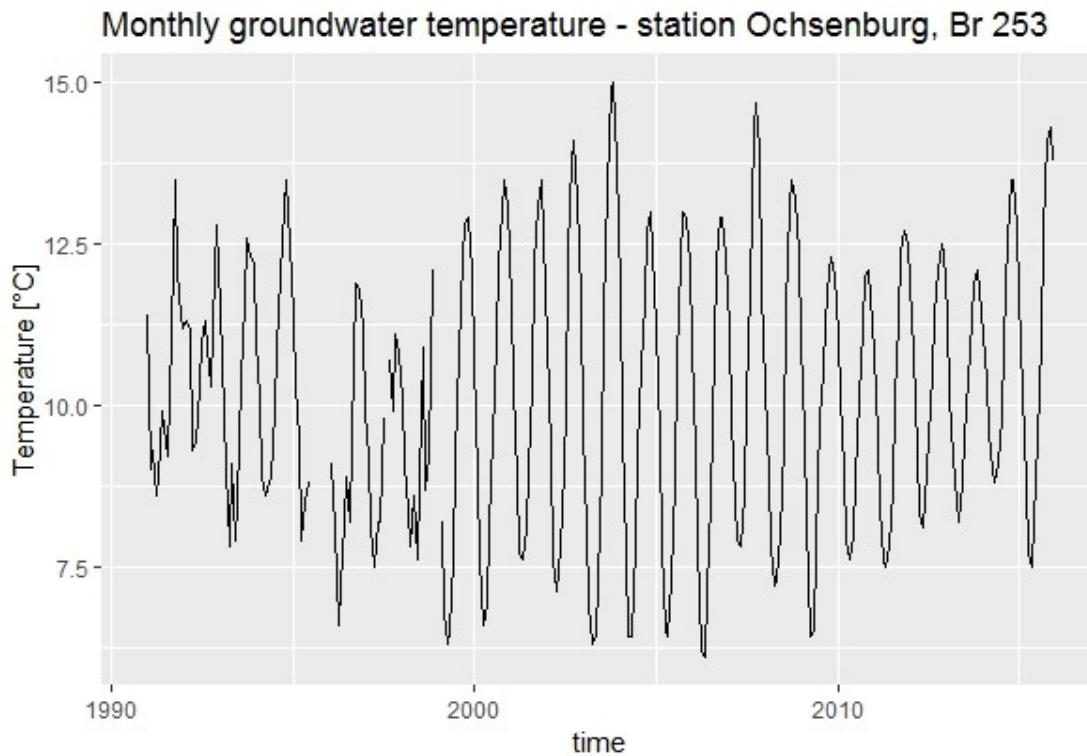


Figure 18: Monthly values of groundwater temperature at station Ochsenburg, Br 253

The data belongs to another body of groundwater (Traisental) than the body of groundwater in question (Pielachtal) so the temperature distribution of the used groundwater data may deviate from the data of the actual groundwater body. Nevertheless is it feasible to assume that the differences in the temperature distributions are small enough to be used for our model, as the two groundwater bodies are located next to each other in the same lithotectonic unit (Rhenodanubian Flysch Zone).

As there are no measured groundwater discharge rates, it was not possible to compare the modelled slow component to real-world data, which is also an element of uncertainty as groundwater is an important factor for stream temperature, especially in small basins (Caissie, 2006).

2.2.7 Altitude distribution

To get the altitude distribution of the catchment, a digital elevation model (DEM), specifically the SRTM 90m resolution data, available as raster data, from Jarvis et al. (2008) was used. To extract data from the DEM to use in the hydrological model, several steps were required and a GIS software was used, QGIS 2.16.3 (QGIS Development Team, 2017).

First the orographic catchment area was computed, with a program called `r.water-outlet` from GRASS GIS 7 (GRASS Development Team, 2017) which is integrated into QGIS. This resulted in an area of 288.91 km². The official area, specified in the data-sheet of the gauge Hofstetten is 289.50 km², which is 0.2% larger than the computed area.

For the input of the hydrological model, the area in km² per 100 m elevation band is needed, which was computed with the program `r.recode` from GRASS GIS 7.

Then the DEM raster data was converted to vector data using the GDAL program `gdal_polygonize.py` inside QGIS. This program produces a polygon feature layer from a raster (GDAL Development Team, 2017). The resulting map can be seen in Figure 19.

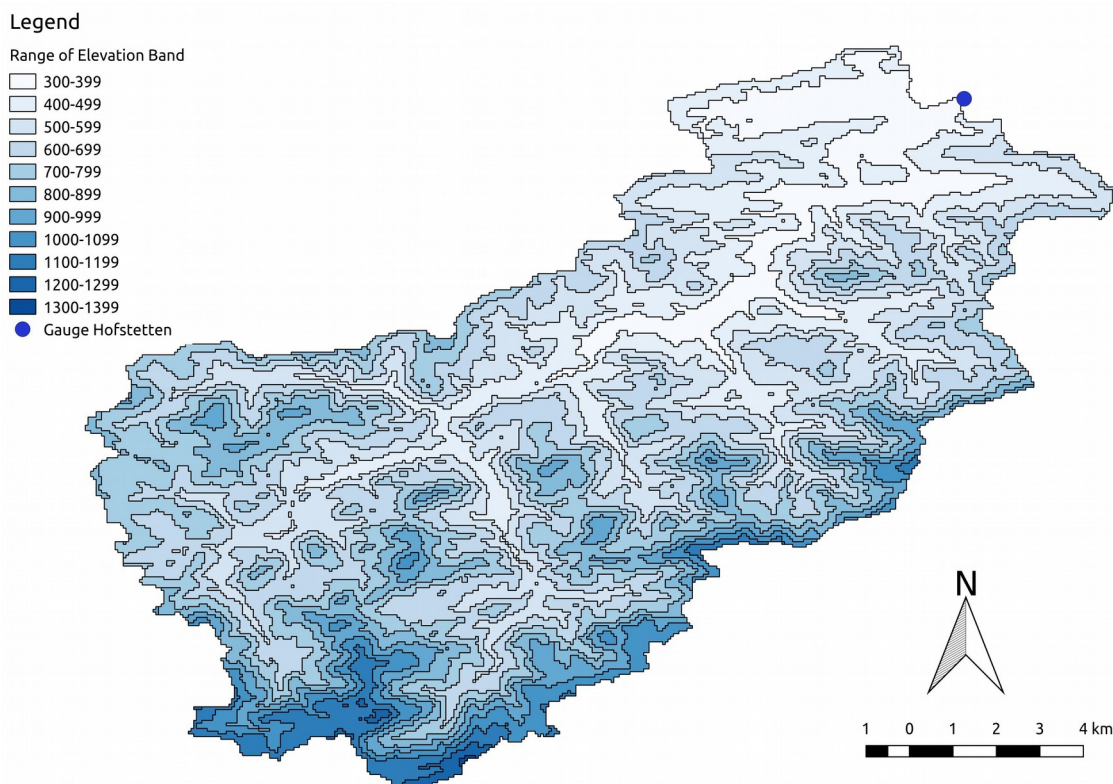


Figure 19: Drainage area of gauge Hofstetten categorized into eleven elevation bands

For each elevation band the area was calculated. The elevation of the catchment area of the gauge Hofstetten ranges from 313 m a.s.l. to 1324 m a.s.l., the elevation bands where the largest area is concentrated are four adjacent bands with a range from 400 m a.s.l. to 799 m a.s.l. (see Table 5) with a combined area of 207.28 km², or 71.75% of the whole Hofstetten catchment.

Table 5: Area per elevation band

Range of elevation band	Area [km²]
300-399	22.96
400-499	43.30
500-599	55.94
600-699	62.48
700-799	45.56
800-899	25.75
900-999	14.35
1 000-1 099	10.28
1 100-1 199	7.06
1 200-1 299	1.19
1 300-1 399	0.06

2.3 Hydrological model

2.3.1 Introduction to MODMOD

The Modular Conceptual Water Balance Model, short BOKU_ModMod or MODMOD was developed at the Institute of Water Management, Hydrology and Hydraulic Engineering, University for Natural Resources and Life Science in Vienna by Hubert Holzmann, Carolina Massmann and Klara Stangl (2014a). It was used to model the discharge at gauge Hofstetten, and to discern the two different components of the discharge, the slow and the fast component, see below.

It comprises, as the name implies, several modules, where each one describes a (dominant) hydrological process. There are eleven modules, all of which are listed in Table 6. The module names printed in bold are used in the hydrological model for this thesis and will be explained in detail below, see Section 2.3.3. The module not implemented yet (“Evapotranspiration”) is italicised, it has to be executed as a separate program.

Table 6: Modules of ModMod (in bold: used for the model for this thesis)

Number of the Module	Modules of ModMod
1	Snow/ Glacier
2	Interception
3	Single Linear Storage
4	Antecedent Precipitation Index (Api) Storage
5	Split Function
6	Root Storage
7	Mobile Soil Water Storage
8	Groundwater Storage
9	Linear Storage Cascade
10	Hortonian Flow
11	Evapotranspiration ¹¹

The module structure models the track of a rain particle and can be described as a sequence of trees which consist of at least one string. A new tree which consists of at least two strings starts after the module “split function”. The model structure of the model used in this thesis can be seen in Figure 20, the numbers in the nodes correspond to the numbers of the modules in Table 6.

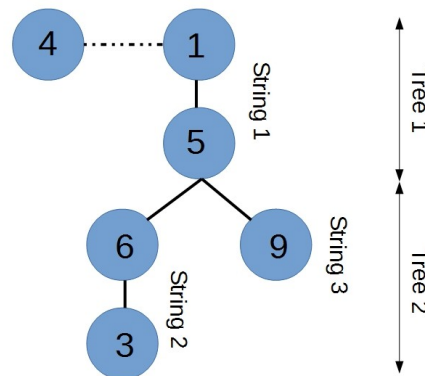


Figure 20: Model structure, modified from Holzmann et al. (2014a)

The source code of the model is written in FORTRAN; Microsoft Visual Studio was used as IDE with the Intel® Visual Fortran integration as the compiler.

¹¹ Calculated by using a separate program

2.3.2 Preparation of input data

The module “Evapotranspiration” is not yet incorporated in MODMOD, so the evapotranspiration had to be calculated externally with a separate FORTRAN program called `etpot_main.for`. As an input, the program takes the area of each of the available elevation bands (described above) and time series of air temperature and precipitation.

To get the required input for MODMOD a meteorological data file, “`PTET_Hofn.txt`” was created which contains the externally computed potential evapotranspiration data, the interpolated precipitation data and the interpolated temperature data.

Another input file, “`Qobs_Hofn.txt`” contains the observed discharge data from the gauge Hofstetten.

The altitude distribution (see section 2.2.7 for how it was created) is stored in the file “`alt_hofstn.txt`” and can be found in Appendix II.

The used time series were split into a calibration period and a validation period. The calibration period comprises a period of thirteen years, from January 1991 to December 2003 and the validation period comprises the eleven years from January 2004 to December 2014.

The parameter input file “`inputmodna.txt`” used for the validation period can be found in Appendix I. The parameter input file for the calibration uses the same parameters but the calibration period of the time series.

2.3.3 Used Modules of MODMOD

As described above, with this model dominant hydrological processes can be represented by a sequence of different modules. The model used in this thesis comprises two trees and three strings. After a split function a new tree with two strings starts. (The structure of the model is given in Figure 20, see above.) The modules which are used are described below. All available modules are listed in Table 6 in Section 2.3.1.

2.3.3.1 Module 1: Snow / Glacier

For this thesis, a model with just the snow module was used, as there is no glacier the according module was not applied. Using the elevation bands, precipitation, and air temperature as inputs, snowmelt and snow accumulation are calculated by applying the degree-day approach. This approach assumes that there is a relationship between air temperature and snow ablation respectively accumulation. To assign temperatures for

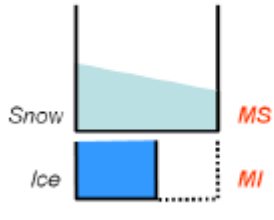
Module concept	Parameters
<p style="text-align: center;">MELT</p> 	<p>MS ... Melt Index Snow</p> <p>MI ... Melt Index Ice</p>

Figure 21: Module 1 (Holzmann et al., 2014a)

each individual elevation band the temperature is interpolated following the standard lapse rate of 0.65 K/100 m from the reference height, which is set at 300 m a.s.l. If there is precipitation it is accumulated as snow if the temperature of a particular elevation band drops below a certain threshold (here: 0°C). If the temperature of a particular elevation band is above the threshold, the precipitation is treated as liquid water and if there is accumulated snow it starts to melt (Holzmann et al., 2014a).

2.3.3.2 Module 3: Single Linear Storage

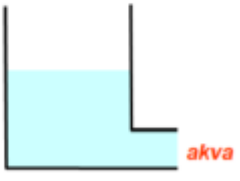
Module concept	Parameters
<p style="text-align: center;">Single Linear Storage</p> 	<p>akva... Recession constant</p>

Figure 22: Module 3 (Holzmann et al., 2014a)

The Single Linear Storage module is a simple “bucket model” and can be used to model many hydrological processes. The outflow is directly proportional to the height of the water level. In this thesis, it represents the contribution of groundwater to the discharge.

2.3.3.3 Module 4: Antecedent Precipitation Index (API) Storage

The Antecedent Precipitation Index (API) module represents the soil moisture content in the catchment. The input is the precipitation and the output is a runoff coefficient (ψ). The relation of API and the runoff coefficient is described by the red line in the

Module concept	Parameters
<p style="text-align: center;">Antecedent Precipitation Index</p>	<p>apikval... recession constant</p> <p>stlow... lower moisture content</p> <p>stup... upper moisture content</p> <p>psilow... runoff coefficient at stlow</p> <p>psiup... runoff coefficient at stup</p>

Figure 23: Module 4 (Holzmann et al., 2014a)

figure above: When the soil moisture content is low, ψ is fixed until the soil moisture reaches the lower threshold, from there ψ rises linearly until the soil moisture reaches an upper threshold. If the soil moisture keeps rising, ψ stays the same until the soil moisture drops again below the upper threshold.

The module output (the runoff coefficient) is used as input to the Split Function module (see below).

2.3.3.4 Module 5: Split Function

Module concept	Parameters
<p style="text-align: center;">SPLIT FUNCTION</p>	<p>isplitme ... Split method</p> <p>splitpro ... constant percentage factor</p> <p>splitswe ... threshold factor</p>

Figure 24: Module 5 (Holzmann et al., 2014a)

The Split Function module divides the inflow into two outflows. In this thesis the Split Function module is used to split up (faster) surface flow from (slower) subsurface flow. There are three split methods available, in this thesis the variable runoff coefficient is used, which is calculated by the API module (see above).

2.3.3.5 Module 6: Root Storage

The Root Storage module takes inflow and potential evapotranspiration as input and is used to simulate the actual evapotranspiration in the root zone. When the storage is full percolation occurs, when there is no precipitation, the storage empties by evapotran-

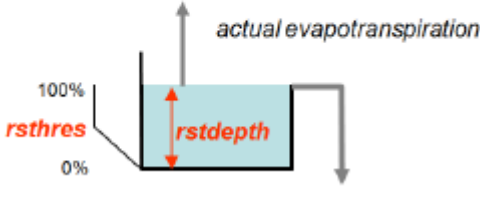
Module concept	Parameters
<p style="text-align: center;">Root Storage</p> 	<p><code>rstdepth...</code> root storage depth</p> <p><code>rsthres...</code> root depth/ root stress ratio</p>

Figure 25: Module 6 (Holzmann et al., 2014a)

spiration. The actual evapotranspiration equals the potential evapotranspiration until the storage reaches the threshold `rsthres`, then the actual evapotranspiration decreases linearly until it reaches zero.

2.3.3.6 Module 9: Linear Storage Cascade

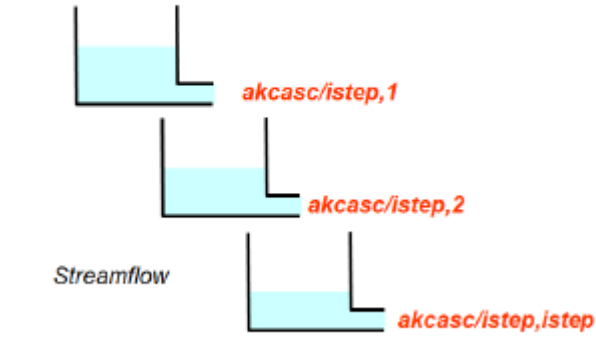
Module concept	Parameters
<p style="text-align: center;">Linear Storage Cascade</p> 	<p><code>akcasc ...</code> retention constant</p> <p><code>istep ...</code> number of storages</p>

Figure 26: Module 9 (Holzmann et al., 2014a)

The Linear Storage Cascade module simulates the routing branch of the model. It consists of a series of Single Linear Storage modules (see above). In the hydrological model for this thesis a cascade of two linear storages was used.¹²

2.3.4 Execution of the hydrological model

2.3.4.1 Creation of the inputmodna.txt file

When the program is executed for the first time, a parameter input file is generated, partially on the basis of inputs from the user, partially with predefined specifications.

¹² For the test run at gauge Loich a “cascade” of just one linear storage was used, so it was practically equal to (and had the same output as) Module 3.

In a first step a name has to be chosen, then the model structure has to be entered, in the form of various modules, arranged in trees and strings, see Figure 20 in section 2.3.1. After this is done, the user has to alter the generated “inputmodna.txt” file by adapting the file paths to the input and output folders and potentially changing the pre-defined parameters.

2.3.4.2 Running the model

When the program is executed a second time, the model is run with the model structure and the parameters according to the previously generated “inputmodna.txt” file.

2.3.5 Preparation of the output data

An R-script is used to manipulate the output of the hydrological model. Then the total discharge is calculated by adding together the output of the linear storage cascade (which represents the fast flow) and the single linear storage (slow flow). The precipitation is calculated by summing up the modelled discharge and the modelled evapotranspiration.

As described above, the time series was split into a calibration period (1991 to 2003) and a validation period (2004 to 2014).

2.3.6 Goodness of fit and parameter adaption

After the preparation of the output data, the sums of the observed and the simulated values of the discharge were compared. The sums of precipitation and the expected precipitation (observed discharge plus simulated evapotranspiration) and the sum of simulated discharge and simulated evapotranspiration were also compared. This was done to get a rough estimate if the model was fulfilling the water balance equation, see section 3.1.1.

After that first check, the time series of observed and simulated discharge were compared with each other using following goodness-of-fit measures: Nash-Sutcliffe efficiency (NSE) (Nash & Sutcliffe, 1970) see equation (9) and Kling-Gupta efficiency (KGE) (Gupta, Kling, Yilmaz, & Martinez, 2009), see equations (10) and (11).

$$NSE = 1 - \left[\frac{\sum_{i=1}^n (y_i^{obs} - y_i^{sim})^2}{\sum_{i=1}^n (y_i^{obs} - y_i^{mean})^2} \right] \quad (9)$$

$$KGE = 1 - ED \quad (10)$$

$$ED = \sqrt{(r-1)^2 + (\alpha-1)^2 + (\beta-1)^2} \quad (11)$$

With:

- r as the Pearson product-moment correlation coefficient
- α as the ratio between the standard deviation of the simulated values and the standard deviation of the observed ones
- β as the ratio between the mean of the simulated values and the mean of the observed ones (bias) (Zambrano-Bigiarini, 2017)

The discharge time series with daily values was used for parameter optimization. The parameter optimization was done manually. The calibration time series was split up in yearly segments, so that it was easier to visually compare simulated and observed discharge and to help with the process of parameter optimization. To show the effects of the parameter optimization, see Figure 27, Figure 28 and Figure 29. They display a comparison of observed and modelled discharge over the whole calibration time series, including goodness of fit parameters. They are set, in chronological order, at the beginning of parameter estimation, after some 20 iterations, and at the final model output after 51 iterations, respectively. An example of how the yearly segments look like can be seen in Figure 30, Figure 31 and Figure 32 which cover the year 1997 at the beginning of parameter estimation, after some iterations, and with the final parameter set, respectively. The year 1997 was chosen as it represents the year responsible for the biggest boost in NSE.

The initial values are the parameter set which was optimized for the gauge Loich. In Table 7 all parameters which were changed in the optimization process are depicted including how they changed. The three columns correspond to the values of Figures 27, 28, and 29.

Table 7: Change of parameters due to parameter optimization

Parameter	Values for Fig. 27	Values for Fig. 28	Values for Fig. 29
corr_etp	1.10	1.10	1.20
stup	30.00	40.00	30.00
psilow	0.15	0.30	0.20
psiup	0.70	0.50	0.50
Root storage (mm)	90.00	50.00	60.00
Depth-Ratio of Rootstress (0 - 1)	0.50	0.50	0.10
akcasc	2.00	1.50	1.50
istep	1	2	2
NSE	0.52	0.602	0.617
KGE	0.74	0.724	0.74

After reaching the threshold for optimizing the model, the daily time series was aggregated to a monthly time series as seen in Figure 33. A result of this aggregation is a smoothed time series, the NSE and the KGE become higher (0.78 and 0.87, respectively) as extremely high and low daily values are cumulated in monthly values.

After optimizing the parameters using the calibration period, the model was applied to the validation period. In Figure 34 the comparison between observed and simulated values, already monthly aggregated, can be seen. The NSE and the KGE here are 0.63 and 0.76, respectively.

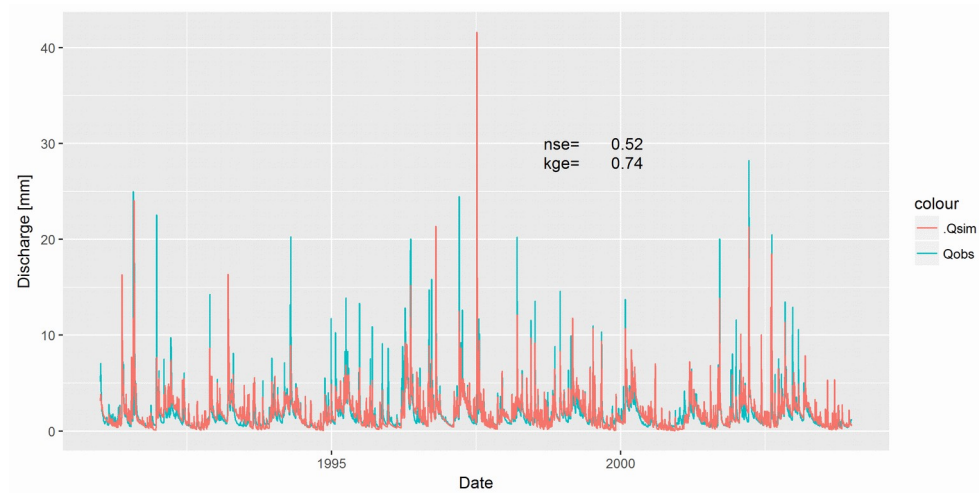


Figure 27: Daily values of observed and modelled discharge using the starting parameter set

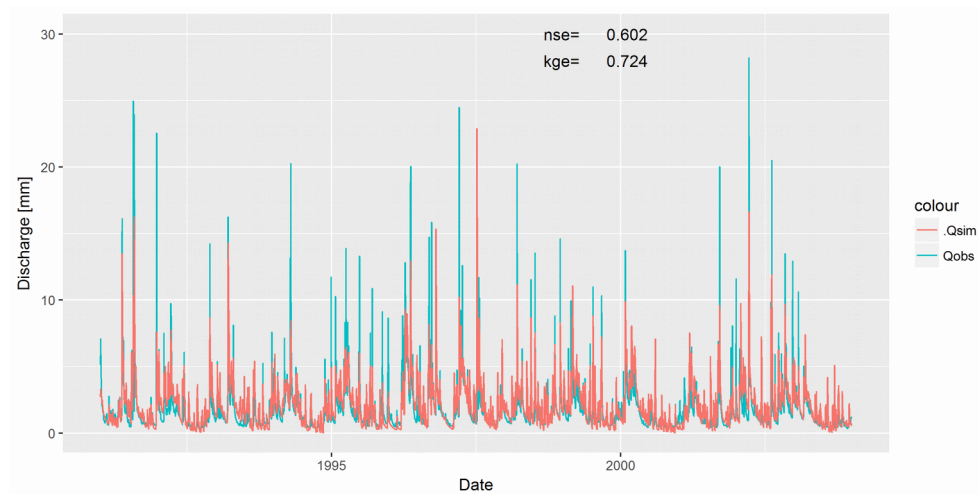


Figure 28: Daily values of observed and modelled discharge after 20 iterations of parameter optimization

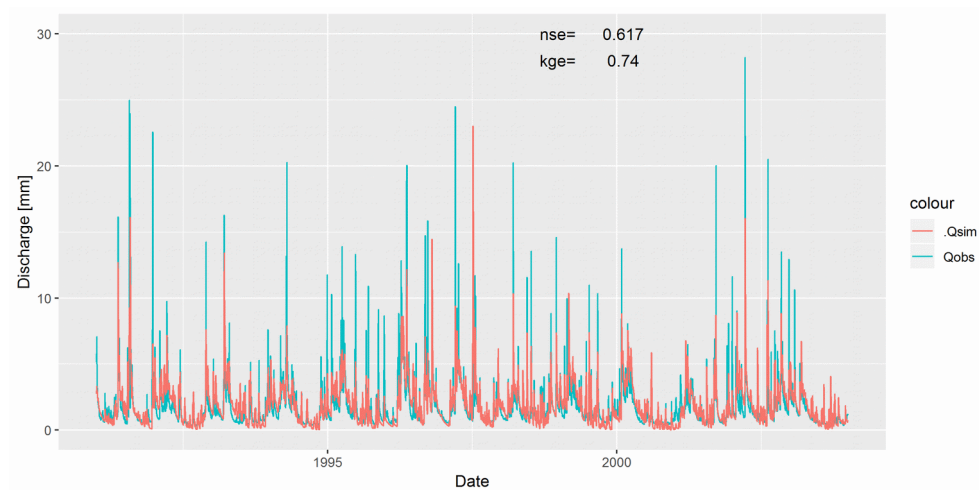


Figure 29: Daily values of observed and modelled discharge, final parameter set.

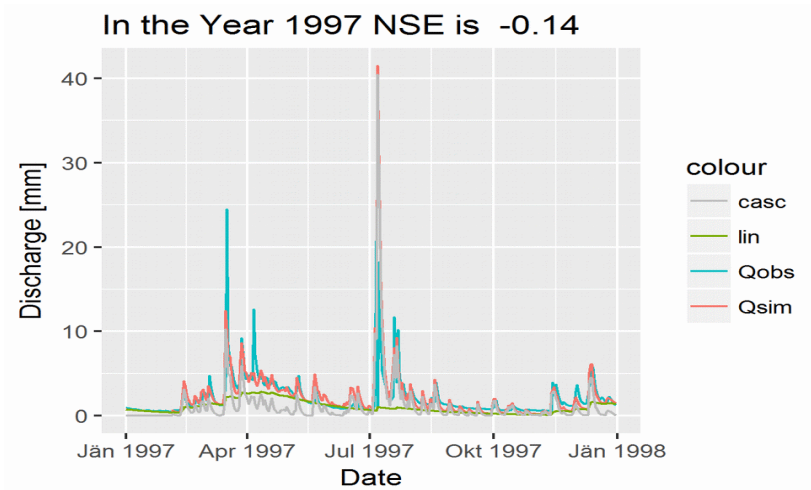


Figure 30: Starting parameter set - sample year 1997

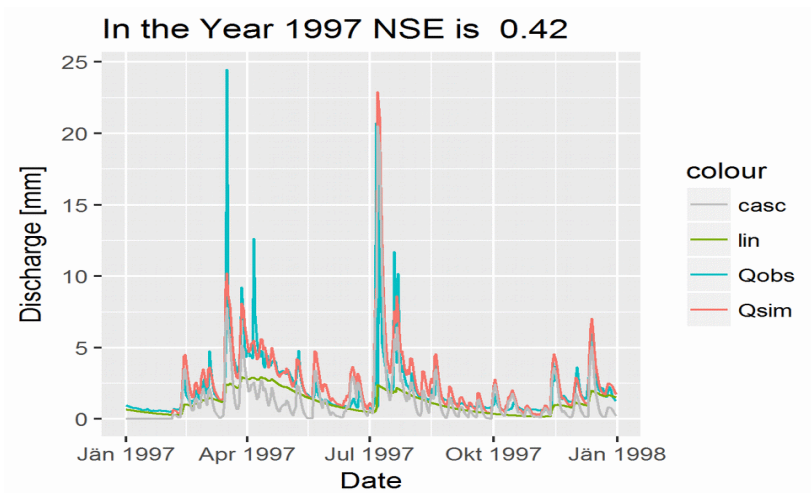


Figure 31: After 20 iterations - sample year 1997

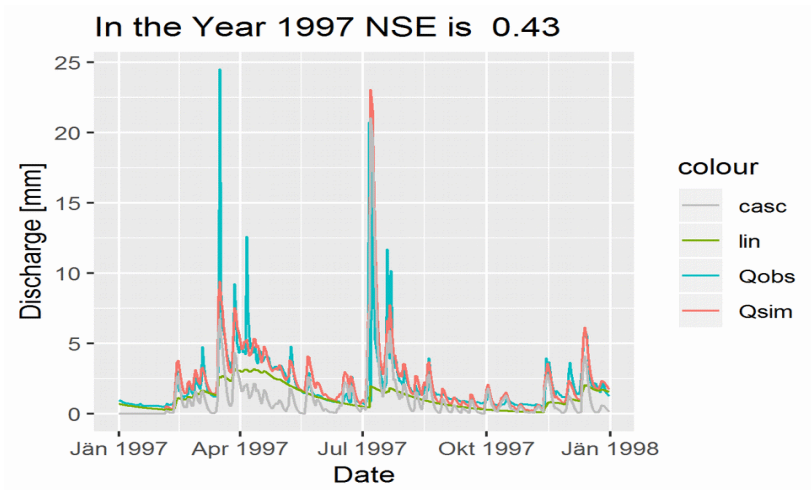


Figure 32: Final parameter set after 51 iterations - sample year 1997

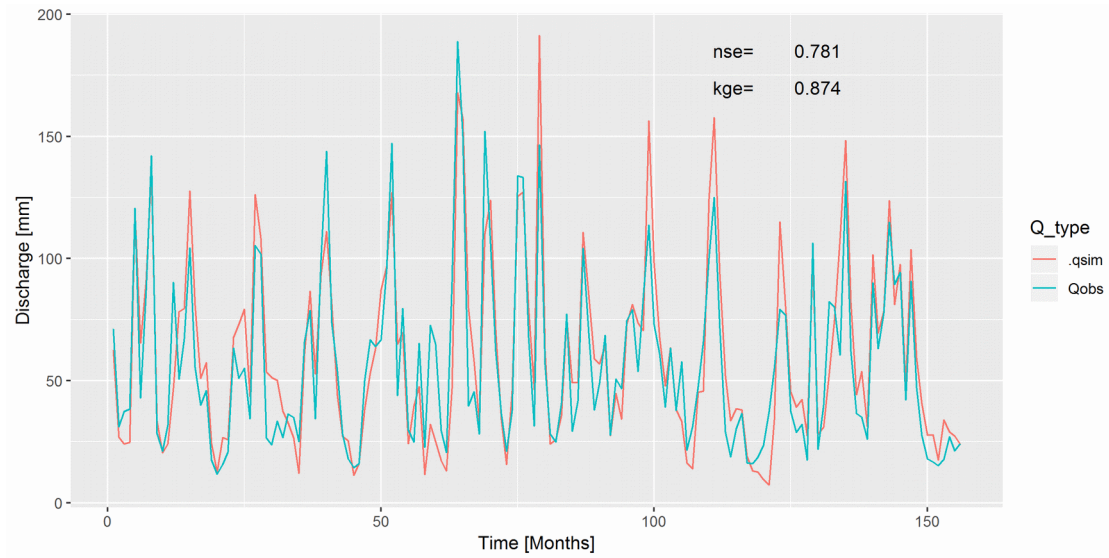


Figure 33: Monthly comparison of observed and simulated runoff values (calibration period)

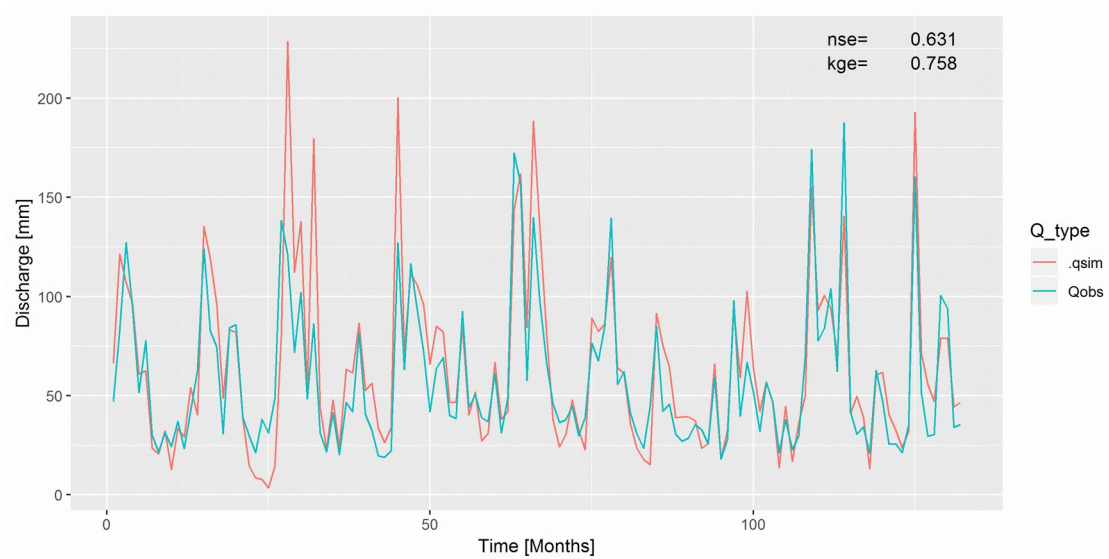


Figure 34: Monthly comparison of observed and simulated discharge values (validation period)

2.4 Statistical model

A simple hydrology-based discharge-weighted model was compared to a linear and a non-linear regression model and to an unweighted version of the hydrology-based model.

2.4.1 Discharge-weighted hydrology-based model

The proposed model in this thesis assigns temperatures to the two different components of water, one slow flowing component which corresponds to the groundwater and one fast flowing component which corresponds to the surface runoff. These two components form the output of the hydrological model and are represented as the green line (slow component) and the grey line (fast component) in Figures 30 to 32. At each point in time the total runoff consists of the sum of these two components, so the proportions of the components can be given as percentages by dividing them by the total runoff. The temperature is weighted by the component's proportion of the runoff, as equation (12) shows.

$$T_{Stream_S} = T_{Air} * \frac{V_{fast}}{V_{tot}} + T_{Groundwater} * \frac{V_{slow}}{V_{tot}} \quad (12)$$

With T_{Stream_S} as the simulated stream temperature, T_{Air} , and $T_{Groundwater}$ as the observed temperature of the air and the groundwater, respectively, and V_{fast} and V_{slow} as the amount of fast and slow discharge, respectively. V_{tot} is the total amount of discharge.

2.4.2 Linear regression model

To have a comparison for the proposed model's output, a multiple linear regression model was used (equation (13)), where T_{Stream_S} is the simulated stream temperature and T_{Air} , and $T_{Groundwater}$ are the observed temperatures of the air and the groundwater, respectively. The variable a is the intercept, and β_1 and β_2 are the coefficients of the air temperature and the groundwater temperature, respectively.

$$T_{Stream_S} = a + \beta_1 * T_{Air} + \beta_2 * T_{Groundwater} \quad (13)$$

2.4.3 Non-linear regression model

For the non-linear regression model, the model from Mohseni et al. (1998) was used as depicted in equation (14) and Figure 35.

$$T_s = \mu + \frac{\alpha - \mu}{1 + e^{\gamma(\beta - T_a)}} \quad (14)$$

With:

- T_s = estimated stream temperature
- T_a = measured air temperature
- α = estimated maximum stream temperature
- μ = estimated minimum stream temperature
- β = temperature at inflection point
- γ = function of the slope ($\tan(\theta)$) and is calculated by equation (15):

$$\gamma = \frac{4 \tan(\theta)}{\alpha - \mu} \quad (15)$$

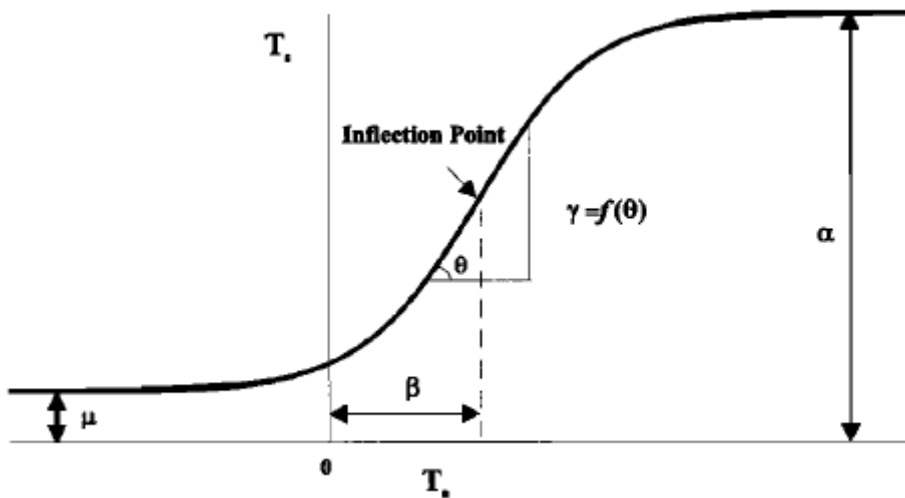


Figure 35: Schematic representation of the logistic function parameters (O. Mohseni et al., 1998)

The parameters α and μ are estimated directly, the parameters β and γ are estimated using the method by Nelder and Mead (1965), minimising lambda in equation (16).

$$\lambda = \sum_{i=1}^n \left(T_{obs} - \mu - \frac{\alpha - \mu}{1 + e^{\gamma(\beta - T_s)}} \right)^2 \quad (16)$$

3 Results and Discussion

3.1 Hydrological model

3.1.1 Comparing modelled discharge values with observed values (calibration period)

The modelled mean yearly discharge for the calibration time period of 1991 to 2003 is 722 mm compared to the observed discharge for the same period of 684 mm. This means the modelled discharge overestimates the observed discharge by six per cent or 38 mm per year.

The simulated evapotranspiration was adapted so that the sum of the yearly mean simulated discharge and the yearly mean simulated evapotranspiration amounts to 1271 mm. The observed yearly areal precipitation amounts to 1270 mm, so that there is a difference of only 0.01 percent..

The observed and simulated time series were compared using the performance criteria NSE and KGE, see section 2.3.6 above, which amount to 0.62 and 0.74, respectively for the daily values, the monthly aggregated NSE and KGE values amount to 0.78 and 0.87, respectively.

3.1.2 Comparing fast and slow runoff (validation period)

The output of the hydrological model, (the split of the discharge into a slow and a fast component) can be seen in Figure 36 and Figure 37 which depict the whole validation period and a sample year (2005), respectively. These values are used as input for the statistical model for water temperature estimation, see below.

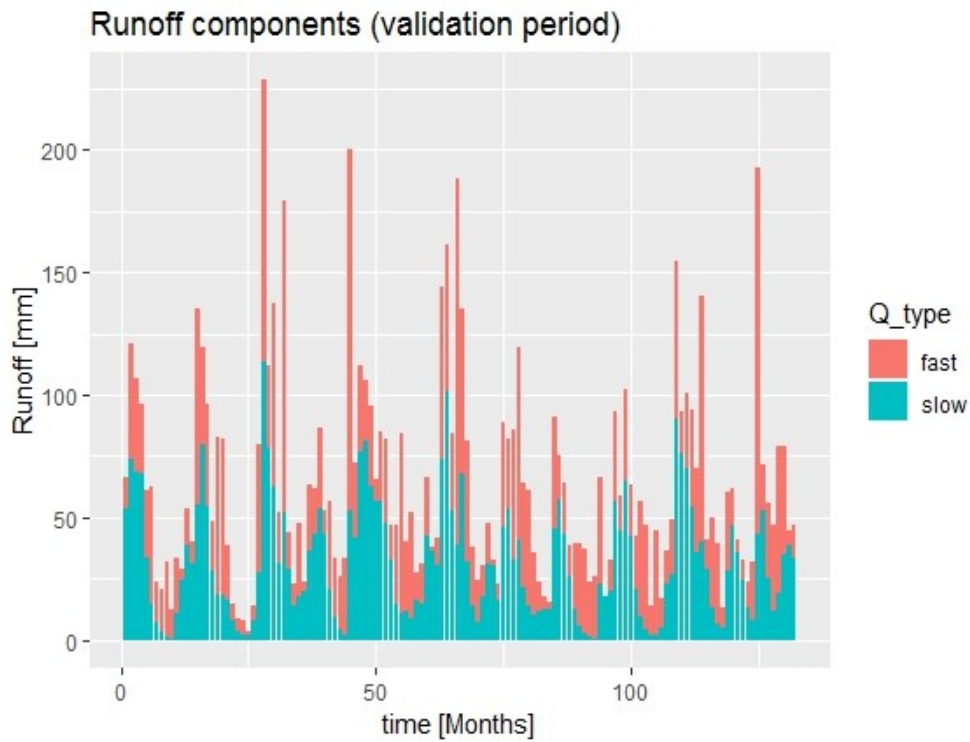


Figure 36: Fast (red) and slow (blue) runoff components of the validation period (of the hydrological model).

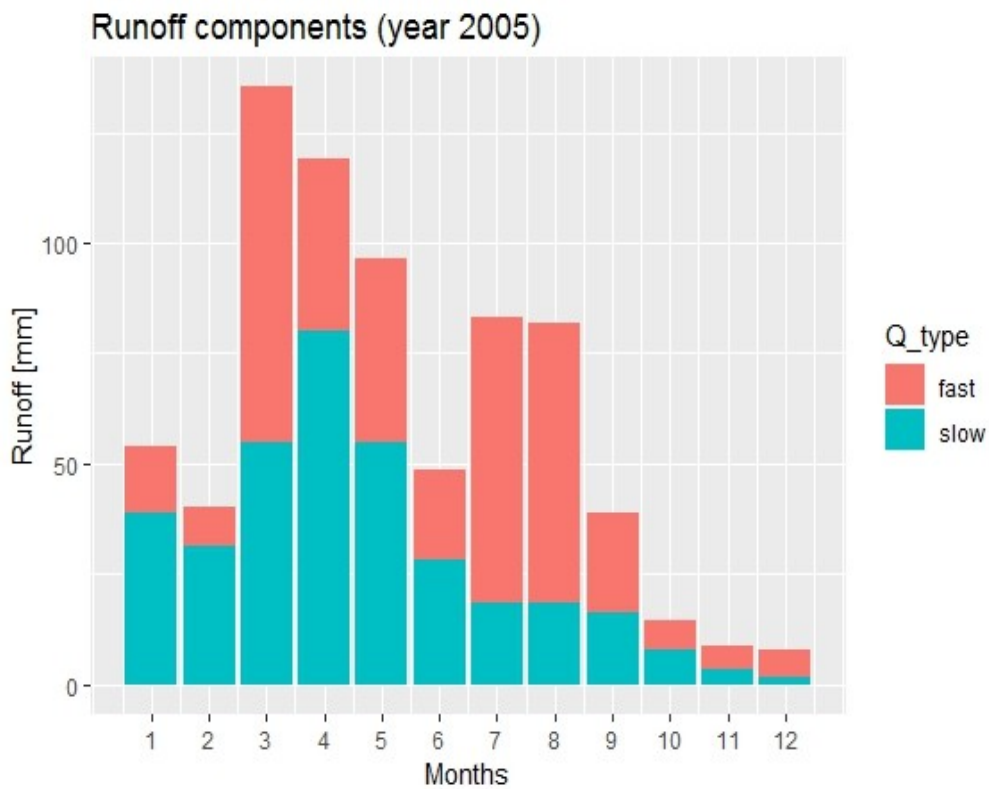


Figure 37: Fast (red) and slow (blue) runoff components of the year 2005.

3.2 Statistical model

This statistical model aims to establish a connection between the quantity of the slow and the fast discharge, their associated temperatures (groundwater temperature and air temperature, respectively) and the stream temperature.

Weekly and monthly intervals are commonly used for predicting stream temperatures (Caissie, 2006). In this master thesis, monthly intervals are used to model the stream temperature.

3.2.1 Preparations

For the statistical analysis the stream temperature time series was split in a calibration period and a validation period, n.b., that these time periods are different from the ones used for the hydrological model, see below 3.2.1.1.

3.2.1.1 Stream temperature

As written above, there was a gap in the available time series for stream temperature, which amounted to 853 missing data points, see Figure 12 above. As the data was aggregated to monthly means, this number shrank accordingly to 30 missing data points, from June 2004 to October 2006 and June 2008. Each month with incomplete data was counted as missing (in June 2004, October 2006 and June 2008 there were some days with data, but the month as a whole was not taken into consideration.)

As there was no possibility to compare simulated stream temperatures to observed values in this period and the gap separates the timeline in two time periods, these periods were used as the (new) calibration period and validation period. The calibration period comprises 161 data points or 62 % of the available data, (January 1991 to May 2004) and the validation period comprises 98 data points or 38% of the available data, (November 2006 to December 2014). As a longer calibration period results in more robust results (van der Spek & Bakker, 2017) this was considered an appropriate splitting. The hydrological validation period (2004 to 2014) compasses the whole statistical validation period (Nov 2006 to Dec 2014). Figure 38 illustrates the gap and the two periods.

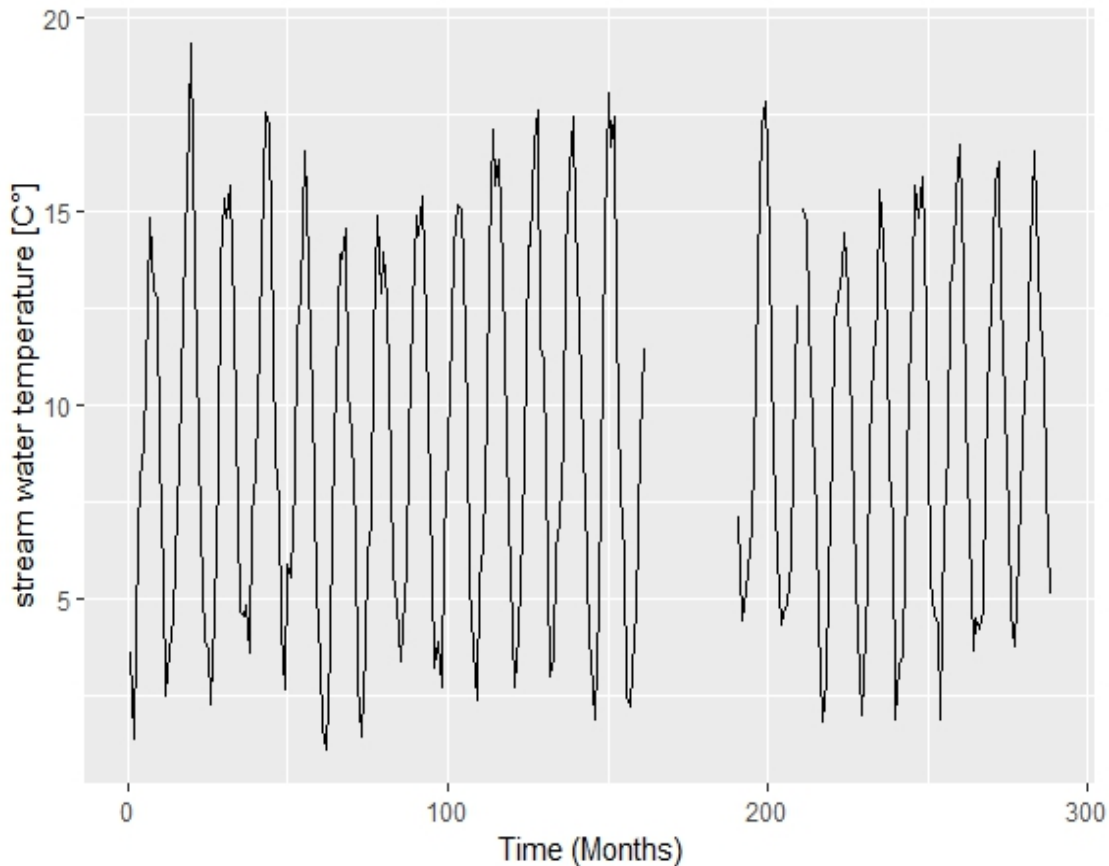


Figure 38: Time series of observed water temperature (gap divides calibration and validation period)

3.2.1.2 Groundwater temperature

The discharge-weighted model assumes that the stream temperature is dependent on the temperatures of a fast and a slow component. The temperature of the fast component is assumed to be the same as the air temperature, see below, the temperature of the slow component is assumed to be the temperature of the groundwater.

Since the groundwater temperature usually lags behind stream and air temperature (O. Mohseni & Stefan, 1999) the peaks of the slow component is not aligned to the peaks of the stream temperature, potentially resulting in poor model results – if the peaks were aligned the model would yield better stream temperature results. To achieve this the groundwater temperature has to be shifted to be aligned to the stream temperature (stream and air temperature are closely aligned, see Figure 17 above and the cross-correlation of the stream and air temperature in Figure 41 below).

To find out how big the lag is between stream temperature and groundwater temperature, a cross-correlation between groundwater temperature and stream temperature was conducted. This was done for the calibration period, for the validation period and

for the entire time series. The results were similar with either the highest correlation was at lag 3 (calibration period, with a value of 0.85) or at lag 4 (validation period and entire time series, with values of 0.89 and 0.86, respectively). Figure 39 gives the resulting graph for the whole time series. As the correlations are quite similar, a lag of 4 was used for the discharge-weighted model. That means the groundwater temperature was shifted four months back to align it to the stream temperature. In Figure 40 the groundwater and air temperature curves are plotted for a period of three years, to make the lag clearly visible.

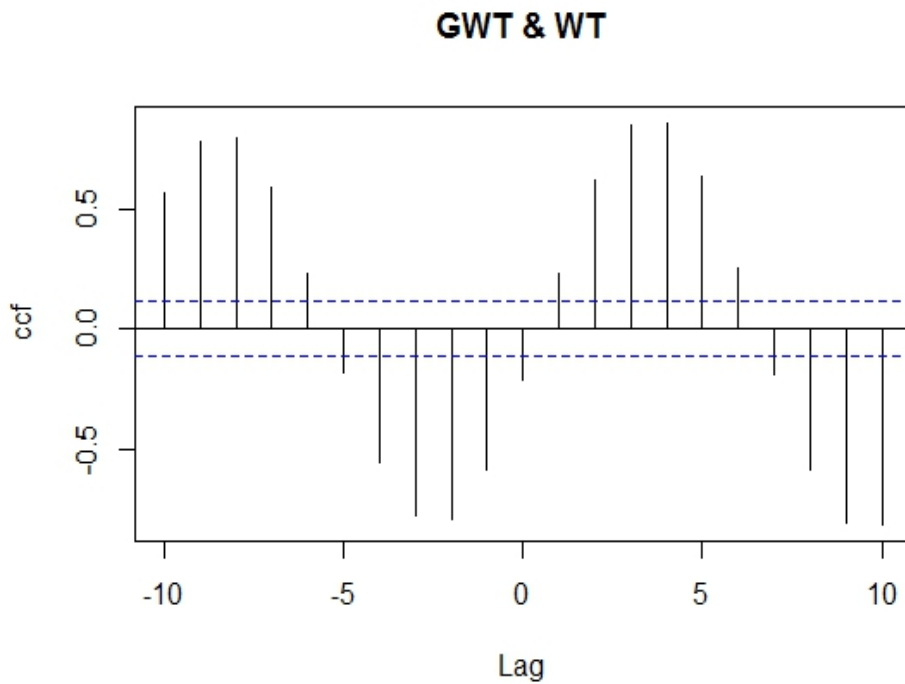


Figure 39: Cross-correlation of groundwater temperature and stream temperature, highest value at lag 4 with 0.86

The first four values were excluded from the period and the four subsequent values were included. (January, February, March, April 2015)

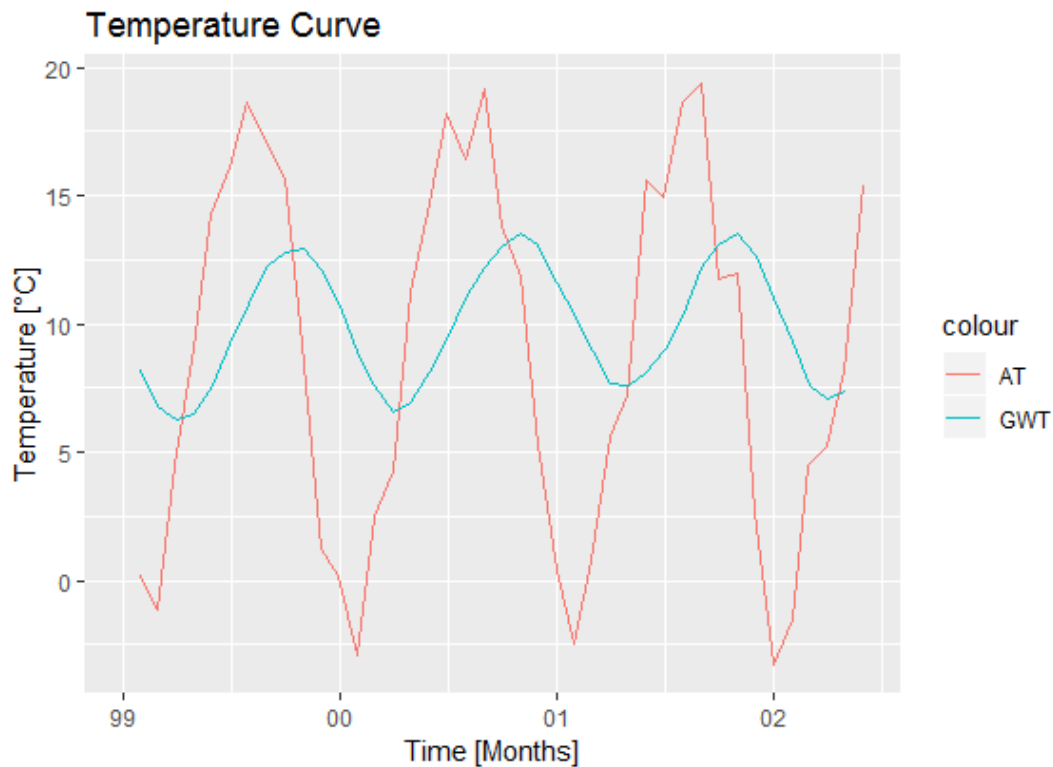


Figure 40: Comparison of air (AT) and groundwater (GWT) temperature

3.2.1.3 Air temperature

The temporal resolution of the air temperature time series was averaged to a monthly time series as the other input data for the water temperature prediction model is also in monthly resolution.

It is assumed that the fast component used in the discharge-weighted model has the same temperature as the air. To compare the relationship between stream temperature and air temperature a cross-correlation was conducted. As the lag which results in the maximum value (0.98) is zero, see Figure 41, there was no lag for the air temperature introduced in the model.

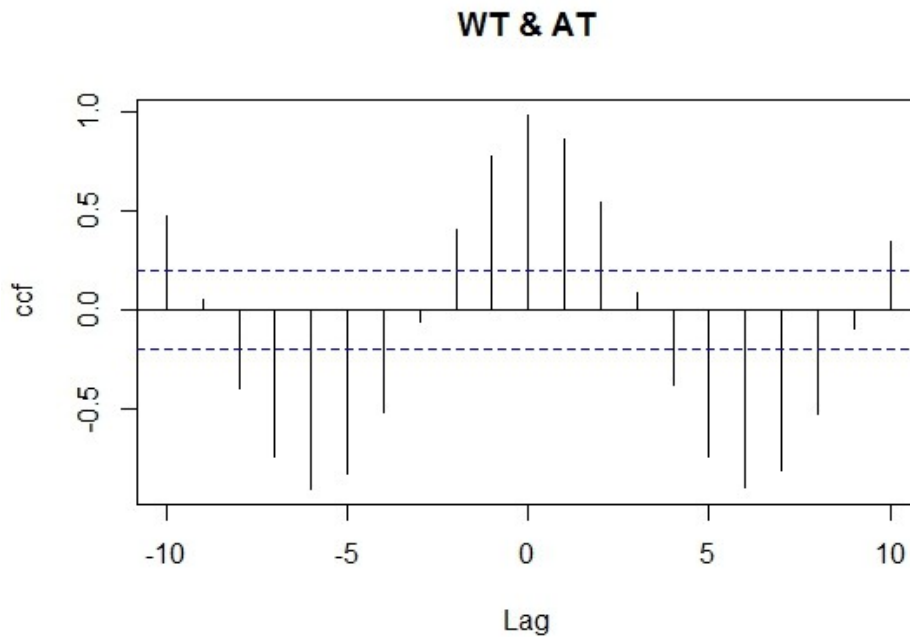


Figure 41: Cross-correlation of air and stream temperature, highest value at lag 0 with 0.98

3.2.2 Model results

The results in this section are all concerned with the (statistical) validation period from November 2006 to December 2014.

3.2.2.1 Discharge-weighted model

The proposed model for this thesis, a discharge-weighted model, is calculated using equation (17).

$$T_{Stream_S} = T_{Air} * \frac{V_{fast}}{V_{tot}} + T_{Groundwater} * \frac{V_{slow}}{V_{tot}} \quad (17)$$

With T_{Stream_S} as the simulated stream temperature, T_{Air} , and $T_{Groundwater}$ as the observed temperature of the air and the groundwater, respectively, and V_{fast} and V_{slow} as the amount of fast and slow discharge, respectively. V_{tot} is the total amount of discharge.

The resulting temperature graph is represented by the blue line in Figure 42, the dotted black line represents the observed time series (the big black dots are the observed values).

It is apparent at first glance that the discharge-weighted model fails to account for low temperatures, especially below 5 °C. The NSE and the KGE (depicted in the blue

box next to the graph, see equations (9) and (10) in section 2.3.6 for how they are calculated) are relatively low (compared with some other models, see below) at 0.62 and 0.67 respectively.

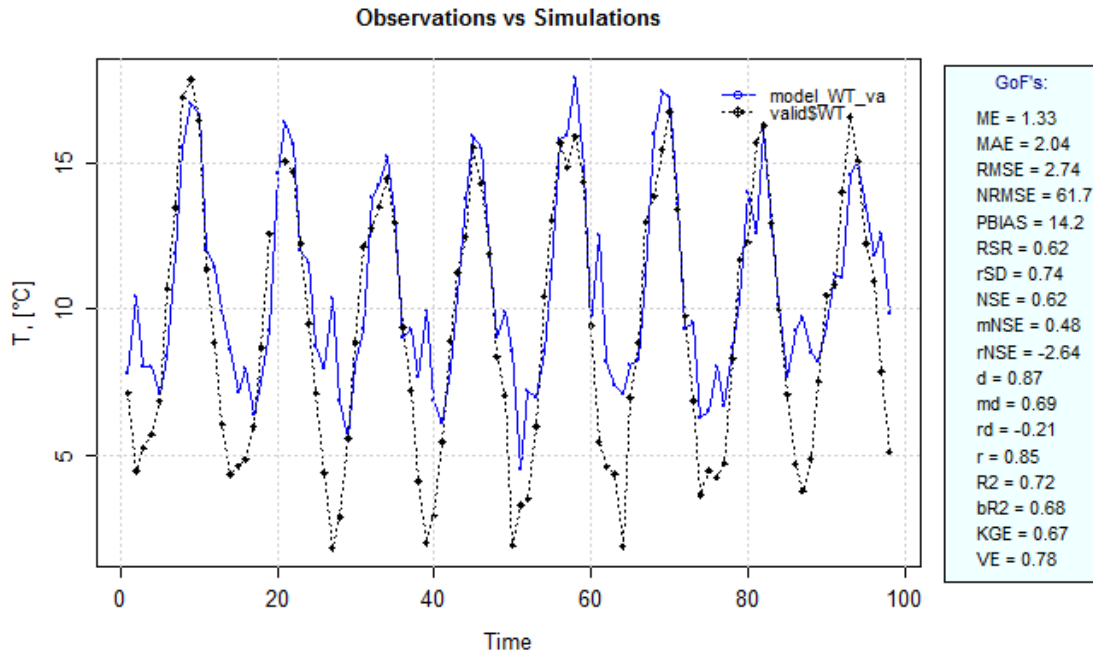


Figure 42: Discharge-weighted model without lagged groundwater temperature (blue line: model, black dots: observed values), for the validation period

3.2.2.2 Discharge-weighted model with lagged groundwater temperature

As described above in section 3.2.1.2 the groundwater time series was shifted back 4 months, otherwise the procedure was the same as for the unlagged groundwater time series, so equation (17) was used to estimate the stream temperature. The resulting graph in Figure 43 shows that with the lagged groundwater time series the modelled (blue) line maps the lower areas better, which results in a remarkable increase of values of NSE (0.87 vs. 0.62 unlagged) and KGE (0.88 vs. 0.67 unlagged).

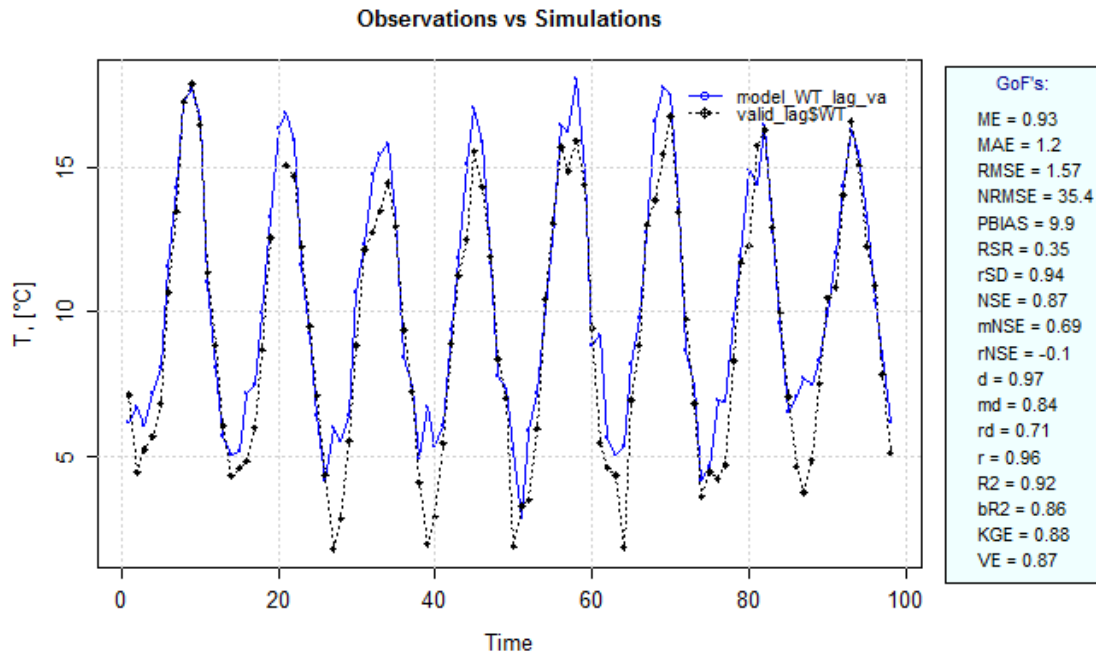


Figure 43: Discharge-weighted model with lagged groundwater temperature (blue line: model, black dots: observed values), for the validation period

3.2.3 Comparison to the linear regression model

A multiple linear regression model (see equation (13) in section 2.4.2) was used to establish a relationship between stream temperature and the explanatory variables air and groundwater temperature. For building the model, the calibration period mentioned above (in section 3.2.1.1) was used. The intercept and the coefficients for the resulting linear regression can be found in Table 8. These coefficients were then used with the air and groundwater temperature values of the validation period to get a simulated stream temperature.

Table 8: Intercept and coefficients of the multiple linear regression model

Intercept	Air temperature	Groundwater temperature
2.833633	0.649950	0.092851

The blue line in Figure 44 illustrates this simulated stream temperature, the black dots on the black line are the observed stream temperature values (monthly means) of the validation period. The goodness of fit parameters are listed in the light blue box on the right side of the figure; the NSE and the KGE are extremely high with 0.97 and 0.98 respectively.

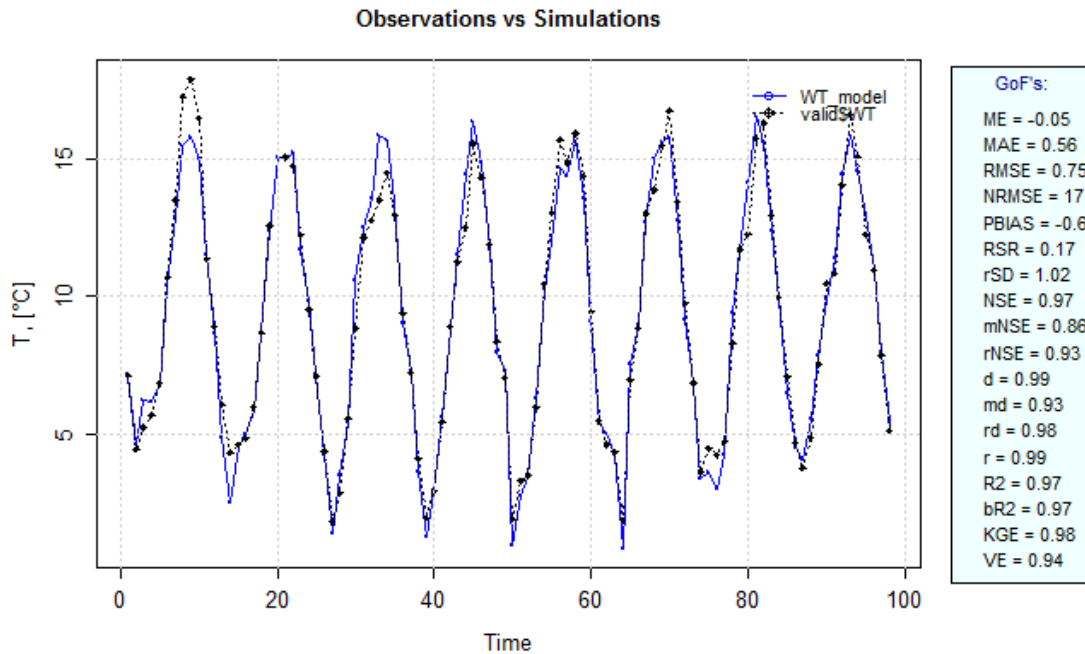


Figure 44: Linear regression model (blue line: model, black dots: observed values), for the validation period

3.2.4 Comparison to the non-linear regression model

A non-linear regression model developed by Mohseni et al. (1998) with air temperature as the only input parameter was used for comparison. In Table 9 the parameters of the model can be seen, see section 2.4.3 for further information on how the model was built.

Table 9: Parameters of the non-linear regression model

Alpha	Mu	Beta	gamma
20.00	0.00	9.60	0.14

The non-linear regression model looks strikingly similar to the linear regression model see Figure 45. The NSE and the KGE even have the same values, 0.97 and 0.98, respectively. As stated above in section 1.3.3, this is probably the case because the effects which cause the non-linearity of the air-temperature-water-temperature relationship (freezing and evaporative cooling) are averaged out in the monthly scale.

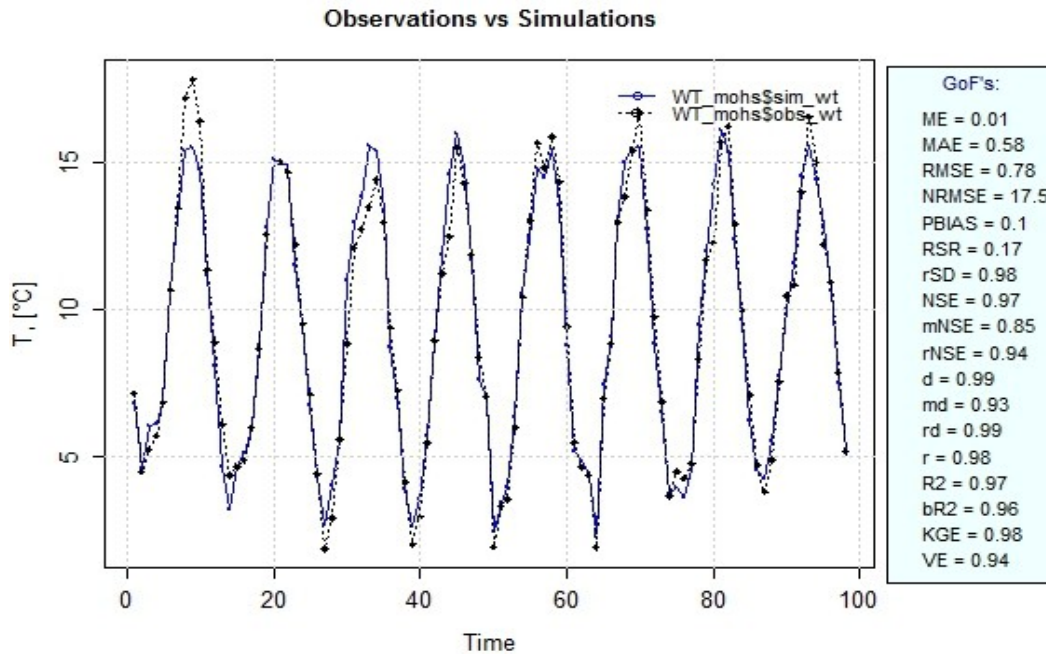


Figure 45: Non-linear regression model (blue line: model, black dots: observed values), for the validation period

3.2.5 Comparison to the unweighted model

To get information about the impact of the discharge weighting in this section another model was built, where the air temperature and the groundwater temperature are weighted equally. This can be achieved by adapting equation (12), so that for V_{fast} and V_{slow} the value 0.5 is used instead of the percentage of the respective discharges as in equation (18). Then the observed temperatures are no longer discharge-weighted but have an equal share of influence on the stream temperature.

$$T_{Stream_S} = T_{Air} * 0.5 + T_{Groundwater} * 0.5 \quad (18)$$

Again, see above, two different groundwater time series were used, one without lag and one with a lag of 4 months.

3.2.5.1 Unweighted without lagged groundwater temperature

As can be seen in Figure 46, when not weighted for discharge, the simulated stream temperature (blue line) fits the observed stream temperature considerably better than the discharge-weighted model. The NSE is 0.88 which is higher than the NSE of the discharge-weighted model (0.62) and even slightly better than the NSE of the dis-

charge-weighted model with lagged groundwater temperature (0.87). The KGE is 0.75, which is higher than the KGE of the discharge-weighted model without lag (0.67) but lower than the KGE of the discharge-weighted model with lagged groundwater temperature (0.88).

Noticeable is the shift of the unweighted curve downwards. Another striking change is the temporal alignment of the minimal values, even before lagging the groundwater temperature, this is the main reason for the much higher NSE value.

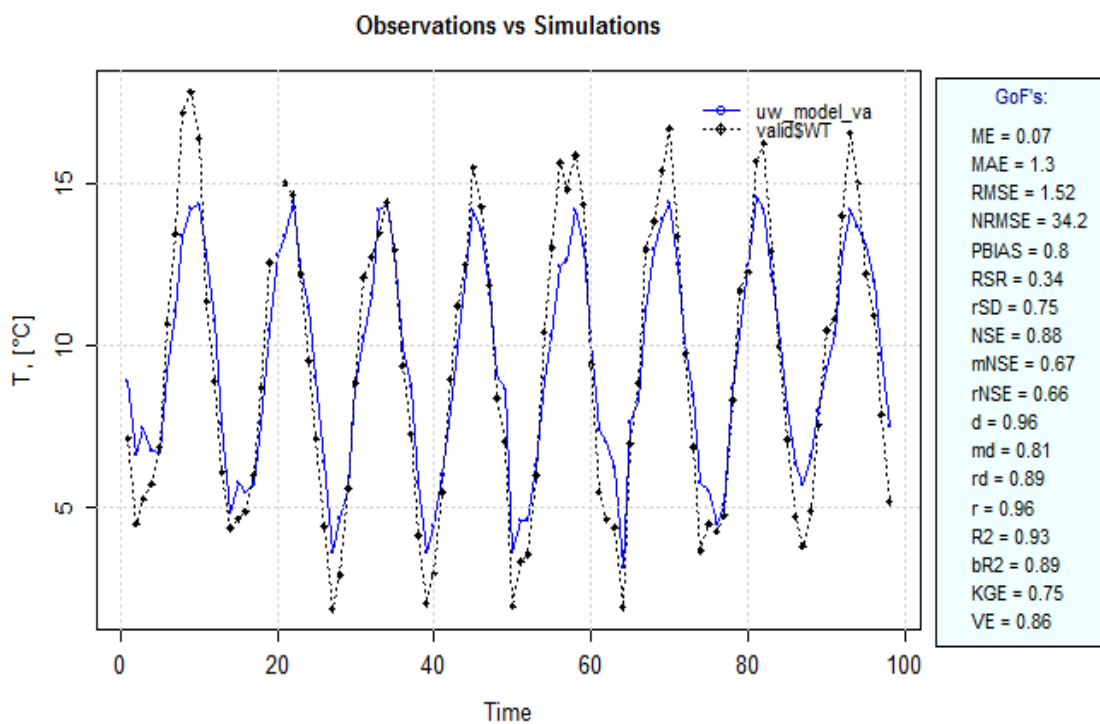


Figure 46: Unweighted-discharge model without lagged groundwater temperature (blue line: model, black dots: observed values), for the validation period

3.2.5.2 Unweighted with lagged groundwater temperature

The outcome of the model with a shift of groundwater temperature for four data points (months) is displayed in Figure 47. The simulated stream temperature, represented by the blue line, shows an almost perfect fit to the observed stream temperature (black line). This is also evident by looking at the values of NSE (0.97) and KGE (0.98) which are practically the same (rounded to the second decimal place) as in the linear regression model.

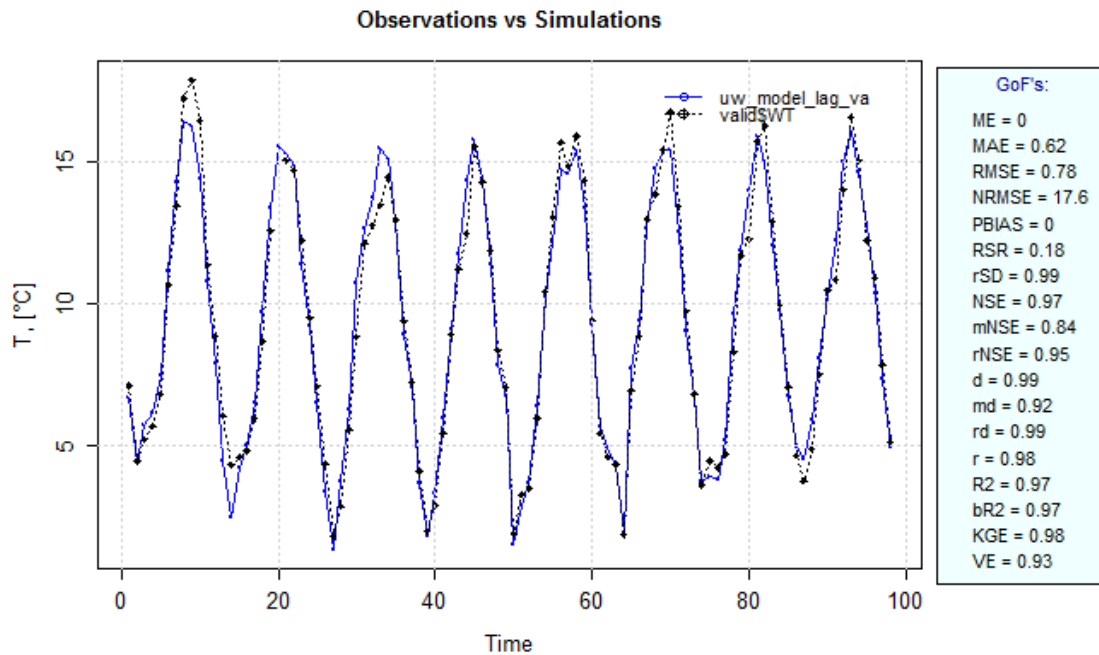


Figure 47: Unweighted-discharge model with lagged groundwater temperature (blue line: model, black dots: observed values), for the validation period

In Table 10 the observed stream temperature is compared to the discharge-weighted model, the linear regression model and the unweighted model. The range of the observed stream temperature is higher than each of the simulated temperatures' range, the linear regression model is closest to the observed values for the mean and the range. The discharge-weighted model is closest to the max value, and the unweighted model to the minimum value. The values of the discharge-weighted model are with the exception of the maximum value far off the observed values, the linear regression model and the unweighted model less so, unsurprisingly.

Table 10: Comparison of stream temperatures, observed values, linear regression model, discharge-weighted and unweighted model with lagged groundwater temperature (all values in °C) with closest values in bold.

Variable	Observed values	Lin-reg model	Discharge - weighted model	Unweighted model
mean	9.34	9.35	10.33	9.41
min	1.83	0.85	2.89	1.35
max	17.86	16.54	18.01	16.45
Range (abs.values)	16.03	15.69	15.01	15.10

3.2.5.3 Reasons for outperforming the discharge-weighted model

The reason why the unweighted model outperforms the discharge-weighted model lies in the core characteristic of the discharge-weighted model: it is weighted by the discharge, to be precise, by the fast and slow discharge component expressed in percentages. As can be seen in Figure 48 for a sample year (2010)¹³, the fast component (in grey) starts near zero, has a clear maximum in the middle of the year and decreases again towards the end of the year. This means that the influence of the fast component is very low at the beginning and the end of the year, in contrast to the slow component which is very influential at these times.

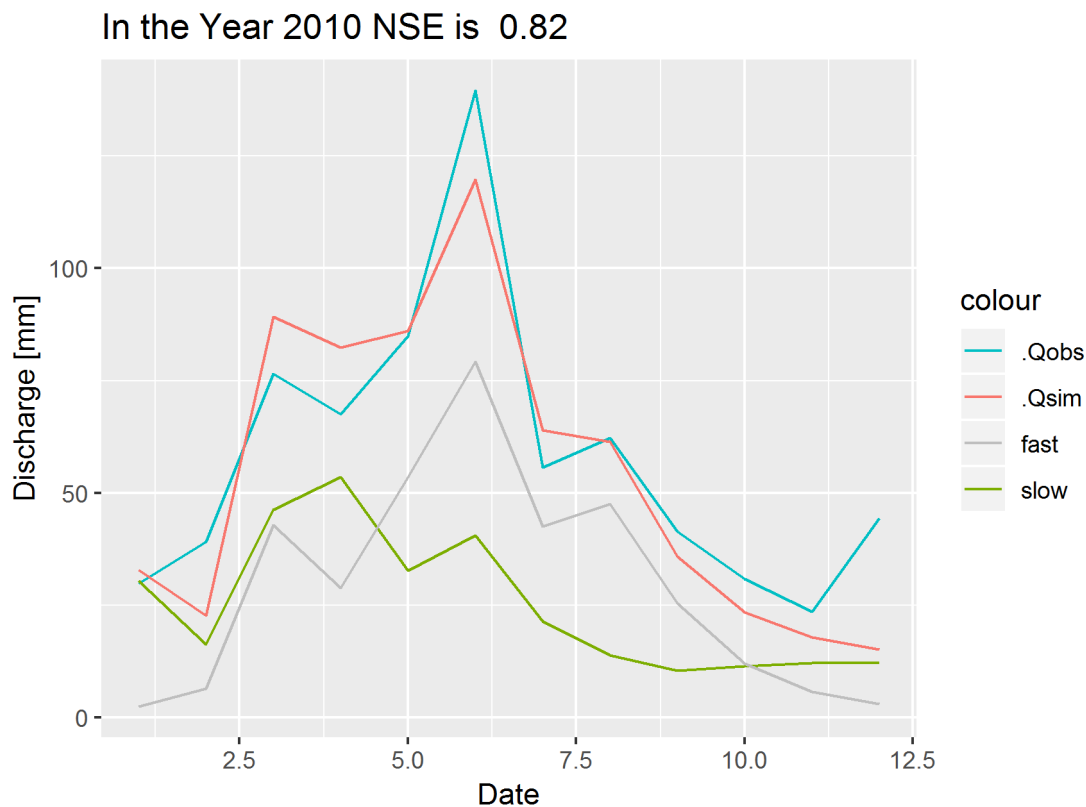


Figure 48: Observed discharge (blue) and simulated discharge (red) which is split up into the fast (grey) and slow (green) component

The air, groundwater and stream temperature distributions throughout the year 2010 can be seen in Figure 49. When taking a closer look at January the groundwater temperature (11.10 °C) is weighted with 92.4% of the discharge (slow component), and the air temperature (-3.99 °C) is weighted with 7.6% of the discharge (fast component). This means that in January 2010 the discharge-weighted model's output is 9.95 °C (groundwater temperature times slow component weight plus air temperature times

¹³ The year 2010 was not chosen arbitrarily as it shows a clear deviation of the weighted model at both the beginning and the end of the year, but it is also by no means unusual.

fast component weight) which is 8 °C above the observed temperature of 1.98 °C. The unweighted model which averages groundwater and air temperature generates a simulated stream temperature of 3.56 °C which is 1.6 °C above the observed temperature. These values are also shown in Table 11.

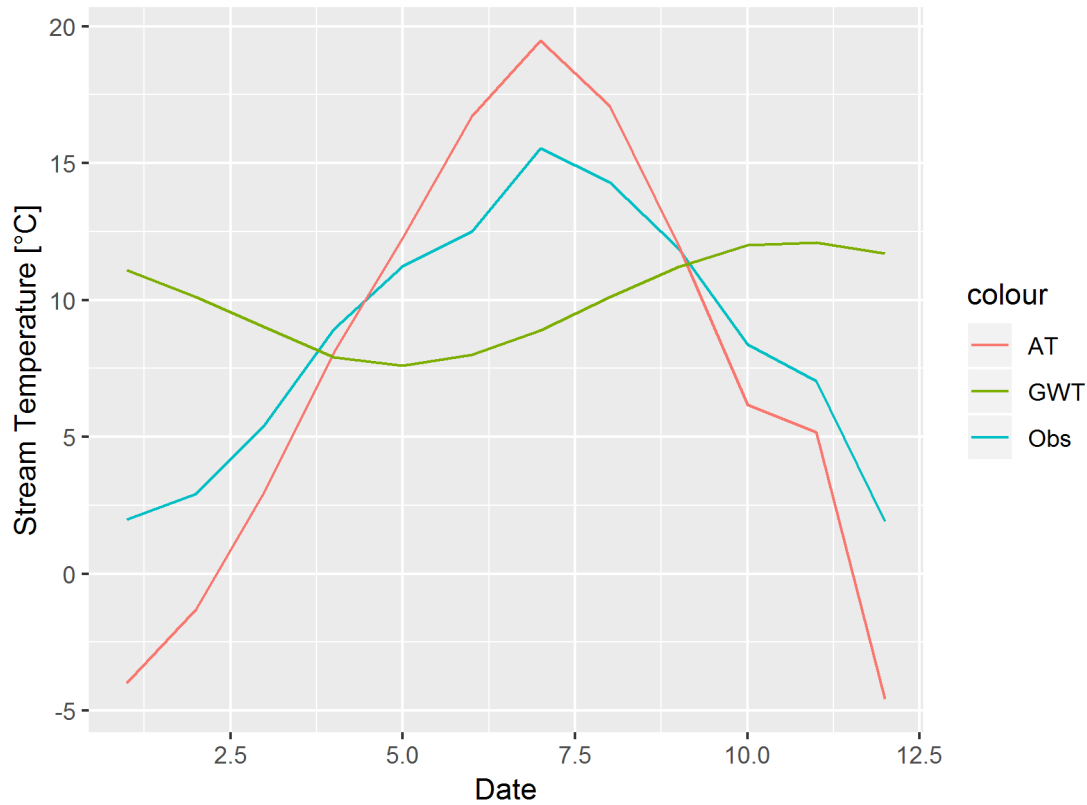


Figure 49: Temperature distributions of air (red), groundwater (green) and stream (blue) temperature

Table 11: Discharge components, temperature components and model results for January 2010

Slow C. [%]	Fast C. [%]	GWT [°C]	AT [°C]	W.M. [°C]	UW.M. [°C]	ObsT [°C]
92.4	7.6	11.10	-3.99	9.95	3.56	1.98

As can be seen in Figure 50 the discharge-weighted model introduces a large spike at the beginning of the year, at the end of the year there is also a smaller peak and in December the difference between observed and simulated discharge is over 6 °C. These peaks are the main reason that the NSE of the discharge-weighted model is just 0.45 compared to the NSE of the unweighted model of 0.94. When the first value of the discharge-weighted model is omitted, the NSE rises to 0.64, when additionally the last value is omitted, the NSE rises to 0.80.

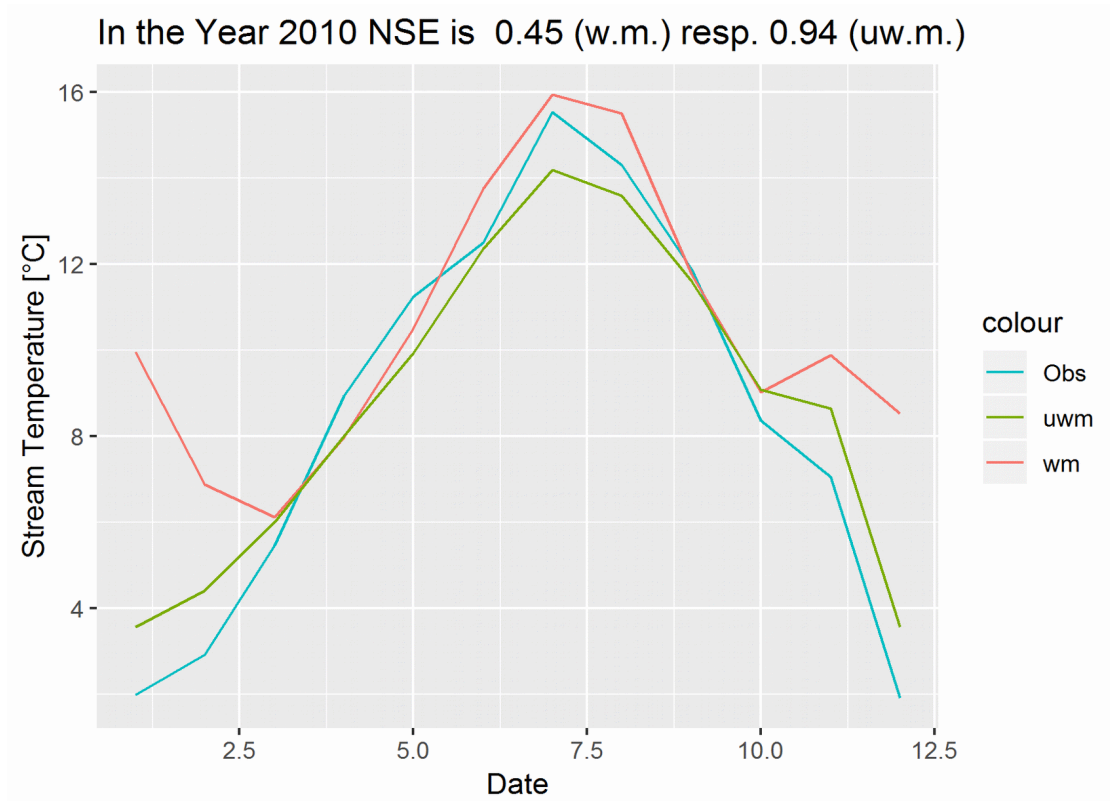


Figure 50: Observed temperature (blue), discharge-weighted model output (red), unweighted model output (green) for the year 2010

4 Conclusion

The discharge of the river Pielach was divided into two distinct components (slow and fast) and two separate temperature distributions were assigned to each component. These two temperature distributions were combined to estimate the stream temperature. The size of the discharge components, determined with the rainfall-runoff model MODMOD, was used for weighting the two temperature profiles.

The discharge-weighted hydrology-based model, although giving good results in modelling stream temperature (with an NSE of 0.87 and an KGE of 0.88) was not able to beat the more simple linear and non-linear models (both with an NSE of 0.97 and a KGE of 0.98). More importantly the model which didn't use the discharge components as weights had also higher goodness-of-fit parameters, again an NSE of 0.97 and a KGE of 0.98.

One reason for this performance is that for the discharge-weighted model the groundwater temperature was overrepresented at the beginning and the end of a given year. This behaviour occurs because the slow component, used as a weighting factor, accounts for the major part of the total discharge (often over 90%) at these points of time, thus pushing the simulated stream temperature high above the observed temperature. These peaks lead to reduced NSE values in comparison with the unweighted model where the air and groundwater temperature were just averaged for each month.

For future utilization of this model it may be beneficial to validate the hydrological model output by incorporating real-world data about groundwater inflows or to introduce some correction factor for instances where the weight of a discharge component drops below a certain threshold, for example $>25\%$.

For estimating the slow and fast component more accurately one option is to apply ground-based infrared thermography, as Schuetz & Weiler (2011) propose. As Beven and Germann (2013) attest, a physical theory which could also help with this issue seems not to be around the corner.

5 Appendices

Appendix I: inputmodna.txt (Gauge Hofstetten, for the validation period)

```
INPUT FUER NA_MODELL MODNA
-----
#Anzahl der Module nmodule und der Stränge
      6      3
#Länge der Stränge istlen
      3      2      1
#Modulesequenz: ( Baum / Strang / Modulcode
      1      4      5      6      3      9
      1      1      1      4      5
      2      2      6      3
      2      3      9
#Verwendung des Moduls für Bilanz-Summary - logout
      1      0      0      0      1      1
Pfad- und Dateinamen der Inputfiles *****
#Pfad der Dateistruktur pfad
C:\Users\Russ\Desktop\master\daten\
#Kurzbezeichnung (3 Zeichen) shortdesc
ha3
#Gebietsfile (Höhenverteilung, Expositionsklassen) elevfile
alt_hofstn.txt
#Glätscherfile (Höhenverteilung) glazfile
-999
#Meteorologiefile (Lufttemperatur, Niederschlag) metfile
PTET_V_Hofn.txt
#Verdunstungsfile (Pot ETP) petfile (-999 bei
-999
#Abflussfile (Beobachteter Abfluss) qfile
Qobs_V_Hofn.txt
#Rosaliafile (dat,time, n1,n2,n3,q) rosfile
-999
#Zeitdiskretisierung (Zeitschritte pro Tag) deltad
1.000000
#Seehöhe der Referenztemperatur aus metfile alttem
300.
#Hypsometrischer Gradient (Temperaturgradient/ Lapse Rate) hypgrad
-6.5000001E-03
#Correction factor precip [-] corr_ns
1.000000
#Correction factor ETpot [-] corr_etp
1.200000
Snow / Glacier *****
#Glätschschmelze berücksichtigt? (0=no, 1=yes) iglaz
0
# Strahlungsgradient radgrad
5.5000000E-02
#Schmelztemperatur (Schwellenwert in oC) thres
0.0000000E+00
#Grad-Tag-Faktor fuer Schnee fak
7.000000
#Grad-Tag-Faktor fuer Eis fakice
8.500000
#Strahlungsfaktor fuer Schnee fakrad
2.5000000E-02
#Strahlungsfaktor fuer Eis fakradice
```

```

9.9999998E-03
#Gewichtungsfaktor Temperaturindexanteil alpha
0.7000000
#Gewichtungsfaktor Strahlungsindex-anteil beta
0.3000000
#Mindestniederschlag (mm), ab dem albedo zurueckgesetzt wird ansalb
5.000000
#Minimumswert (Tageszahl des hydrol. Jahres) (31. Janner)
ishift=91+31
122
#Maximum des Tagestemperaturgang (Stunde 15h) shift
15
#Reduktionsfaktor / Streckungsfaktor des Tagesgangs (Gewichtung)
reduc
1.000000
#Jahresamplitude (+/-) des Grad-Tag-Faktors famp
1.000000
#Jahresamplitude der Schwellentemperatur tamp
0.0000000E+00
#Methode der Schmelzberechnung meltmethod
1
#Beruecksichtigung von albedo (1=ja,0=nein) ialb
0
#Verwendung von "Cold-Content" (1=ja,0=nein)icc
0
#"Cold-Content" threshold, sum of temperatu re for snow melt
0
#Verwendung von Expositionsgewichtung (1=ja,0=nein) iexp
0
# Prozentanteil des direkten Schmelzabflusses proz
40.00000
#Speicherkoeffizient des Linearspeichers fürSchneeabfluss sk
7.000000
#Speicherkoeffizient des Linearspeichers fürGletscherabfluss gsk
1.100000
API storage *****
#Retention constant apikval
7.000000
#Initial state of storage apistat
30.0000000E+00
#storage content lower stlow
0.0000000E+00
#storage content upper stup
30.00000
#runoff coefficient lower psilow
0.200000E+00
#runoff coefficient upper psiup
0.5000000
Split function *****
#Splitmethode (1=konst., 2=variabel, 3=Schwellenwert) isplitmet
2
#Aufteilung in Prozent (z.B. 30% = 0.30) splitproz
0.3000000
#Schwellenwert (z.B. 3m^2/s) splitswel
3
Plant available water storage
*****
Depth of Root storage (mm)
60.00000
Depth-Ratio of Rootstress (0 - 1)

```

```

0.100000
actual Water content (in mm)
30.000000
Single Linear Storage *****
#Retention constant akval
40.000000
#Initial state of storage aktstat
2.5000000E+00
Linear storage cascade
*****
#Retention constant akcasc (will be subdivided by istep)
1.500000
#Anzahl der Speicher istep
2
#Initial state of storage actcasc(5)
0.0000000E+00 0.0000000E+00 0.0000000E+00 0.0000000E+00
0.0000000E+00

```

Appendix II: alt_hofstn.txt

```

300, 100
22.95628
43.2980
55.93803
62.47877
45.55520
25.7518
14.34674
10.27744
7.057441
1.193843
0.057676

```

Appendix III: ALL_DATA.txt

```

year,month,WTemp,AirTemp,GWTemp,GWTemp_lag,slow_p,fast_p
1991,1,3.61,-1.116,11.4,8.9,0.852,0.148
1991,2,1.368,-4.382,9,9.9,0.861,0.139
1991,3,6.645,5.348,9.3,9.4,0.639,0.361
1991,4,8.05,5.943,8.6,9.2,0.389,0.611
1991,5,8.932,8.816,8.9,11.1,0.351,0.649
1991,6,12.627,14.73,9.9,13.5,0.667,0.333
1991,7,14.826,18.084,9.4,12.1,0.255,0.745
1991,8,12.935,17.287,9.2,11.4,0.401,0.599
1991,9,12.78,14.73,11.1,11.2,0.758,0.242
1991,10,8.803,7.19,13.5,11.3,0.6,0.4
1991,11,5.473,2.497,12.1,11.2,0.234,0.766
1991,12,2.471,-3.281,11.4,9.3,0.416,0.584
1992,1,3.665,0.965,11.2,9.4,0.739,0.261
1992,2,4.521,1.514,11.3,10.3,0.703,0.297
1992,3,5.987,3.765,11.2,11,0.642,0.358
1992,4,8.557,7.547,9.3,11.3,0.767,0.233
1992,5,12.474,13.284,9.4,10.9,0.748,0.252
1992,6,14.197,16.543,10.3,10.3,0.3,0.7
1992,7,17.277,18.723,11,12.1,0.343,0.657
1992,8,19.335,21.432,11.3,12.8,0.303,0.697
1992,9,13.623,13.71,10.9,11.5,0.065,0.935
1992,10,9.077,7.126,10.3,10.7,0.032,0.968
1992,11,6.787,4.607,12.1,9,0.336,0.664
1992,12,3.945,-1.884,12.8,7.8,0.797,0.203
1993,1,3.736,0.884,11.5,9.1,0.691,0.309

```

1993,2,2.25,-2.757,10.7,7.9,0.936,0.064
1993,3,4.539,1.987,9,8.5,0.487,0.513
1993,4,8.413,8.44,7.8,10.4,0.719,0.281
1993,5,13.645,14.965,9.1,11.6,0.82,0.18
1993,6,15.327,16.42,7.9,12.6,0.386,0.614
1993,7,14.858,16.497,8.5,12.3,0.191,0.809
1993,8,15.681,17.297,10.4,12.2,0.117,0.883
1993,9,12.213,12.92,11.6,11,0.159,0.841
1993,10,9.668,8.761,12.6,10.1,0.118,0.882
1993,11,4.683,0.117,12.3,8.9,0.524,0.476
1993,12,4.539,1.445,12.2,8.6,0.556,0.444
1994,1,4.858,2.306,11,8.8,0.68,0.32
1994,2,3.596,-0.139,10.1,8.9,0.867,0.133
1994,3,7.139,6.897,8.9,9.9,0.617,0.383
1994,4,8.257,7.567,8.6,10.9,0.615,0.385
1994,5,11.652,12.913,8.8,12,0.577,0.423
1994,6,13.877,16.733,8.9,13.1,0.495,0.505
1994,7,17.561,20.461,9.9,13.5,0.385,0.615
1994,8,17.216,19.229,10.9,12.5,0.191,0.809
1994,9,14.37,14.897,12,11.4,0.194,0.806
1994,10,8.645,7.219,13.1,10.3,0.065,0.935
1994,11,7.54,6.823,13.5,9.5,0.214,0.786
1994,12,4.229,0.606,12.5,7.9,0.608,0.392
1995,1,2.687,-1.91,11.4,8.5,0.702,0.298
1995,2,5.914,4.379,10.3,8.8,0.669,0.331
1995,3,5.552,2.332,9.5,NA,0.681,0.319
1995,4,8.05,8.687,7.9,NA,0.648,0.352
1995,5,11.845,12.881,8.5,NA,0.748,0.252
1995,6,12.833,14.73,8.8,NA,0.314,0.686
1995,7,16.584,20.384,NA,NA,0.435,0.565
1995,8,15.323,16.365,NA,NA,0.123,0.877
1995,9,11.567,11.987,NA,NA,0.111,0.889
1995,10,10.361,10.429,NA,9.1,0.374,0.626
1995,11,5.147,0.017,NA,8.1,0.306,0.694
1995,12,3.452,-2.306,NA,6.6,0.672,0.328
1996,1,1.687,-5.174,NA,7.2,0.99,0.01
1996,2,1.128,-3.954,9.1,8.2,0.778,0.222
1996,3,3.729,-0.039,8.1,8.9,0.526,0.474
1996,4,6.96,7.187,6.6,8.2,0.47,0.53
1996,5,10.71,12.887,7.2,10.7,0.566,0.434
1996,6,13.917,16.293,8.2,11.9,0.632,0.368
1996,7,13.781,16.39,8.9,11.8,0.421,0.579
1996,8,14.587,16.597,8.2,11.2,0.339,0.661
1996,9,10.36,10.39,10.7,9.9,0.267,0.733
1996,10,9.29,8.981,11.9,9.2,0.477,0.523
1996,11,6.803,4.707,11.8,8.1,0.816,0.184
1996,12,2.855,-4.384,11.2,7.5,0.958,0.042
1997,1,1.462,-4.345,9.9,8.2,1,0
1997,2,3.731,1.589,9.2,8.2,0.506,0.494
1997,3,6.143,4.113,8.1,9.8,0.523,0.477
1997,4,6.939,4.917,7.5,NA,0.69,0.31
1997,5,11.677,13.555,8.2,10.7,0.664,0.336
1997,6,14.901,17.123,8.2,9.9,0.515,0.485
1997,7,12.908,16.929,9.8,11.1,0.236,0.764
1997,8,13.927,17.339,NA,10.8,0.498,0.502
1997,9,12.751,13.45,10.7,10.1,0.58,0.42
1997,10,8.239,6.161,9.9,9.1,0.261,0.739
1997,11,5.706,3.233,11.1,8.4,0.421,0.579
1997,12,4.852,0.748,10.8,7.8,0.624,0.376
1998,1,3.371,-0.384,10.1,8.6,0.871,0.129

1998,2,4.211,2.6,9.1,7.6,0.624,0.376
1998,3,5.758,3.265,8.4,8.8,0.553,0.447
1998,4,9.047,8.71,7.8,10.9,0.716,0.284
1998,5,12.46,13.352,8.6,8.7,0.614,0.386
1998,6,14.923,17.323,7.6,9.2,0.287,0.713
1998,7,14.4,18.071,8.8,12.1,0.122,0.878
1998,8,15.425,18.216,10.9,NA,0.132,0.868
1998,9,11.995,13.293,8.7,NA,0.044,0.956
1998,10,9.781,9.716,9.2,8.2,0.237,0.763
1998,11,5.609,1.357,12.1,6.8,0.625,0.375
1998,12,3.244,-1.745,NA,6.3,0.673,0.327
1999,1,3.888,0.174,NA,6.5,0.792,0.208
1999,2,2.742,-1.104,8.2,7.6,0.724,0.276
1999,3,6.429,4.474,6.8,9.2,0.599,0.401
1999,4,8.953,9.063,6.3,10.8,0.735,0.265
1999,5,11.908,14.281,6.5,12.3,0.549,0.451
1999,6,14.11,16.147,7.6,12.8,0.35,0.65
1999,7,15.191,18.616,9.2,12.9,0.127,0.873
1999,8,15.041,17.094,10.8,12.1,0.098,0.902
1999,9,13.589,15.703,12.3,10.7,0.12,0.88
1999,10,9.603,9.232,12.8,8.9,0.121,0.879
1999,11,5.401,1.257,12.9,7.6,0.064,0.936
1999,12,3.73,0.177,12.1,6.6,0.541,0.459
2000,1,2.389,-2.874,10.7,6.9,0.614,0.386
2000,2,5.499,2.521,8.9,8.1,0.612,0.388
2000,3,6.344,4.297,7.6,9.5,0.635,0.365
2000,4,9.842,11.22,6.6,11,0.825,0.175
2000,5,13.812,14.69,6.9,12.2,0.718,0.282
2000,6,17.114,18.21,8.1,13,0.5,0.5
2000,7,15.693,16.442,9.5,13.5,0.211,0.789
2000,8,16.368,19.168,11,13.1,0.098,0.902
2000,9,13.499,13.793,12.2,11.6,0.089,0.911
2000,10,11.339,11.848,13,10.3,0.062,0.938
2000,11,7.111,5.283,13.5,8.9,0.029,0.971
2000,12,4.148,0.448,13.1,7.7,0.06,0.94
2001,1,2.692,-2.494,11.6,7.6,0.609,0.391
2001,2,4.109,0.796,10.3,8.1,0.586,0.414
2001,3,6.796,5.619,8.9,9,0.528,0.472
2001,4,8.587,7.203,7.7,10.3,0.681,0.319
2001,5,14.137,15.568,7.6,12.2,0.696,0.304
2001,6,14.134,14.927,8.1,13.1,0.364,0.636
2001,7,16.704,18.645,9,13.5,0.162,0.838
2001,8,17.625,19.345,10.3,12.6,0.115,0.885
2001,9,11.503,11.727,12.2,11,0.21,0.79
2001,10,11.182,11.984,13.1,9.3,0.815,0.185
2001,11,5.643,2.747,13.5,7.6,0.413,0.587
2001,12,3.015,-3.258,12.6,7.1,0.65,0.35
2002,1,3.464,-1.535,11,7.4,0.548,0.452
2002,2,6.25,4.5,9.3,8.3,0.672,0.328
2002,3,6.98,5.219,7.6,9.9,0.563,0.437
2002,4,8.987,8.19,7.1,12.4,0.829,0.171
2002,5,13.813,15.384,7.4,13.8,0.741,0.259
2002,6,16.07,18.82,8.3,14.1,0.275,0.725
2002,7,17.435,19.074,9.9,13.2,0.228,0.772
2002,8,14.912,18.329,12.4,11.7,0.204,0.796
2002,9,12.131,12.463,13.8,9.6,0.297,0.703
2002,10,8.849,7.897,14.1,8.1,0.569,0.431
2002,11,7.659,5.833,13.2,6.9,0.632,0.368
2002,12,3.927,-1.158,11.7,6.3,0.759,0.241
2003,1,3.455,-1.787,9.6,6.4,0.747,0.253

2003,2,1.859,-4.739,8.1,7.3,0.97,0.03
2003,3,4.861,4.081,6.9,9,0.633,0.367
2003,4,7.992,7.043,6.3,11.4,0.774,0.226
2003,5,14.437,15.442,6.4,13.4,0.545,0.455
2003,6,18.041,20.53,7.3,14.9,0.36,0.64
2003,7,16.674,19.316,9,15,0.173,0.827
2003,8,17.458,20.665,11.4,13.8,0.127,0.873
2003,9,12.196,12.75,13.4,11.8,0.029,0.971
2003,10,7.781,5.426,14.9,9.6,0.324,0.676
2003,11,6.134,4.353,15,7.7,0.668,0.332
2003,12,2.475,-1.832,13.8,6.4,0.742,0.258
2004,1,2.211,-3.281,11.8,6.4,0.811,0.189
2004,2,4.055,1.525,9.6,7.8,0.607,0.393
2004,3,4.634,1.487,7.7,9.3,0.642,0.358
2004,4,9.063,8.753,6.4,10.6,0.706,0.294
2004,5,11.462,11.765,6.4,11.6,0.548,0.452
2004,6,NA,15.89,7.8,12.7,0.24,0.76
2004,7,NA,17.81,9.3,13,0.31,0.69
2004,8,NA,17.923,10.6,12.4,0.162,0.838
2004,9,NA,12.887,11.6,11.2,0.047,0.953
2004,10,NA,9.897,12.7,9.5,0.057,0.943
2004,11,NA,3.567,13,7.8,0.335,0.665
2004,12,NA,-1.181,12.4,6.5,0.832,0.168
2005,1,NA,-0.558,11.2,6.4,0.716,0.284
2005,2,NA,-3.514,9.5,7.3,0.778,0.222
2005,3,NA,1.11,7.8,8.8,0.406,0.594
2005,4,NA,8.07,6.5,10.7,0.671,0.329
2005,5,NA,13.077,6.4,12.2,0.568,0.432
2005,6,NA,16.273,7.3,13,0.584,0.416
2005,7,NA,17.694,8.8,12.9,0.223,0.777
2005,8,NA,15.49,10.7,12.2,0.224,0.776
2005,9,NA,13.867,12.2,10.9,0.415,0.585
2005,10,NA,9.123,13,9.3,0.531,0.469
2005,11,NA,2.093,12.9,7.8,0.406,0.594
2005,12,NA,-1.726,12.2,6.2,0.224,0.776
2006,1,NA,-6.658,10.9,6.1,0.607,0.393
2006,2,NA,-2.107,9.3,7.1,0.559,0.441
2006,3,NA,0.687,7.8,8.5,0.35,0.65
2006,4,NA,8.147,6.2,10.9,0.497,0.503
2006,5,NA,12.329,6.1,12.2,0.695,0.305
2006,6,NA,16.473,7.1,12.9,0.455,0.545
2006,7,NA,20.323,8.5,12.9,0.6,0.4
2006,8,NA,14.826,10.9,12.3,0.289,0.711
2006,9,NA,15.483,12.2,11.2,0.653,0.347
2006,10,NA,9.929,12.9,9.8,0.608,0.392
2006,11,7.123,4.843,12.9,8.5,0.369,0.631
2006,12,4.467,0.958,12.3,7.9,0.834,0.166
2007,1,5.237,3.648,11.2,7.8,0.577,0.423
2007,2,5.699,3.714,9.8,8.6,0.707,0.293
2007,3,6.837,4.845,8.5,10.1,0.62,0.38
2007,4,10.67,10.517,7.9,11.8,0.822,0.178
2007,5,13.463,14.281,7.8,14.3,0.371,0.629
2007,6,17.234,18.2,8.6,14.7,0.281,0.719
2007,7,17.863,18.49,10.1,14,0.173,0.827
2007,8,16.442,17.026,11.8,11.8,0.062,0.938
2007,9,11.363,11.28,14.3,10.3,0.263,0.737
2007,10,8.871,6.871,14.7,8.9,0.58,0.42
2007,11,6.068,1.14,14,7.8,0.686,0.314
2007,12,4.336,-2.206,11.8,7.2,0.772,0.228
2008,1,4.612,1.181,10.3,7.3,0.657,0.343

2008,2,4.846,2.039,8.9,8,0.862,0.138
2008,3,5.986,3.584,7.8,9.4,0.67,0.33
2008,4,8.681,7.897,7.2,11.5,0.577,0.423
2008,5,12.566,13.677,7.3,13.1,0.695,0.305
2008,6,NA,17.647,8,13.5,0.314,0.686
2008,7,15.043,17.384,9.4,13.2,0.126,0.874
2008,8,14.706,17.381,11.5,12.4,0.297,0.703
2008,9,12.234,11.763,13.1,11,0.175,0.825
2008,10,9.515,8.826,13.5,9.6,0.591,0.409
2008,11,7.105,4.813,13.2,8.2,0.469,0.531
2008,12,4.374,0.406,12.4,6.4,0.633,0.367
2009,1,1.834,-3.794,11,6.5,0.955,0.045
2009,2,2.871,-0.3,9.6,7.8,0.721,0.279
2009,3,5.571,2.81,8.2,9.8,0.515,0.485
2009,4,8.845,10.983,6.4,10.5,0.63,0.37
2009,5,12.135,13.977,6.5,11.3,0.625,0.375
2009,6,12.759,15.413,7.8,12.1,0.207,0.793
2009,7,13.481,18.606,9.8,12.3,0.5,0.5
2009,8,14.459,18.216,10.5,12,0.39,0.61
2009,9,12.954,14.637,11.3,11.1,0.377,0.623
2009,10,9.379,7.755,12.1,10.1,0.288,0.712
2009,11,7.238,5.12,12.3,9,0.588,0.412
2009,12,4.106,-0.481,12,7.9,0.652,0.348
2010,1,1.978,-3.987,11.1,7.6,0.924,0.076
2010,2,2.92,-1.296,10.1,8,0.717,0.283
2010,3,5.458,3.003,9,8.9,0.519,0.481
2010,4,8.93,8.09,7.9,10.1,0.649,0.351
2010,5,11.239,12.261,7.6,11.2,0.379,0.621
2010,6,12.487,16.707,8,12,0.339,0.661
2010,7,15.538,19.484,8.9,12.1,0.335,0.665
2010,8,14.309,17.077,10.1,11.7,0.225,0.775
2010,9,11.881,12,11.2,10.8,0.291,0.709
2010,10,8.364,6.165,12,9.5,0.488,0.512
2010,11,7.044,5.177,12.1,8.4,0.679,0.321
2010,12,1.91,-4.584,11.7,7.6,0.805,0.195
2011,1,3.3,-1.665,10.8,7.5,0.497,0.503
2011,2,3.513,-0.375,9.5,7.8,0.768,0.232
2011,3,5.976,4.142,8.4,8.7,0.668,0.332
2011,4,10.436,10.363,7.6,10.1,0.66,0.34
2011,5,13.043,13.058,7.5,11.3,0.314,0.686
2011,6,15.686,17.097,7.8,12.4,0.142,0.858
2011,7,14.858,16.51,8.7,12.7,0.072,0.928
2011,8,15.903,18.319,10.1,12.5,0.053,0.947
2011,9,14.364,14.877,11.3,11.9,0.022,0.978
2011,10,9.429,7.832,12.4,10.8,0.345,0.655
2011,11,5.462,2.087,12.7,9.3,0.986,0.014
2011,12,4.619,1.603,12.5,8.3,0.606,0.394
2012,1,4.363,0.471,11.9,8.1,0.604,0.396
2012,2,1.873,-4.596,10.8,8.5,0.76,0.24
2012,3,6.953,5.9,9.3,9.5,0.637,0.363
2012,4,8.854,8.27,8.3,10.5,0.668,0.332
2012,5,12.983,13.968,8.1,11.4,0.486,0.514
2012,6,13.86,17.44,8.5,12.1,0.163,0.837
2012,7,15.445,18.31,9.5,12.5,0.096,0.904
2012,8,16.738,18.442,10.5,12.4,0.15,0.85
2012,9,13.413,13.647,11.4,11.4,0.038,0.962
2012,10,9.753,7.974,12.1,10.1,0.318,0.682
2012,11,6.848,4.377,12.5,9.2,0.634,0.366
2012,12,3.643,-0.965,12.4,8.5,0.542,0.458
2013,1,4.475,-0.358,11.4,8.2,0.584,0.416

2013,2,4.241,-1.175,10.1,8.8,0.815,0.185
2013,3,4.723,0.894,9.2,9.5,0.699,0.301
2013,4,8.303,8.85,8.5,10.4,0.579,0.421
2013,5,11.701,12.49,8.2,11.3,0.506,0.494
2013,6,12.276,16.087,8.8,11.9,0.286,0.714
2013,7,15.714,19.732,9.5,12.1,0.699,0.301
2013,8,16.275,18.161,10.4,11.8,0.267,0.733
2013,9,12.923,13.063,11.3,11.1,0.163,0.837
2013,10,9.988,9.139,11.9,10.4,0.36,0.64
2013,11,7.081,3.907,12.1,9.6,0.463,0.537
2013,12,4.68,0.871,11.8,9,0.765,0.235
2014,1,3.781,0.303,11.1,8.8,0.875,0.125
2014,2,4.868,2.704,10.4,9.1,0.752,0.248
2014,3,7.529,6.319,9.6,9.8,0.569,0.431
2014,4,10.469,9.593,9,11,0.247,0.753
2014,5,10.839,11.874,8.8,12.6,0.226,0.774
2014,6,14.022,16.563,9.1,13.5,0.74,0.26
2014,7,16.583,18.619,9.8,13.5,0.458,0.542
2014,8,15.051,16.423,11,12.8,0.249,0.751
2014,9,12.234,13.773,12.6,11.7,0.24,0.76
2014,10,10.925,10.532,13.5,10.2,0.443,0.557
2014,11,7.87,5.97,13.5,8.8,0.88,0.12
2014,12,5.13,2.213,12.8,7.7,0.72,0.28

6 Bibliography

- Benyahya, L., Caissie, D., St-Hilaire, A., Ouarda, T. B. M. J., & Bobée, B. (2007). A Review of Statistical Water Temperature Models. *Canadian Water Resources Journal*, 32(3), 179–192. <https://doi.org/10.4296/cwrj3203179>
- Benyahya, L., St-Hilaire, A., Ouarda, T. B. M. J., Bobée, B., & Dumas, J. (2008). Comparison of non-parametric and parametric water temperature models on the Nivelle River, France. *Hydrological Sciences Journal*, 53(3), 640–655. <https://doi.org/10.1623/hysj.53.3.640>
- Beven, K., & Germann, P. (2013). Macropores and water flow in soils revisited: REVIEW. *Water Resources Research*, 49(6), 3071–3092. <https://doi.org/10.1002/wrcr.20156>
- BMLFUW. (2014). *Flächenverzeichnis der Flussgebiete: Donaugebiet von der Enns bis zur Leitha*. (No. 62). Retrieved from <https://www.bmnt.gv.at/dam/jcr:33699a3d-88fd-4dbc-8081-4d28c80f83bc/Beitrag%2062.pdf>
- BMNT. (2018a). *Pegel Hofstetten(Bad)*. Wien: Bundesministerium für Nachhaltigkeit und Tourismus.
- BMNT. (2018b). *Pegel Loich*. Wien: Bundesministerium für Nachhaltigkeit und Tourismus.
- Brown, G. W. (1969). Predicting Temperatures of Small Streams. *Water Resources Research*, 5(1), 68–75. <https://doi.org/10.1029/WR005i001p00068>
- Caissie, D. (2006). The thermal regime of rivers: a review. *Freshwater Biology*, 51(8), 1389–1406. <https://doi.org/10.1111/j.1365-2427.2006.01597.x>
- Carr, G. M., Duthie, H. C., & Taylor, W. D. (1997). Models of aquatic plant productivity: a review of the factors that influence growth. *Aquatic Botany*, 59(3–4), 195–215. [https://doi.org/10.1016/S0304-3770\(97\)00071-5](https://doi.org/10.1016/S0304-3770(97)00071-5)

- Costanza, R., d'Arge, R., de Groot, R., Farber, S., Grasso, M., Hannon, B., ... van den Belt, M. (1997). The value of the world's ecosystem services and natural capital. *Nature*, 387(6630), 253–260. <https://doi.org/10.1038/387253a0>
- Crozier, L. G., Zabel, R. W., Hockersmith, E. E., & Achord, S. (2010). Interacting effects of density and temperature on body size in multiple populations of Chinook salmon. *Journal of Animal Ecology*, 79(2), 342–349. <https://doi.org/10.1111/j.1365-2656.2009.01641.x>
- Delpla, I., Jung, A.-V., Baures, E., Clement, M., & Thomas, O. (2009). Impacts of climate change on surface water quality in relation to drinking water production. *Environment International*, 35(8), 1225–1233. <https://doi.org/10.1016/j.envint.2009.07.001>
- Demars, B. O. L., Russell Manson, J., Ólafsson, J. S., Gíslason, G. M., Gudmundsdóttir, R., Woodward, G., ... Friberg, N. (2011). Temperature and the metabolic balance of streams: Temperature and the metabolic balance of streams. *Freshwater Biology*, 56(6), 1106–1121. <https://doi.org/10.1111/j.1365-2427.2010.02554.x>
- E. Rieman, B., Isaak, D., Adams, S., Horan, D., David, N., Luce, C., & Myers, D. (2007). Anticipated climate warming effects on bull trout and their habitats across the Interior Columbia River Basin. *Transactions of the American Fisheries Society*, 136, 1552–1565. <https://doi.org/10.1577/T07-028.1>
- Eckel, O., & Reuter, H. (1950). Zur Berechnung des Sommerlichen Wärmeumsatzes in Flussläufen. *Geografiska Annaler*, 32(3–4), 188–209. <https://doi.org/10.1080/20014422.1950.11880830>
- Edinger, J. E., Duttweiler, D. W., & Geyer, J. C. (1968). The Response of Water Temperatures to Meteorological Conditions. *Water Resources Research*, 4(5), 1137–1143. <https://doi.org/10.1029/WR004i005p01137>
- European Environment Agency (Ed.). (2008). *Energy and environment report 2008*. Copenhagen, Denmark : Luxembourg: European Environment Agency ; Office for Official Publications of the European Communities.

- European Environment Agency, European Commission, & World Health Organization (Eds.). (2008). *Impacts of Europe's changing climate: 2008 indicator-based assessment: joint EEA-JRC-WHO report*. Copenhagen : Luxembourg: European Environment Agency ; Office for Official Publications of the European Communities [distributor].
- Ficke, A. D., Myrick, C. A., & Hansen, L. J. (2007). Potential impacts of global climate change on freshwater fisheries. *Reviews in Fish Biology and Fisheries*, 17(4), 581–613. <https://doi.org/10.1007/s11160-007-9059-5>
- Foerster, H., & Lilliestam, J. (2010). Modeling thermoelectric power generation in view of climate change. *Regional Environmental Change*, 10(4), 327–338. <https://doi.org/10.1007/s10113-009-0104-x>
- GDAL Development Team. (2017). *GDAL - Geospatial Data Abstraction Library, Version 2.1.3*. Retrieved from <http://www.gdal.org>
- Grant, P. J. (1977). WATER TEMPERATURES OF THE NGARURORO RIVER AT THREE STATIONS. *Journal of Hydrology (New Zealand)*, 16(2), 148–157.
- GRASS Development Team. (2017). *Geographic Resources Analysis Support System (GRASS GIS) Software, Version 7.2*. Retrieved from <http://grass.osgeo.org>
- Gupta, H. V., Kling, H., Yilmaz, K. K., & Martinez, G. F. (2009). Decomposition of the mean squared error and NSE performance criteria: Implications for improving hydrological modelling. *Journal of Hydrology*, 377(1–2), 80–91. <https://doi.org/10.1016/j.jhydrol.2009.08.003>
- Haas, W., Moshhammer, H., Muttarak, R., Balas, M., Ekmekcioglu, C., Formayer, H., ... Lemmerer, K. (2018). *Pre-Print Österreichischer Special Report Gesundheit, Demographie und Klimawandel – Synthese (ASR18)*.
- Haidekker, A., & Hering, D. (2008). Relationship between benthic insects (Ephemeroptera, Plecoptera, Coleoptera, Trichoptera) and temperature in small and medium-sized streams in Germany: A multivariate study. *Aquatic Ecology*, 42(3), 463–481. <https://doi.org/10.1007/s10452-007-9097-z>

- Hamilton, J. M., Maddison, D. J., & Tol, R. S. J. (2005). Climate change and international tourism: A simulation study. *Global Environmental Change*, *15*(3), 253–266. <https://doi.org/10.1016/j.gloenvcha.2004.12.009>
- Hannah, D. M., & Garner, G. (2015). River water temperature in the United Kingdom: Changes over the 20th century and possible changes over the 21st century. *Progress in Physical Geography*, *39*(1), 68–92. <https://doi.org/10.1177/0309133314550669>
- Hawkins, C. P., Hogue, J. N., Decker, L. M., & Feminella, J. W. (1997). Channel Morphology, Water Temperature, and Assemblage Structure of Stream Insects. *Journal of the North American Benthological Society*, *16*(4), 728–749. <https://doi.org/10.2307/1468167>
- Hemsen, J. (1967). *Die Pielach. Österreichs Fischerei-ZEITSCHRIFT FÜR DIE GESAMTE FISCHEREI, FÜR LIMNOLOGISCHE, FISCHEREIWISSENSCHAFTLICHE UND GEWÄSSERSCHUTZ-FRAGEN*(August/September 1967), 117–131.
- Hockey, J. B., Owens, I. F., & Tapper, N. J. (1982). *EMPIRICAL AND THEORETICAL MODELS TO ISOLATE THE EFFECT OF DISCHARGE ON SUMMER WATER TEMPERATURES IN THE HURUNUI RIVER*. 13.
- Holzmann, H., Massmann, C., & Stangl, K. (2014a). *MODMOD User Manual* (No. Version 1.0; p. 31). Vienna: University for Natural Resources and Life Science.
- Holzmann, H., Massmann, C., & Stangl, K. (2014b). Modular Conceptual Water Balance Model BOKU_ModMod (Version xx).
- Hunter, P. R. (2003). Climate change and waterborne and vector-borne disease. *Journal of Applied Microbiology*, *94*(s1), 37–46. <https://doi.org/10.1046/j.1365-2672.94.s1.5.x>
- Isaak, D. J., Young, M. K., Nagel, D. E., Horan, D. L., & Groce, M. C. (2015). The cold-water climate shield: delineating refugia for preserving salmonid fishes through the 21st century. *Global Change Biology*, *21*(7), 2540–2553. <https://doi.org/10.1111/gcb.12879>

- Jarvis, A., Reuter, H. I., Nelson, A., & Guevara, E. (2008). *Hole-filled SRTM for the globe Version 4, available from the CGIAR-CSI SRTM 90m Database*. Retrieved from (<http://srtm.csi.cgiar.org>)
- Jobling, M. (1997). Temperature and growth: modulation of growth rate via temperature change. In C. M. Wood & D. G. McDonald (Eds.), *Global Warming* (pp. 225–254). <https://doi.org/10.1017/CBO9780511983375.010>
- Johnson, F. A. (1971). Stream temperatures in an Alpine area. *Journal of Hydrology*, *14*(3–4), 322–336. [https://doi.org/10.1016/0022-1694\(71\)90042-4](https://doi.org/10.1016/0022-1694(71)90042-4)
- Johnson, S. L. (2004). Factors influencing stream temperatures in small streams: substrate effects and a shading experiment. *Canadian Journal of Fisheries and Aquatic Sciences*, *61*(6), 913–923. <https://doi.org/10.1139/f04-040>
- Kingsolver, J. G. (2009). The Well-Tempered Biologist: (American Society of Naturalists Presidential Address). *The American Naturalist*, *174*(6), 755–768. <https://doi.org/10.1086/648310>
- Lillehammer, A., Brittain, J. E., Saltveit, S. J., & Nielsen, P. S. (1989). Egg Development, Nymphal Growth and Life Cycle Strategies in Plecoptera. *Holarctic Ecology*, *12*(2), 173–186.
- Macan, T. T. (1958). The temperature of a small stony stream. *Hydrobiologia*, *12*(2–3), 89–106. <https://doi.org/10.1007/BF00034143>
- Mandlburger, G., Hauer, C., Wieser, M., & Pfeifer, N. (2015). Topo-Bathymetric LiDAR for Monitoring River Morphodynamics and Instream Habitats—A Case Study at the Pielach River. *Remote Sensing*, *7*(5), 6160–6195. <https://doi.org/10.3390/rs70506160>
- McMichael, A. J., Woodruff, R. E., & Hales, S. (2006). Climate change and human health: present and future risks. *The Lancet*, *367*(9513), 859–869. [https://doi.org/10.1016/S0140-6736\(06\)68079-3](https://doi.org/10.1016/S0140-6736(06)68079-3)
- Melcher, A. H., & Schmutz, S. (2010). The importance of structural features for spawning habitat of nase *Chondrostoma nasus* (L.) and barbel *Barbus barbus*

- (L.) in a pre-Alpine river. *River Systems*, 19(1), 33–42.
<https://doi.org/10.1127/1868-5749/2010/019-0033>
- Mohseni, O., & Stefan, H. G. (1999). Stream temperature/air temperature relationship: a physical interpretation. *Journal of Hydrology*, 218(3–4), 128–141.
[https://doi.org/10.1016/S0022-1694\(99\)00034-7](https://doi.org/10.1016/S0022-1694(99)00034-7)
- Mohseni, O., Stefan, H. G., & Erickson, T. R. (1998). A nonlinear regression model for weekly stream temperatures. *Water Resources Research*, 34(10), 2685–2692.
<https://doi.org/10.1029/98WR01877>
- Morse, W. L. (1970). Stream Temperature Prediction Model. *Water Resources Research*, 6(1), 290–302. <https://doi.org/10.1029/WR006i001p00290>
- Nash, J. E., & Sutcliffe, J. V. (1970). River flow forecasting through conceptual models part I — A discussion of principles. *Journal of Hydrology*, 10(3), 282–290. [https://doi.org/10.1016/0022-1694\(70\)90255-6](https://doi.org/10.1016/0022-1694(70)90255-6)
- Nelder, J. A., & Mead, R. (1965). A Simplex Method for Function Minimization. *The Computer Journal*, 7(4), 308–313. <https://doi.org/10.1093/comjnl/7.4.308>
- Pletterbauer, F., Melcher, A., & Graf, W. (2018). Climate Change Impacts in Riverine Ecosystems. In S. Schmutz & J. Sendzimir (Eds.), *Riverine ecosystem management: science for governing towards a sustainable future* (pp. 203–224). Retrieved from <http://dx.doi.org/10.1007/978-3-319-73250-3>
- Pletterbauer, F., Melcher, A. H., Ferreira, T., & Schmutz, S. (2015). Impact of climate change on the structure of fish assemblages in European rivers. *Hydrobiologia*, 744(1), 235–254. <https://doi.org/10.1007/s10750-014-2079-y>
- Poertner, H.-O., & Peck, M. A. (2011). TEMPERATURE | Effects of Climate Change. In *Encyclopedia of Fish Physiology* (pp. 1738–1745).
<https://doi.org/10.1016/B978-0-12-374553-8.00197-0>
- Poole, G. C., & Berman, C. H. (2001). An Ecological Perspective on In-Stream Temperature: Natural Heat Dynamics and Mechanisms of Human-Caused Thermal Degradation. *Environmental Management*, 27(6), 787–802.
<https://doi.org/10.1007/s002670010188>

- Pröbstl, U., Prutsch, A., Formayer, H., Landauer, M., Grabler, K., Kulnig, A., ...
Krajasits, C. (2008, August 15). *Climate change in winter sport destinations – transdisciplinary research for implementing sustainable tourism*. 165–173.
<https://doi.org/10.2495/ST080171>
- QGIS Development Team. (2017). *QGIS Geographic Information System*. Retrieved from <http://qgis.osgeo.org>
- Ramaker, T. A. B., Meuleman, A. F. M., Bernhardt, L., & Cirkel, G. (2005). Climate change and drinking water production in The Netherlands: a flexible approach. *Water Science and Technology*, 51(5), 37–44.
<https://doi.org/10.2166/wst.2005.0104>
- Rice, J. A., Breck, J. E., Bartell, S. M., & Kitchell, J. F. (1983). Evaluating the constraints of temperature, activity and consumption on growth of largemouth bass. *Environmental Biology of Fishes*, 9(3–4), 263–275.
<https://doi.org/10.1007/BF00692375>
- Schmitz, W. (1954). Grundlagen der Untersuchung der Temperaturverhältnisse in den Fließgewässern. *Berichte der Limnologischen Flußstation Freudenthal*, 6, 29–50.
- Schuetz, T., & Weiler, M. (2011). Quantification of localized groundwater inflow into streams using ground-based infrared thermography: QUANTIFICATION OF GROUNDWATER INFLOW. *Geophysical Research Letters*, 38(3), n/a-n/a.
<https://doi.org/10.1029/2010GL046198>
- Schulte, P. M. (2011). TEMPERATURE | Effects of Temperature: An Introduction. In *Encyclopedia of Fish Physiology* (pp. 1688–1694).
<https://doi.org/10.1016/B978-0-12-374553-8.00159-3>
- Sinokrot, B. A., & Stefan, H. G. (1993). Stream temperature dynamics: Measurements and modeling. *Water Resources Research*, 29(7), 2299–2312.
<https://doi.org/10.1029/93WR00540>

- Smith, K. (1972). River water temperatures - an environmental review. *Scottish Geographical Magazine*, 88(3), 211–220.
<https://doi.org/10.1080/00369227208736229>
- Smith, K. (1975). WATER TEMPERATURE VARIATIONS WITHIN A MAJOR RIVER SYSTEM. *Hydrology Research*, 6(3), 155–169.
<https://doi.org/10.2166/nh.1975.0011>
- Stefan, H. G., & Preud'homme, E. B. (1993). STREAM TEMPERATURE ESTIMATION FROM AIR TEMPERATURE. *Journal of the American Water Resources Association*, 29(1), 27–45. <https://doi.org/10.1111/j.1752-1688.1993.tb01502.x>
- Steinhauser, F., Eckel, O., & Lauscher, F. (Eds.). (1960). *Klimatographie von Österreich*. <https://doi.org/10.1007/978-3-7091-5724-4>
- Sun, C., Chen, Y., Li, X., & Li, W. (2016). Analysis on the streamflow components of the typical inland river, Northwest China. *Hydrological Sciences Journal*, 1–12. <https://doi.org/10.1080/02626667.2014.1000914>
- van der Spek, J. E., & Bakker, M. (2017). The influence of the length of the calibration period and observation frequency on predictive uncertainty in time series modeling of groundwater dynamics: CALIBRATION PERIOD OF TIME SERIES MODELS. *Water Resources Research*, 53(3), 2294–2311.
<https://doi.org/10.1002/2016WR019704>
- van Vliet, M. T. H., Ludwig, F., Zwolsman, J. J. G., Weedon, G. P., & Kabat, P. (2011). Global river temperatures and sensitivity to atmospheric warming and changes in river flow: SENSITIVITY OF GLOBAL RIVER TEMPERATURES. *Water Resources Research*, 47(2). <https://doi.org/10.1029/2010WR009198>
- van Vliet, M. T. H., Vögele, S., & Rübhelke, D. (2013). Water constraints on European power supply under climate change: impacts on electricity prices. *Environmental Research Letters*, 8(3), 035010. <https://doi.org/10.1088/1748-9326/8/3/035010>

- Walker, J., & Lawson, J. (1977). Natural stream temperature variations in a catchment. *Water Research*, 11(4), 373–377. [https://doi.org/10.1016/0043-1354\(77\)90025-2](https://doi.org/10.1016/0043-1354(77)90025-2)
- Ward, J. V. (1985). Thermal characteristics of running waters. *Hydrobiologia*, 125(1), 31–46. <https://doi.org/10.1007/BF00045924>
- Ward, J. V. (1994). Ecology of alpine streams. *Freshwater Biology*, 32(2), 277–294. <https://doi.org/10.1111/j.1365-2427.1994.tb01126.x>
- Ward, J. V., & Stanford, J. A. (1982). Thermal Responses in the Evolutionary Ecology of Aquatic Insects. *Annual Review of Entomology*, 27(1), 97–117. <https://doi.org/10.1146/annurev.en.27.010182.000525>
- Webb, B. W., Hannah, D. M., Moore, R. D., Brown, L. E., & Nobilis, F. (2008). Recent advances in stream and river temperature research. *Hydrological Processes*, 22(7), 902–918. <https://doi.org/10.1002/hyp.6994>
- World Health Organization. (2017). *Guidelines for drinking-water quality*.
- Zambrano-Bigiarini, M. (2017). *hydroGOF: Goodness-of-fit functions for comparison of simulated and observed hydrological time series*. [R package version 0.3-10]. <https://doi.org/10.5281/zenodo.840087>